

FINISHING OF LARGE DIAMETER AND LARGE BATCH  
ADVANCED CERAMIC BALLS ( $\text{Si}_3\text{N}_4$ ) FOR BEARING  
APPLICATIONS USING MAGNETIC  
FLOAT POLISHING

By

ASHOK LAKSHMANAN

Bachelor of Engineering

University of Madras

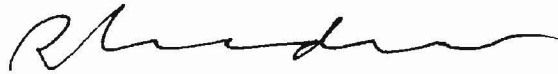
Madras, India

1997

Submitted to the Faculty of the  
Graduate College of the  
Oklahoma State University  
in partial fulfillment of  
the requirements for  
the degree of  
MASTER OF SCIENCE  
July, 2000

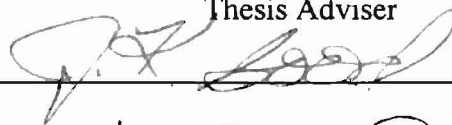
FINISHING OF LARGE DIAMETER AND LARGE BATCH  
ADVANCED CERAMIC BALLS ( $\text{Si}_3\text{N}_4$ ) FOR BEARING  
APPLICATIONS USING MAGNETIC  
FLOAT POLISHING

Thesis Approved:



---

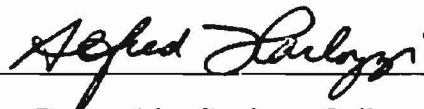
Thesis Adviser



---



---



---

Dean of the Graduate College



## PREFACE

Advanced ceramics, especially silicon nitride, which possess advantages such as low density, higher hardness, higher elastic modulus, high thermal and chemical resistance are being given increasing importance as an alternative to conventional bearings that are used in extreme conditions. Some of the major lacunae that are faced while using either pure ceramic or hybrid bearings are the cost of manufacturing and the time it takes to finish a batch of balls. Lack of sufficient reliability also acts as one of the major disadvantage of conventional processes such as grinding and polishing.

Roughing, semi-finishing and final finishing are the three stages that constitute this polishing process. High material removal rate is given importance in the initial stages; emphasis is laid on the removal rate along with the sphericity in the semi-finishing stage, while sphericity, required final size and the surface finish are considered to be important in the final stage. The main objective of this investigation is to develop a methodology by which large  $\text{Si}_3\text{N}_4$  balls (0.5 inch) constituting a large batch, are finished for bearing applications with good sphericity and good surface finish. Another aim of this investigation is to reduce the total setup time for the process which in turn reduces the overall process time.

The optimum load and speed conditions were found out using an experimental design based on Taguchi approach. Non-diamond abrasives such as  $B_4C$ , SiC and  $CeO_2$  of various grit sizes are used for polishing the batch. For the polishing process, the chamber needs to be aligned with the polishing spindle. As the entire process involves lot of polishing runs, any misalignment in setting up the chamber tends to multiply through all the runs. In order to overcome this problem, five to six runs were combined in such a way that only the magnetic fluid was replaced without disturbing the setting. This method reduced the entire process time by almost one-third of the original process time in addition to introducing the element of repeatability in aligning the polishing apparatus.

The variation in the critical parameters such as the sphericity, the surface finish, and the diametric tolerance among the sample size selected and in a single ball was found out using average and range charts. Sphericity values as low as  $0.20\mu m$  has been achieved along with a good surface finish of 7.2-10.4 nm for the large batch of balls. Acceptable diametric tolerance was also obtained for the finished batch of balls.

## ACKNOWLEDGEMENTS

I would first like to thank my adviser, Dr. Ranga Komanduri, for his guidance, and his advice throughout this work. I would like to express my special appreciation for Mr. Srihari Raghava Rao, former research assistant at MAERL, OSU, for his support. Special thanks to Mr. Satish Ramanathan for assisting me in performing the polishing. I would also like to thank Mr. Nagasubramanian Chandrasekaran, Mr. Sriram Rao, Mr. Venkatesh Thiyagarajan, Mr. Ananthapadmanabhan Chandrasekaran and Mr. Ashutosh Kuperkar for their co-operation, help and valuable-discussions.

I'm indebted to my family Mr. C. S. Lakshmanan, Mrs. L. Baghirathi, and Ms. L. Jayashree who were always encouraging in times of need, and without whose ever present support and sacrifices I would not have come this far. Finally, I would like to thank one and all for helping me in completing this work.

This project is sponsored by grants from the National Science Foundation (NSF) on "Tribological Interactions in Polishing of Advanced Ceramics and Glasses," (CMS-9414610), and "Design, Construction and Optimization of magnetic Field Assisted Polishing," (DMI-9402895) and DOD's DEPSCoR program on "Finishing of Advanced Ceramics," (DAAH04-96-1-0323) and CATT's program on " Finishing Silicon Nitride Balls for Bearing Applications," (Contract No. F34601-95-D-0376).

## TABLE OF CONTENTS

<b>Chapter</b>		<b>Page</b>
1.	Introduction	1
	1.1 Conventional Finishing Method for Ceramic Balls	5
2.	Literature Review	8
	2.1 Lapping and Polishing Technology	8
	2.2 Literature on Magnetic Float Polishing	13
3.	Problem Statement	23
4.	Approach	25
	4.1 Introduction	25
	4.2 Silicon Nitride Workmaterial	25
	4.3 Abrasives	28
	4.4 Salient Features of Magnetic Float Polishing	29
	4.5 Evaluation of Surface Integration	31
	4.6 Experimental work	36
5.	Magnetic Float Polishing (MFP)-Methodology	38
	5.1 Equipment for MFP	39
	5.2 Mechanical Polishing	42
	5.3 Chemo-mechanical Polishing	42

6.	Optimum Polishing Conditions for MFP of Large Batch Silicon Nitride Balls Using the Taguchi Approach	44
	6.1 Introduction	44
	6.2 Experiments Design Using Taguchi Approach	47
	6.3 Approach	48
	6.4 Evaluation of Experimental Design Results	51
7.	Apparatus Setting up and Process Time	61
	7.1 Out-of-Roundness	61
	7.2 Surface Finish	65
	7.3 Setting up the Apparatus	65
8.	Statistical Analysis	72
	8.1 Introduction	72
	8.2 Average and Range Charts	73
	8.3 Average (Xbar) and Range ( R ) charts for Large batch and Large Diameter (0.5”) balls.	75
9.	Conclusions	94
10.	Future Work	96
11.	References	98

## LIST OF FIGURES

<b>Figure</b>		<b>Page</b>
Figure 1.1	Friction losses for (a) bearing steel; (b) silicon nitride bearings	3
Figure 1.2	Lapping apparatus for polishing of steel or advanced ceramic balls	6
Figure 2.1	Schematic of apparatus for low stress polishing of spherical objects.	10
Figure 2.2	Schematic of a lapping apparatus	11
Figure 2.3	Schematic of apparatus for polishing spherical objects	12
Figure 2.4	Apparatus for magnetic float polishing	14
Figure 2.5	Schematic of setup with float	15
Figure 2.6	Kinematic model for MFP	16
Figure 2.7	Dynamic model for MFP	18
Figure 2.8.1	(a) Plots of response of each polishing parameter level on Ra.	21
	(b) Plots of response of each polishing parameter level on Ra.	21
	[Jiang and Komanduri, 1998]	
Figure 2.8.2	(a) S/N ratio plots showing the effect of each parameter level on Ra value.	22
	(b) S/N ratio plots showing the effect of parameter levels on Rt.	22

Figure 4.1	Schematic of a talysurf traverse unit laser interferometric transducer system	33
Figure 4.2	Deviation of Ra and Rt parameters	35
Figure 5.1	Schematic of apparatus for MFP of a small batch of advanced ceramic balls	40
Figure 5.2	Schematic of apparatus for MFP of a large batch of advanced ceramic balls	41
Figure 6.1	Condition of the groove on the float after the first test run	56
Figure 6.2	Condition of the groove on the float after the second test run	56
Figure 6.3	Condition of the groove on the float after the third test run	57
Figure 6.4	Condition of the groove on the float after the fourth test run	57
Figure 6.5	Condition of the groove on the float after the fifth test run	58
Figure 6.6	Condition of the groove on the float after the sixth test run	58
Figure 6.7	Condition of the groove on the float after the seventh test run	59
Figure 6.8	Condition of the groove on the float after the eighth test run	59
Figure 6.9	Condition of the groove on the float after the ninth test run	60
Figure 7.1	A typical eccentric Si <sub>3</sub> N <sub>4</sub> ball	64
Figure 8.1	R-Chart (Variation of Sphericity within a ball)	79
Figure 8.2	Xbar-Chart (Variation of Sphericity within the sample size)	80
Figure 8.3	R-Chart (Variation of diameter within a ball)	82
Figure 8.4	Xbar-Chart (Variation of diameter within the sample size)	83
Figure 8.5	R-Chart (Variation of Ra within a ball)	85
Figure 8.6	Xbar-Chart (Variation of Ra within the sample size)	86

Figure 8.7	R-Chart (Variation of $R_t$ within a ball)	88
Figure 8.8	Xbar-Chart (Variation of $R_t$ within the sample size)	89
Figure 8.9	Roundness profile of a finished $Si_3N_4$ ball (Talyrond 250)	90
Figure 8.10	Roundness profile of a finished $Si_3N_4$ ball (Talyrond 250)	91
Figure 8.11	Surface Roughness profile of a finished $Si_3N_4$ ball (Talysurf 120L)	92
Figure 8.12	Surface Roughness profile of a finished $Si_3N_4$ ball (Talysurf 120L)	93
Figure 10.1	Integrated chip on a single crystal silicon ball	97



## LIST OF TABLES

<b>Table</b>		<b>Page</b>
Table 1.1	Properties of advanced ceramics and bearing steel	2
Table 4.1	Chemical composition of NBD-200 Si <sub>3</sub> N <sub>4</sub> ball [Hah et al.,1995]	27
Table 4.2	Typical abrasives	28
Table 6.1	Conditions for finishing a small batch (13 balls) Si <sub>3</sub> N <sub>4</sub> balls (0.5")	45
Table 6.2	Abrasives used and their properties	45
Table 6.3	Test Conditions used	46
Table 6.4	Parameters used for the test	48
Table 6.5	L <sub>9</sub> (3 <sup>4</sup> ) Orthogonal arrays used	50
Table 6.6	Design of Experiment	50
Table 6.7	Results of the trial runs	55
Table 7.1	Total process time for Si <sub>3</sub> N <sub>4</sub> balls (large batch, diameter-7/32", 9/32", 11/32")	68
Table 7.2	Total process time (theoretical) for Si <sub>3</sub> N <sub>4</sub> balls (large batch, diameter-17/32")	69
Table 7.3	Total process time with MRR (Large batch: 55 Si <sub>3</sub> N <sub>4</sub> balls)	69
Table 7.4	Split up times for the entire polishing process.	71
Table 8.1	Values of constants for different sub-group sizes	75
Table 8.2	Measured sphericity values in μm. Sample Size=15, Subgroup,n=8	78

Table 8.3	Measured diameter values in mm. Sample size=15, Subgroup size, n=8	81
Table 8.4	Measured values of Ra (nm), Sample Size=15, Subgroup size, n=8	84
Table 8.5	Measured values of Rt (nm), Sample Size=15, Subgroup size, n=8	87

## LIST OF SYMBOLS

Ra	Arithmetic average roughness height
Rt	Maximum roughness height in five cutoffs: the vertical height between the heighest and the lowest points of the profile within the evaluation length.
n	Subgroup size
UCL	Upper Control Limit
LCL	Lower Control Limit

# Chapter 1

## Introduction

Steel ball bearings have been traditionally used for bearing applications in many mechanical and aerospace industries. Considerable number of disadvantages have been experienced while using steel balls in places of high temperatures, as they have to be lubricated for having a satisfactory and optimum life. The arrival of high-speed spindles (speeds upto 180,000 rpm) for machining centers increased the need for an alternate material that can overcome the drawbacks of steel balls. Advanced ceramics are being widely considered as a replacement for steel balls in bearings for such high speed and high temperature applications. The concept of using hybrid ball bearings, which were made up of ceramic balls and steel races, is also widely used in order to increase the life span of the hybrid bearing. For high-speed applications, the life of a hybrid bearing is about two to three times the life of an all-steel bearing.

Silicon nitride is the material of choice for the hybrid bearings due to many of its superior properties. These include higher hardness, high elastic modulus or higher stiffness, higher thermal and chemical stability and lower density compared to traditional steel balls and higher fracture toughness when compared to other advanced ceramics. The comparison of properties of silicon nitride with other advanced ceramics and the traditional steel balls are shown in the Table 1.1. As advanced ceramics have high compressive strength but low tensile strength, they are not suitable for the bearing races. Also the problem of different thermal coefficient between an all-ceramic bearing and the metal shaft makes it advantageous to use ceramic balls with steel bearing braces.

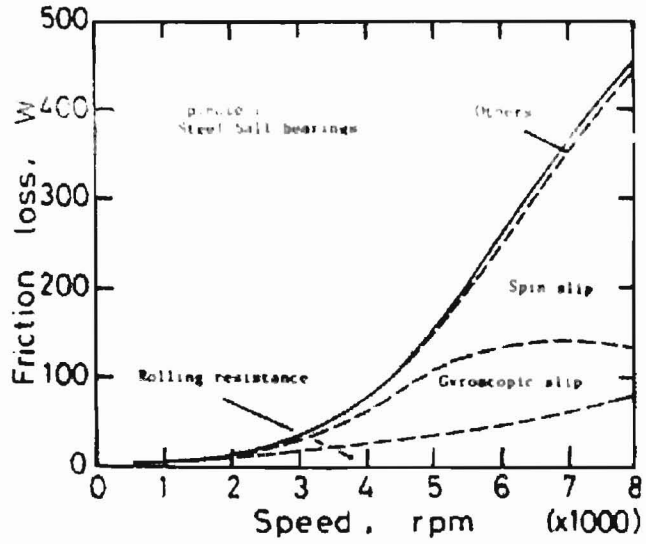
Table 1.1 Properties of advanced ceramics and bearing steel [Jiang, 1998]

	Si <sub>3</sub> N <sub>4</sub>	B <sub>4</sub> C	Al <sub>2</sub> O <sub>3</sub>	Bearing Steel
Density (g/cm <sup>3</sup> )	3.24	2.52	3.78	7.85
Young's Modulus (Gpa)	314	448	360	200
Thermal Exp. Coeff. (/°C)	3.2*10 <sup>-6</sup>	5.8*10 <sup>-6</sup>	8*10 <sup>-6</sup>	11.6*10 <sup>-6</sup>
Thermal Conductivity (W/m°K)	32	26	25	40
Flexural Strength (Mpa)	700	300	240	2500
Fracture Toughness (MNm <sup>-3/2</sup> )	7	3	4.9	20
Max. Work Temp. (°C)	1100	1750	1200	200
Hardness (Hv10Kg) (Gpa)	16	28	22	7
Corrosion Resistance	High	High	High	Moderate
Failure Mode	Spalling	Fracture	Fracture	Spalling

Hirotoishi et al. (1988) investigated the temperature rise of angular-contact bearings for machine tools (having steel rings and silicon nitride balls) and conventional steel ball bearings with grease lubrication and oil-air lubrication. According to Hirotoishi et al., the key advantages of silicon nitride balls are reduction of centrifugal forces and gyroscopic moments. These advantages have been attributed to the low density of silicon nitride. The frictional losses were found to decrease for the silicon nitride balls with the rise in speed. At speeds as high as 8000 rpm, the bearing losses or the friction (as shown in the Figures 1.1a and 1.1b) for silicon nitride ball bearings were about 30 to 50 percent lower than for steel ball bearings. This trend was found similar to that of the temperature

rise in the ceramic and the steel bearings with the rise in temperature. It was also concluded that the reduction of gyroscopic moment by using silicon nitride balls worked effectively for bearings having large contact angles.

(a)



(b)

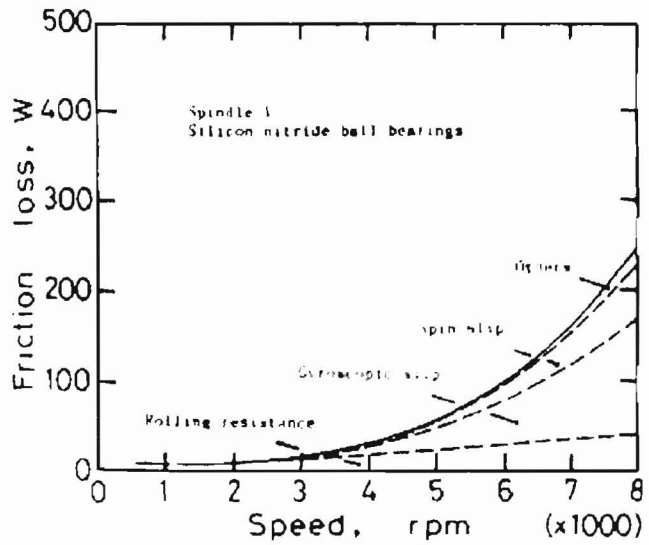


Figure 1.1 Friction losses for (a) bearing steel; (b) silicon nitride bearings

Dezzani and Pearson (1996) compared the resistance to various failures of hybrid bearings with steel bearings. Test conditions similar to those of aircraft turbine main-shaft bearings were simulated to compare the performance of M50 and M50 NiL hybrid ceramic bearings with steel bearings. Full-scale tests were run with NBD-200 (Grade-5) silicon nitride balls, under conditions that included 150°C temperature, surface flaws created by hard particle contamination, partial EHD lubrication, and the sliding action of balls under thrust loading. The hybrid bearings had longer life than all steel bearings and demonstrated resistance to the surface-peeling mode of failure initiation. Higher strength of the rolling contact surfaces, high residual compressive stresses in the nitrided layers, and a more favorable action in ceramic to steel rolling contact have been given as the main reasons for the improved performance of the hybrid over all-steel bearings.

Pete et al. (1999) compared silicon nitride ceramic balls and conventional steel bearings using M50 steel balls in terms of heat generation, frictional torque and ball wear. They found that steel balls generate heat more quickly than ceramic balls and heat generation rate and frictional torque are higher for steel ball bearings. Large hertzian contact region for steel balls, due to high inertial load on the outer race and lower Young's modulus, was found out as the reason for high heat generation of the M50 steel balls at speeds above 15,000 rpm. It was also found that higher slip velocities and traction coefficients leads to an increase in wear rate of the steel balls and that it is almost 50 percent more than the ceramic ball. The overall frictional losses for the silicon nitride are about 20 percent less than the steel balls.

## 1.1 Conventional finishing method for ceramic balls

V-groove lapping is the most common technique used for finishing ceramic as well as steel balls. This process is done at loads as high as 10N at low speeds using expensive diamond abrasives. Figure 1.2 is a schematic of this process. This process takes almost twelve to sixteen weeks to finish the ceramic balls from its as-received condition to finish as they operate at very low speeds (~ 50 rpm). Creation of surface imperfections, pits and gouges results due to the use of abrasives that are significantly harder than the ceramic balls at high loads and low speeds. Nucleation sites of cracks are caused due to the presence of surface imperfections on the advanced ceramics, which are very hard and brittle. This leads to a high rate of fatigue crack propagation, which in turn leads to catastrophic failure during operation.

Gentle conditions are required during polishing in order to overcome the above-mentioned defects. Magnetic float polishing (MFP) is a new technique, which uses low loads and high speeds. The abrasives used in this method are slightly harder or even less hard than the ceramic material due to which the surface quality of the ceramic material has been considerably improved. As a result, this technique is also known as a “gentle” finishing process. MFP uses low loads (~1N/ball), high speeds (~2000 to 5000 rpm for small batches and ~200 to 300 rpm for large batches), and abrasives such as boron carbide, silicon nitride, and cerium oxide. In addition to the low loads used for polishing, the use of float offers great flexibility to the polishing system i.e. the work material, the polishing shaft and the abrasive slurry. As discussed in the following chapters the work material is supported against the load by a float, which imparts the buoyant forces, caused by the magnetic fluid used for forming the slurry. Any vibrations or excessive forces are



adjusted due to the freedom of the controlled movement of the float in the vertical plane, which resembles a spring-loaded mechanism e.g. a shock absorber.

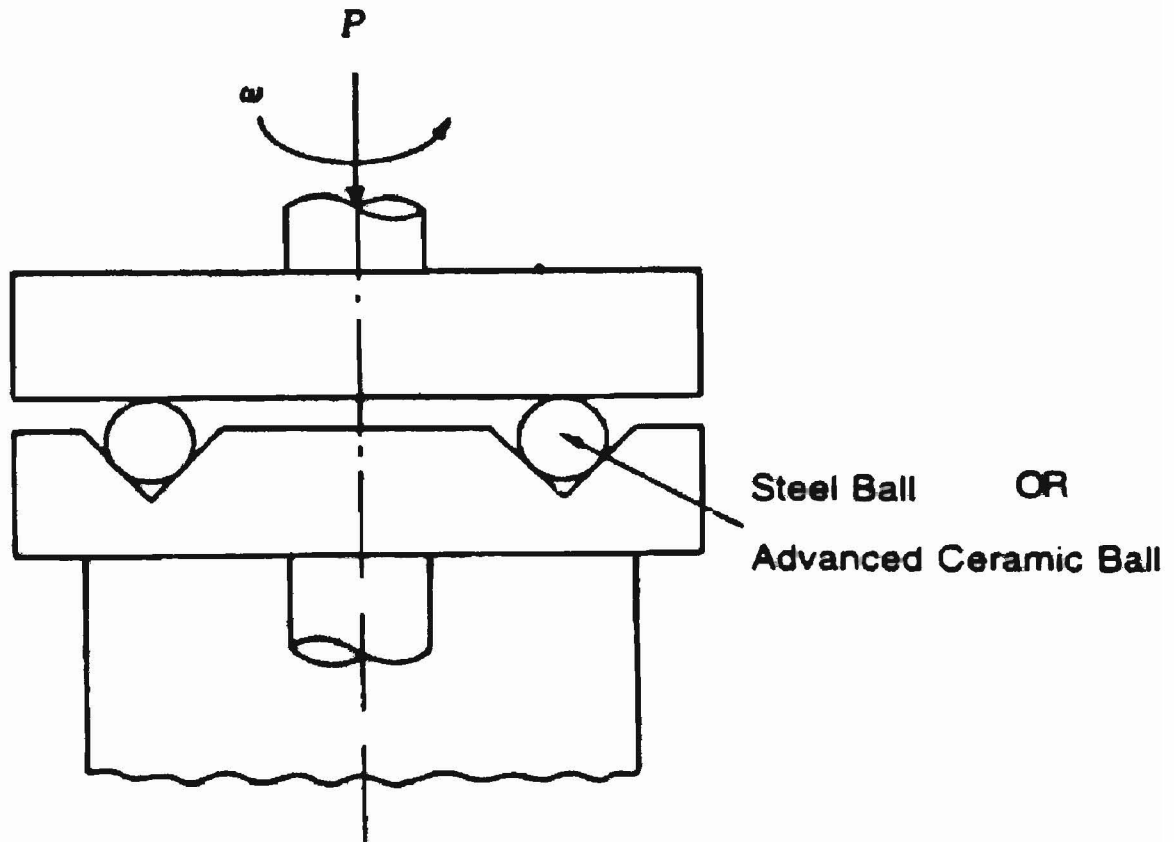


Figure 1.2 Lapping apparatus for polishing of steel or advanced ceramic balls.

Chapter 2 contains the literature review on the development of the magnetic float polishing process. Chapter 3 and Chapter 4 deal with the problem statement and the approach respectively. Chapter 5 deals with the methodology of magnetic float polishing,

while Chapter 6 describes the method used for finding the optimum conditions for this work. Chapter 7 deals with the steps involved in reducing the setup and the overall process time. Chapter 8 describes the statistical analysis of the process for controlled variation using the average and range charts. Chapter 9 lists the conclusions of this particular work, while Chapter 10 discusses future work.

## Chapter 2

### Literature Review

#### 2.1 Lapping and Polishing Technology:

Finishing of spherical blanks requires precise and controlled material removal so that sphericity can be controlled and improved as required. The rolling motion of balls in grinding and polishing plays a very important role in maintaining the sphericity of the balls. Plates, usually two, having a relative rotational motion are used for grinding, polishing or lapping of spherical objects. The plates used for this method of lapping are mostly horizontal but in certain cases they can also be vertical or inclined at an angle. Load on the plates, rotational speed of the plates, type of abrasives used, volume present of the abrasives, abrasive slurry and ball material to be finished are some of the important parameters that control the material removal rate in these processes. Some selected patents that relate to ball finishing technique in lapping and polishing have been discussed.

Messerschmidt (1972) discloses a ball-lapping device comprising two superimposed lapping discs spaced by a working gap. In this case, one disc is stationary and the other moving. The rotatable disc consists of concentric lapping grooves on its face facing the other disc. A rotary magazine, which includes a circular guide path for the balls to be lapped is used for encompassing the discs. The working gap is connected with the guide path by means of a radial recess in the stationary disc. Two modes of operation have been used for the purpose of lapping. In the first mode a guide is used for guiding

the balls into the working gap, as a result of which the balls get lapped for one revolution. The guide then guides the lapped balls to the guide path. In the second mode of operation the connection between the guide path and the working gap are closed due to which the balls in the grooves are continued to be lapped until they have attained the desired surface finish.

London (1990) describes a method and an apparatus for low stress polishing of spherical objects. Figure 2.1 is a schematic of the apparatus, which basically consists of two parallel plates with a clearance so that the spherical objects to be polished can be placed. The face of the plates has been made very smooth. The top plate is made of ceramic material and includes a transparent plate. This transparent plate enables the monitoring of the process by viewing. Concave grooves have been provided on the top plate for the purpose of mixing the balls during polishing. Motion of the balls out of the polishing zone is prevented by using magnets placed on the top plate. Thus the magnets help in keeping the balls within the polishing chamber. The slurry used for polishing in this case is a mixture of glycol and fine diamond powder. The process uses loads on the order of several hundred grams and the rotational speeds used in the range of five to six rpm. A magnet is used in the device due to which the rotation of the ball around an axis is promoted. Good sphericity values upto  $0.15 \mu\text{m}$  have been obtained while maintaining highly uniform diametric values. In this method the polishing is more on that balls that are larger in diameter, which is continued till all the balls are of the same diameter and sphericity. This method claims to produce balls with very minimal or no damage. The polishing process can be carried on continuously for nearly twenty-four hours without any operator attention. The average time taken for completing a lot is  $\sim 10 - 23$  days.

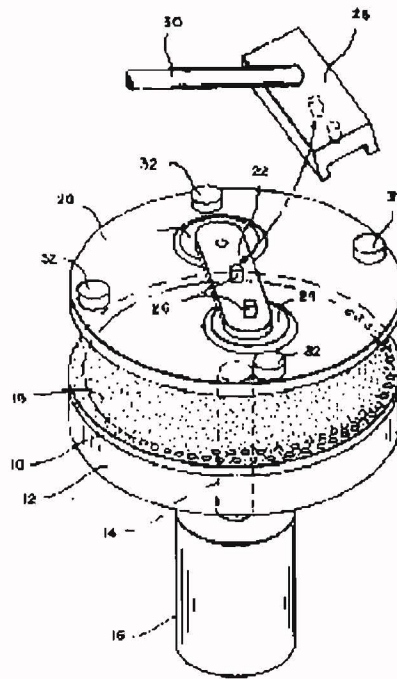


Figure 2.1 Schematic of apparatus for low stress polishing of spherical objects.

A modified lapping apparatus using the above principle is described by US Pat. No. 5, 301, 470 issued in 1994 to Sato. An angle of tilt ( $\alpha$ ) is given to the lapping plates during polishing, while the plates stay horizontal when loading and unloading of the balls. Schematic of the lapping apparatus is shown in Figure-2.2. The plates are protected from the heat generated from the rotating spindle by providing supports to the plates on both sides. The supports also serve the purpose of avoiding any change in the geometry in alignment of the plates while maintaining parallelism and concentricity of the plates with respect to the groove on the other disc.

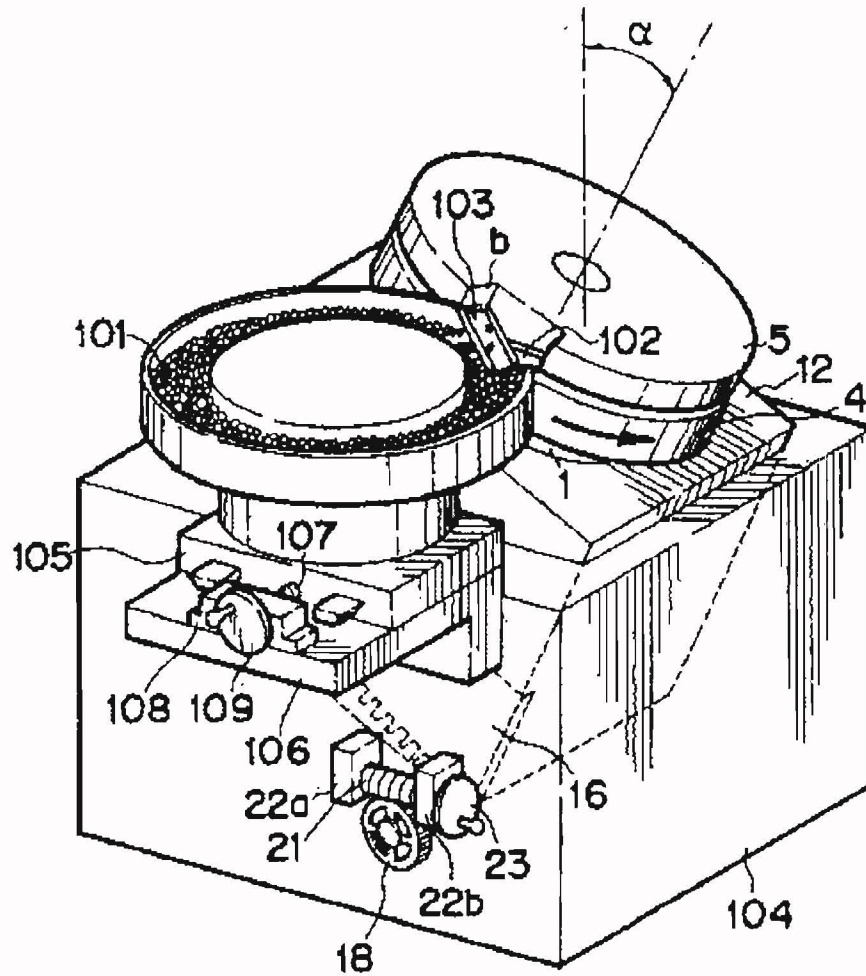
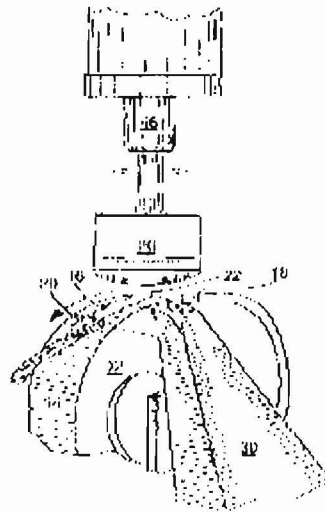


Figure 2.2 Schematic of a lapping apparatus

Kordonsky et al. presents magnetorheological method and describes an apparatus for the same in US Pat No. 5,839,944. This process has its features similar to magnetic float polishing. Mixing the magnetic fluid with the abrasives forms abrasive slurry. In this case a chamber is used for placing the workpiece and the abrasive slurry. The non-magnetic abrasives along with the workpiece are attracted in one direction, while the magnetic field is pulled in the opposite direction due to the action of the magnetic field

on the chamber. Figure-2.3 is a schematic of the apparatus for polishing spherical objects. A channel like polishing chamber is used for accommodating the magnetic fluid and the spherical object. The two vessels used are rotated in opposite directions relative to each other. The electromagnets are used for applied for applying the magnetic field, which is responsible for the relative motion between the workpieces and the abrasive slurry in the opposite direction.

Figure 2.3 Schematic of apparatus for polishing spherical objects



The apparatus and polishing process described by US Pat No. 5, 957, 753 and US Pat No. 5, 931, 718 issued to Komanduri et al. have been discussed in detail later in this chapter and in forthcoming chapters.



## 2.2 Literature on magnetic float polishing

Coats (1940) used the principle of magnetic field assisted finishing for finishing for gun barrels. Subsequently, considerable work in this field was also done in the former U.S.S.R in the late 1950's when Baron (1975) applied this technology for finishing large workpieces and hard to machine materials. This was followed by works in the late 1980's in Japan when Kato and Umehara (1990) and Shinmura et al. (1990) applied this technique for finishing workpieces to obtain a great degree of accuracy and good surface finish. Further advancements in this work were done by Komanduri et al. (1995) in the U.S.

Tani et al (1984) introduced magnetic float polishing but he could polish only very soft materials, such as acrylic resin. Figure-2.4 is a schematic for magnetic float polishing after Tani et al. Material removal in this case is achieved by pressing the non-magnetic abrasive grains against the workpiece due to buoyant levitational force applied by the non-magnetic abrasive grains. The polishing force used in this case was extremely low, so it could only be used to finish very soft materials. The material removal rate obtained was  $\sim 2 \mu\text{m}/\text{min}$  using SiC ( $4 \mu\text{m}$  grain size) abrasive. This work was not successful for finishing hard materials as the material removal rate was found to be extremely low or negligible.



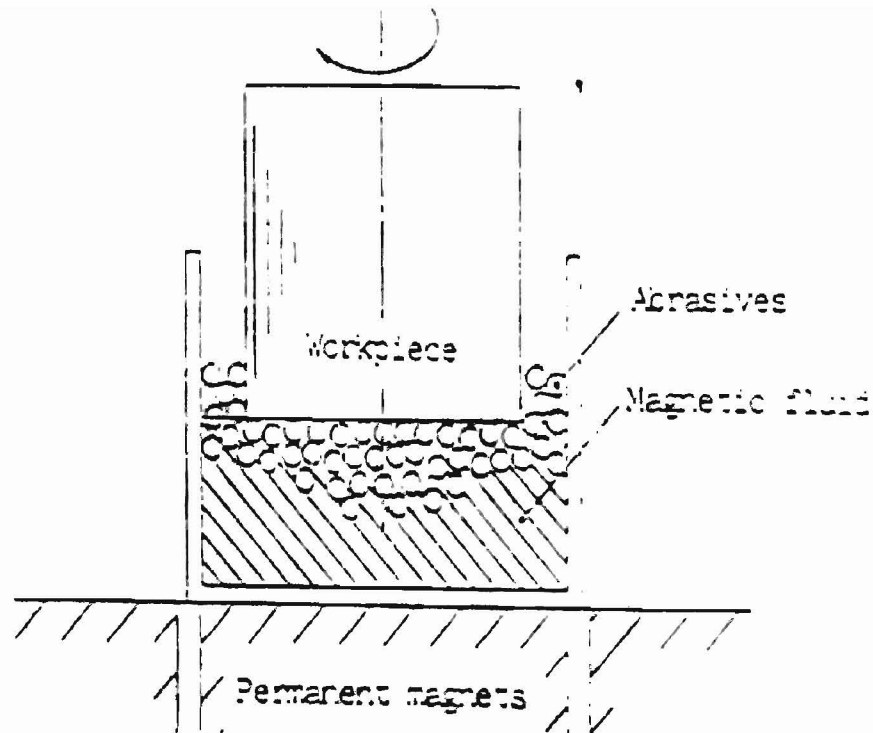


Figure 2.4 Apparatus for magnetic float polishing [Tani et al., 1984]

Major breakthrough was made when Umehara and Kato (1990) introduced the use of a float to produce uniform and sufficiently high load for getting high material removal rates while polishing advanced ceramic balls. The freely rotating float enables a three point contact to the ball (float, chamber wall, and polishing shaft), so the ball moves around a fixed center, leading to considerable improvements in sphericity. It was also found out that the polishing load increases significantly, especially at lower clearances. Stock removal was found to increase with time and that the stock removal is high with

float compared to without the float. Figure-2.5 is a schematic of the apparatus used by Umehara and Kato (1990).

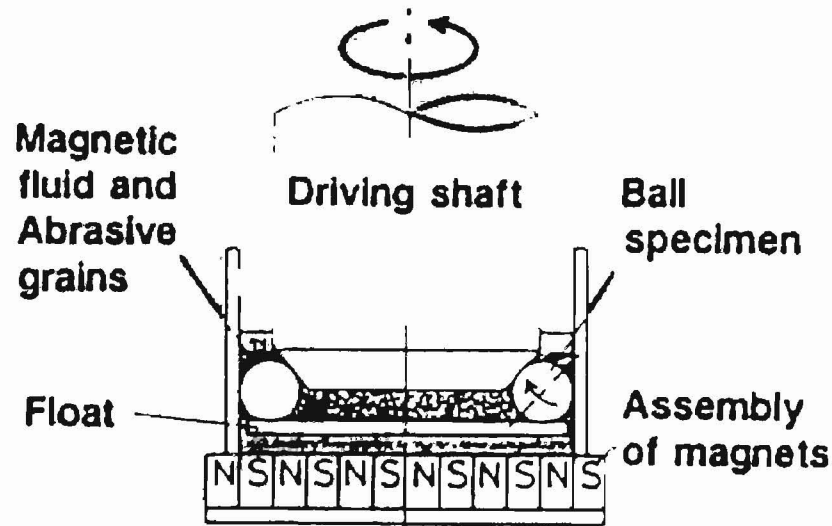
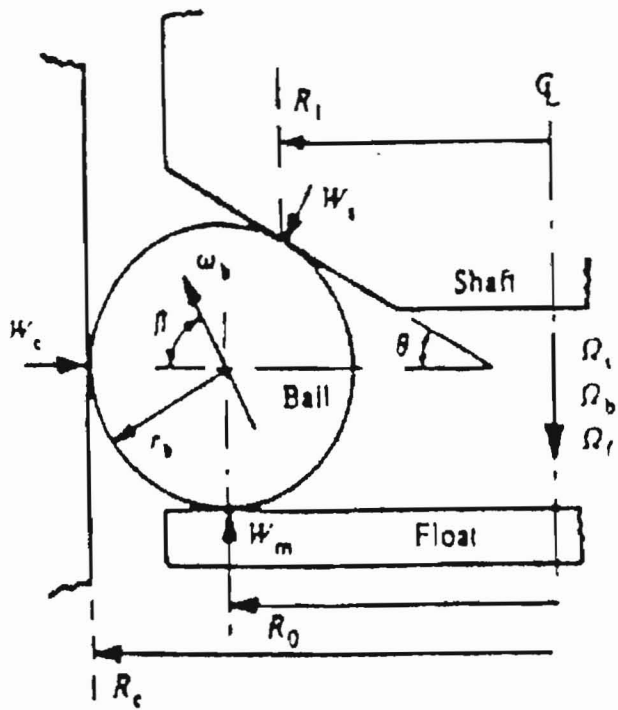


Figure 2.5 MFP apparatus with float [Umehara and Kato, 1990]

A kinematic model of the ball motion was developed by Childs et al. (1994) for calculating the sliding speeds and to estimate the wear coefficients. Material removal was attributed to two-body abrasion caused by the abrasives embedded in the drive shaft. The wear coefficients were attained in the range of (0.04- 0.08), which further supported their theory. Figure-2.6 shows the kinematic model as developed by Childs et al.



$$R_f = R_c - R_b$$

$$R_s = R_f - R_b \sin \theta$$

$$V_c = (R_f \Omega_b - R_b \Omega_b \sin \beta) - 0$$

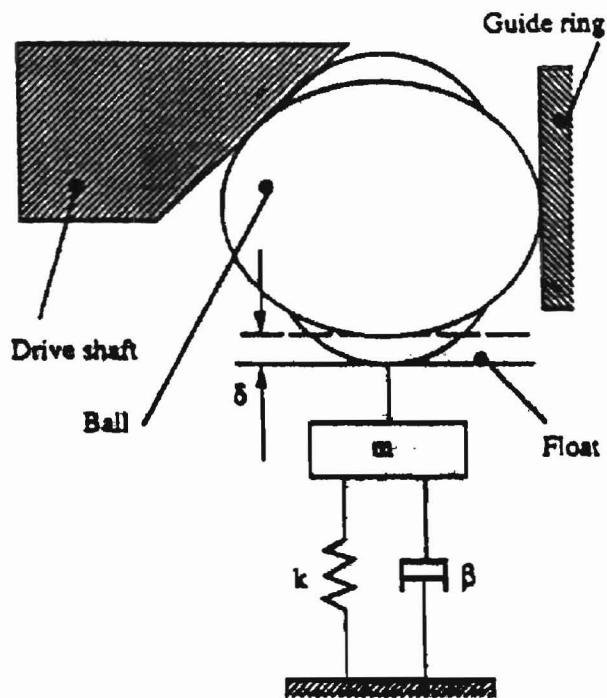
$$V_s = R_s \Omega_s - (R_f \Omega_b + R_b \omega_b \cos (\beta - \theta))$$

$$V_f = (R_f \Omega_b - R_b \omega_b \cos \beta) - R_f \Omega_f$$

Figure 2.6 Kinematic model of ball motion during MFP [Childs et al., 1994]

The possibility of chemo-mechanical action in the magnetic float polishing of silicon nitride balls, using chromium oxide ( $\text{Cr}_2\text{O}_3$ ) and aluminum oxide ( $\text{Al}_2\text{O}_3$ ) abrasive was studied by Komanduri et al. (1996). The abrasives were chosen because of their similar hardness to the workmaterial. The main aim of the study was to investigate the chemical and mechanical aspects of polishing. In chemo-mechanical polishing, a very small amount of material is removed from the surface due to the chemo-mechanical action at the contacting area between the abrasives and the polished material. The material removal of these two abrasives was found to be different when used for silicon nitride balls though they were of similar hardness. Chemo-mechanical action of chromium oxide played a big role in the higher removal rate when used with silicon nitride balls. Pits, possibly formed by abrasion, were observed along with brittle fracture and dislodgment of grains when aluminum oxide, was used for polishing silicon nitride. Polishing with chromium oxide resulted in a relatively smooth surface, with fewer pits, (when compared to the surface produced by using aluminum oxide) which was attributed to the chemo-mechanical action. According to Imanaka et al. (1978), the chemical reaction is caused by the mechanical friction energy and the polishing is done when this very small part is removed by friction.

A dynamic model (see Figure-2.7) of magnetic float polishing of ceramic balls was developed by Zhang, Umehara and Kato (1996) for generating good sphericity. It was concluded that during magnetic float polishing, when the larger diameter positions of ball enter the contact area, the load will increase and a larger amount of material will be removed from this place, and this process was found to continue until a spherical surface is obtained.



$$\Delta P = \kappa \delta$$

$$\kappa = \sqrt{(k - m\omega^2)^2 + (\beta\omega)^2}$$

Figure 2.7 Dynamic model of MFP [Zhang et al., 1996]

Roughing, intermediate semi-finishing and the final finishing were the three stages identified by Ming Jiang and Komanduri (1997) in their investigation of finishing of  $\text{Si}_3\text{N}_4$  balls by magnetic float finishing process. Emphasis was laid on the material removal in the initial roughing stage, whereas the material removal, sphericity, and surface roughness were monitored in the intermediate semi-finishing stage. Importance

was given to required size, sphericity, and the surface roughness values. High material removal rates ( $1\mu\text{m}/\text{min}$ ) with minimal subsurface damage were possible with the use of harder abrasives. The abrasives used were  $\text{B}_4\text{C}$  and  $\text{SiC}$  and these hard abrasives lead to high material removal due to rapid accumulation of minute amounts of material removed by mechanical micro-fracture at high polishing speeds and low loads in the magnetic float polishing process.

Ming Jiang and Komanduri (1998), further extended this study when they investigated the chemo-mechanical polishing of silicon nitride balls with different abrasives for obtaining a good surface finish.  $\text{CeO}_2$  and  $\text{Cr}_2\text{O}_3$  were found to be the most effective among all the abrasives used, followed by  $\text{Fe}_2\text{O}_3$  and  $\text{Cr}_2\text{O}_3$ . The formation of  $\text{SiO}_2$  layer on the surface of silicon nitride balls while using these abrasives was found out using a thermodynamic analysis. Formation of a soft  $\text{SiO}_2$  layer occurs due to the chemo-mechanical interaction between the work material and the abrasives in water environment, which acts as a facilitator for the reaction process. The thermal conductivity and the dissolution of the oil-based fluid is almost zero and thus the oil-film formed between the work material and the abrasive prevents the occurrence of any chemo-mechanical interaction.

Ming Jiang and Komanduri (1998) applied the Taguchi technique to obtain optimum conditions for magnetic float polishing. An orthogonal array was formed to vary the three parameters, namely, load, speed, percentage of abrasive, for obtaining the best condition for good surface quality. It was found that polishing force was the most significant factor, for the overall surface finish. The results from the tests also indicated that within the range of the parameters evaluated, a high level of polishing force

(1.4N/ball), a low level of abrasive concentration (5%) and a high level of polishing speed are optimum for improving both  $R_a$  and  $R_t$ . A surface finish as low as  $15\text{nm}R_a$  and  $150\text{ nm }R_t$  was obtained with SiC ( $1\text{ }\mu\text{m}$ ). Figures 2.8.1 (a) and (b) and 2.8.2 (a) and (b) show the results of the study using Taguchi method.

A polishing run can be considered successful or not based on its ability to improve the sphericity of the ball. Alignment of the polishing chamber, the condition of the groove on the polishing shaft, the groove formed on the float, the groove formed on the side wall and the sphericity of the balls before polish are some of the factors to be monitored before and after each polishing run. Of all these factors, the alignment of the chamber with the polishing shaft plays a very important role in reducing the sphericity of the balls. Any misalignment of the axes of the balls and the tapered contact surface will lead the balls to contact the tapered surface in a line not perpendicular to the axis. This might lead to non-uniform application of the load on the balls, leading to a non-uniform material removal among the balls, which consequentially leads to high sphericity values.

One of the main drawbacks of having a varied load is the improper spinning motion of the balls or the dragging motion of the balls, which not only results in the non-uniform material removal around the surface of the balls but also causes a case where the sphericity of the balls vary highly from ball to ball. Another main factor, which affects the sphericity, is the condition of the groove on the spindle and the uniformity of the groove formed on the float. The repeatability of the alignment of the chamber with the polishing spindle for every run also plays a very important role in obtaining a good sphericity of the balls.

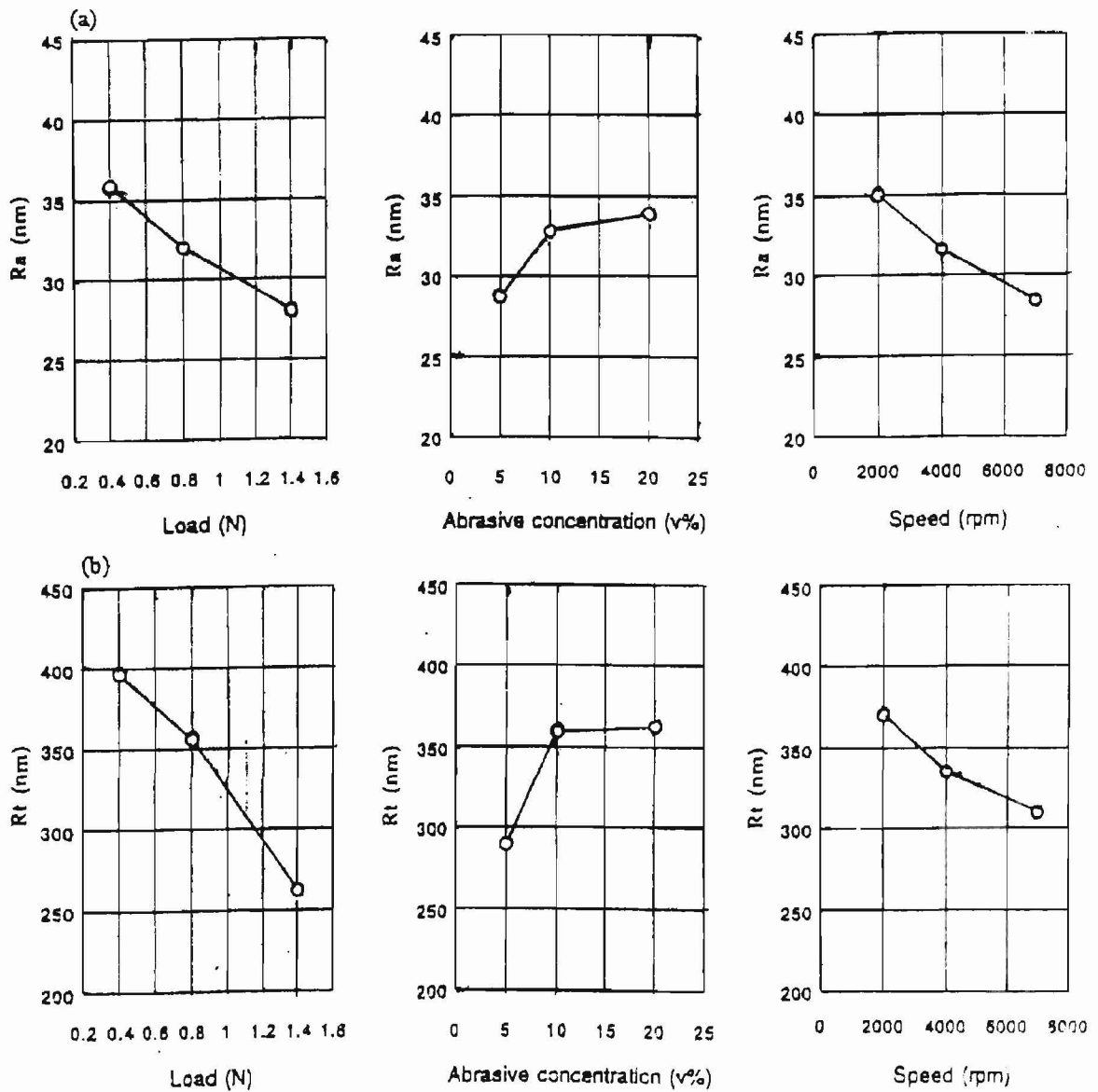


Figure 2.8.1 (a) Plots of response of each polishing parameter level on Ra.

(b) Plots of response of each polishing parameter level on Ra. [Jiang and Komanduri, 1998]



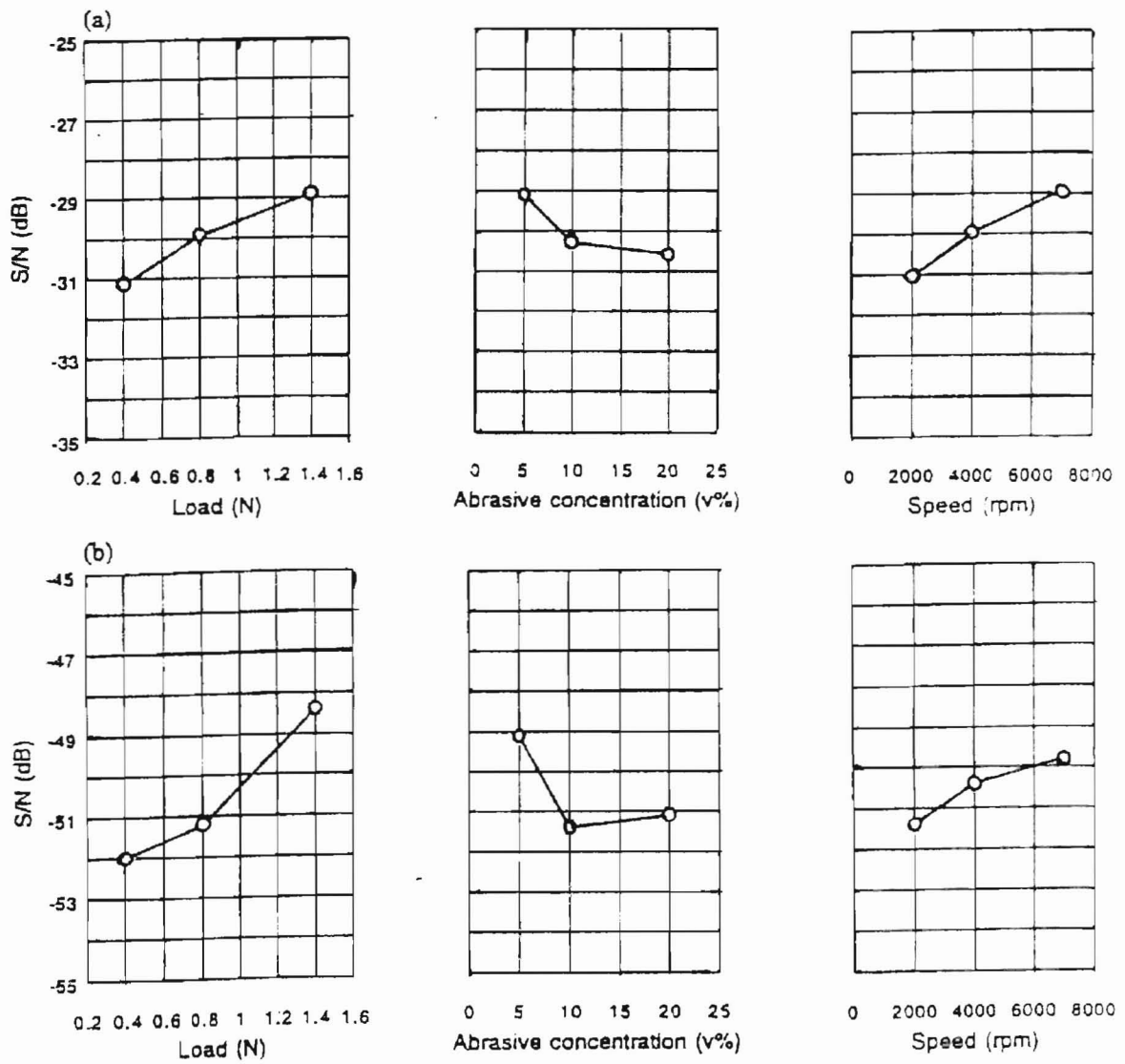


Figure 2.8.2 (a) S/N ratio plots showing the effect of each parameter level on Ra value.  
 (b) S/N ratio plots showing the effect of each parameter level on Rt. [Jiang and Komanduri, 1998]

## Chapter 3

### Problem Statement

Methodology has been previously established for finishing of advanced ceramic balls ( $\text{Si}_3\text{N}_4$ ) of different sizes using the magnetic float polishing technique. However, this technique was applied to the finishing of the small batches as well as large batches of balls whose sizes varied from  $7/32''$  to  $13/32''$ . Even though process parameters had been established for finishing of balls of the above mentioned sizes, the finishing of large size balls ( $17/32''$ ) still remained under investigation. Another important problem faced was the amount of time required for finishing a large batch. Some of the constraints that have to be taken into consideration in design of the polishing shaft are the dimensions of the existing chamber, thickness of the guide ring and the diameter of the balls going to be polished.

The repeatability of the process depends to a large extent on the set up of the apparatus. The set up or the alignment of the polishing chamber with that of the polishing spindle significantly influences the sphericity of the balls. Even though the validity of the setting up process could be maintained by using a vibration sensing equipment (Vibroport) and checking for the resonance [Srihari (1999)], the repeatability of the set up for each polishing run is very important. This repeatability can be affected by human errors, as the apparatus is setup manually using a vernier caliper, which leads to the possibility of a potential offset. This offset can get amplified for each successive run and

thereby affects the uniformity of the groove on the polishing spindle and thus the sphericity of the balls.

The primary objective of this investigation is to

1. Finish a large batch (55 balls) of 17/32"  $\text{Si}_3\text{N}_4$  balls, using the magnetic float polishing technique, to an out of roundness and diametric tolerance as low as possible. Maintaining a good surface finish ( $R_a$  and  $R_t$ ) was also a part of the task.
2. Improve repeatability in the set up of the process and reduce the overall setup time involved in finishing of a set of as-received  $\text{Si}_3\text{N}_4$  balls (17/32") to the required size (16/32").
3. Find the optimum polishing conditions (for a batch of 55 of 17/32" balls) by varying the load and the speed using the Taguchi method
4. Control the sphericity or out of roundness of the balls and lay emphasis on the material removal rate of the balls by varying the abrasives and their grit sizes.
5. Analyze the variations in diameter, out of roundness, and surface finish within the subgroup size selected as well as within the sample size selected using average and range charts.

## **Chapter 4**

### **Approach**

#### **4.1 Introduction**

The major emphasis of this investigation is on finishing of a large batch of 17/32” silicon nitride balls in a polishing chamber, which can hold as many as 55 balls of the above mentioned size. Various constraints such as the dimensions of the already existing chamber and the diameter of the ball to be polished are taken into consideration before designing the polishing shaft. The main aim of the initial roughing phase in the process is maximum material removal. Surface quality of the balls are improved by employing chemo-mechanical polishing. The setup of the apparatus plays a very important role in improving the sphericity of the balls. The experimental approach consisted of trying to make more than one polishing run with the same setup and it also involved the determination of the optimum loading and speed conditions. Importance of the groove on the float and the spindle was taken into consideration for finding the best conditions. Full characterization of the silicon nitride balls including the diameter, sphericity, and the surface roughness are evaluated using micrometer, Talysurf, and Talyrond. The variation in all these parameters are found out for a particular ball as well as the sample size chosen from a particular hatch, using average and range charts.

#### **4.2 Silicon Nitride Workmaterial**

Silicon Nitride ( $\text{Si}_3\text{N}_4$ ) is a ceramic with a hexagonal structure and predominantly covalent bonding [McColm, 1983, Katz et al, 1985]. Silicon has an electron configuration

of Si [ $3s^23p^2$ ](excited electron state:  $sp^3$  hybridization). This yields a tetrahedral arrangement of covalent bond formation with four N atoms producing a  $SiN_4$  tetrahedral building unit. Two other  $SiN_4$  tetrahedrons share the hexagonal  $Si_3N_4$ , which are formed by the tetrahedral units. So each silicon atom in its three dimensional network is covalently bonded with four nitrogen atoms, and each nitrogen atom is covalently bonded with three silicon atoms.

Silicon nitride has two crystalline phases ( $\alpha$ - $Si_3N_4$  and  $\beta$ -  $Si_3N_4$  respectively) in the microstructure. They are both covalently bonded hexagonal structured materials but  $\beta$ -  $Si_3N_4$  grain is more elongated than that of  $\alpha$ - $Si_3N_4$  ( $\alpha$ - $Si_3N_4$ :  $a=0.78$  nm,  $c=0.56$ nm;  $\beta$ -  $Si_3N_4$ :  $a=0.76$ nm,  $c=0.29$ nm). The  $\alpha$ - $Si_3N_4$  is easier to form than  $\beta$ -  $Si_3N_4$  but it get converted to  $\alpha$ - $Si_3N_4$  at high temperatures (1400-1800°C). In general, advanced silicon nitride engineering materials are  $\beta$ -  $Si_3N_4$  because all  $\alpha$ - $Si_3N_4$  transform to  $\beta$ -  $Si_3N_4$  during the shaping process (hot pressing).

Due to the low concentration of vacancies of the covalent solid, sintering cannot be done to high densities merely by heating. According to McColm (1983) several techniques, such as chemical vapor deposition (CVD), reaction bonding, hot pressing (HP), and hot isostatic pressing (HIP) have been available to obtain dense silicon nitride.

#### 4.2.1 Hot Pressed (HP) and Hot Isostatically Pressed (HIP) Process

Sintering of a mixture of  $\alpha$ - $Si_3N_4$  and  $\beta$ -  $Si_3N_4$  to a high density using uni-axial or isostatic high pressure is used for making hot pressed  $Si_3N_4$  material. Densification aids such as MgO or  $Y_2O_3$  are used for mixing  $Si_3N_4$  powders for enabling liquid phase

sintering and are then heated to 1700°C at 20Mpa pressure for HP and heated above 1700°C in a nitrogen atmosphere at high pressure > 300Mpa for HIP. The high-pressure nitrogen gas can yield isostatic material, which results in uniform material.

Tables 4.1 and 4.2[Jiang, 1998] shows the chemical composition of NBD silicon nitride ball ( $\beta$ - $\text{Si}_3\text{N}_4$ , uni-axially pressed with 1 wt.%MgO as main sintering aid). Reaction of  $\text{Si}_3\text{N}_4$  and  $\text{SiO}_2$  with small amounts of MgO creates a glassy phase at the grain boundaries during the high-temperature sintering or hot pressing of  $\text{Si}_3\text{N}_4$ . The complex glassy phase produced during sintering is primarily a magnesium silicate, which is modified by Ca, Fe, Al and other impurities initially present in silicon nitride ( $\text{Si}_3\text{N}_4$ ).

Table 4.1 Chemical composition of NBD-200  $\text{Si}_3\text{N}_4$  ball [Hah et al., 1995]

Mg	Al	Ca	Fe	C	O	$\text{Si}_3\text{N}_4$
0.6-1.0	$\beta$ 0.5	$\beta$ 0.04	$\beta$ 0.17	$\beta$ 0.88	2.3-3.3	94.1-97.1

#### 4.2.2 Chemical Vapor Deposition (CVD) process

In this process, pyrolytically deposited  $\text{Si}_3\text{N}_4$  is formed from  $\text{SiCl}_4$  vapor and  $\text{NH}_3$  gas. The volatile  $\text{SiCl}_4$  and  $\text{NH}_3$  gases react and deposited  $\text{Si}_3\text{N}_4$  on the substrate that is very hot. High density  $\text{Si}_3\text{N}_4$  which is usually thin and amorphous (at 0°C:  $\text{SiCl}_4 + 6\text{NH}_3 \rightarrow \text{Si}(\text{NH})_2 + 4\text{NHCl}$ ; at 1200°C:  $n\text{Si}(\text{NH})_2 \rightarrow a\text{-Si}_3\text{N}_4$ ).

#### 4.2.3 Reaction Bonding Process

Silicon is heated in a nitrogen atmosphere for obtaining the reaction bonding of  $\text{Si}_3\text{N}_4$  material.  $\text{Si}_3\text{N}_4$  material is achieved by compacting silicon powder to high density in an inert atmosphere and then heated in a nitrogen atmosphere at ~1400°C. Complex



shapes can be made using this method, but the final product has porosity of about 20% and 300Mpa flexural strength (at 1400°C:  $3\text{Si} + 2\text{N}_2 \rightarrow \alpha\text{-Si}_3\text{N}_4$ ).

### 4.3 Abrasives

Table 4.2 [Jiang, 1998] shows some of the typical abrasives used.

ABRASIVE	Hardness	
	Mohs	Knoop kg/mm <sup>2</sup>
Diamond	10	7000
Boron Carbide (B <sub>4</sub> C)	9.3	3200
Silicon Carbide (SiC)	9.2	2500
Aluminum Oxide (Al <sub>2</sub> O <sub>3</sub> )	9	2150
Chromium Oxide (Cr <sub>2</sub> O <sub>3</sub> )	8.5	1800
Silicon Nitride (Si <sub>3</sub> N <sub>4</sub> )	8.5	1600
Zirconium Oxide (ZrO <sub>2</sub> )	8	1200
Silicon Oxide (SiO <sub>2</sub> )	7	820
Cerium Oxide (CePO <sub>4</sub> )	6	-
Iron Oxide (Fe <sub>2</sub> O <sub>3</sub> )	6	-
Copper Oxide (CuO)	3.5	225

These abrasives can be classified into two groups, one for mechanical polishing and the other based on those which can used for chemo-mechanical polishing depending on their mechanical hardness. The chemical activity of the abrasive with the work material in a particular environment also influences the type of abrasive. The abrasives

that are used for mechanical polishing are those that are harder than silicon nitride as emphasis is laid on high material removal rates along with material removal to reach a specific diameter. They are fine grain size diamond, boron carbide ( $B_4C$ ), and SiC. In this case the material removal is considered by mechanical microfracture. Abrasives whose hardness is less than or equal to that of silicon nitride are used for chemo-mechanical polishing. The most common abrasives, which can be used for this purpose, are aluminum oxide ( $Al_2O_3$ ), chromium oxide ( $Cr_2O_3$ ), zirconium oxide ( $ZrO_2$ ), silicon oxide ( $SiO_2$ ), cerium oxide ( $CeO_2$ ), iron oxide ( $Fe_2O_3$ ), yttrium oxide ( $Y_2O_3$ ), and molybdenum oxide ( $Mo_2O_3$ ). Cerium oxide was found to be the most suitable ceramic for the chemo-mechanical polishing of  $Si_3N_4$  work material to improve the final surface finish.

#### **4.4 Salient features of magnetic float polishing**

Most prominent characteristics of the magnetic float technology are

1. High material removal rate
2. Excellent surface finish
3. Good sphericity
4. Very low finishing times when compared to conventional techniques
5. Minimal or no sub-surface damage is imparted to the work material
6. Gentle finishing process due to the application of low loads
7. Various parameters can be addressed in this process separately

This technique can handle small as well as large batches and is considerably faster than the conventional V-groove lapping.



#### 4.4.1 High material removal rate

Sliding at the contact region between the workpiece and the abrasives embedded in the tool is the main mechanism of material removal in polishing or lapping. The reasons due to which material removal is much more than in conventional lapping or polishing are

1. The load applied in magnetic float polishing is very low when compared to the loads encountered in lapping, due to which the frictional force at the contact region is significantly reduced, which in turn increases the sliding motion of the balls.
2. The speed in the magnetic float polishing is very high (~50 to 100 times higher) than the conventional lapping process. This increased relative speed also leads to increased sliding motion.

Experimental results show that the material removal is almost 100 times more than that of the conventional lapping.

#### 4.4.2 Good surface finish

Surface as well as sub-surface damages are avoided because the magnetic buoyant force applied during polishing is extremely small (~1N/ball) and controllable. The process of applying a softer abrasive, more commonly known as chemo-mechanical polishing, in the final stage improves the surface finish. The material removal from the ceramic balls is due to the removal of the reaction product during chemo-mechanical polishing by frictional action. The chemical reaction is mainly due to the interaction between the abrasive, the water-based slurry and the balls, thus resulting in a very smooth and a damage free surface.

#### 4.4.3 Good sphericity

The mechanism by which material is removed in lapping as well as polishing is that when balls of larger diameter or the larger diameter portion of the ball comes into contact with the contact area, then the load on that particular portion will increase and that larger amount of material will be removed from this place. The same process is repeated till a spherical surface is obtained. In case of magnetic float polishing, there are three contact points for each ceramic ball. These contact points bring about a rotation motion around the axis parallel to the contact area along with a spinning motion around the axis vertical to the contact area. The rotation motion acts as the motion for polishing and the spinning motion acts as the feed for the polishing. This combination of the rotation motion with the spinning motion during polishing causes the track around the ball to be uniform, which results in good sphericity.

#### **4.5 Evaluation of surface integration**

##### 4.5.1 Evaluation of roundness by number

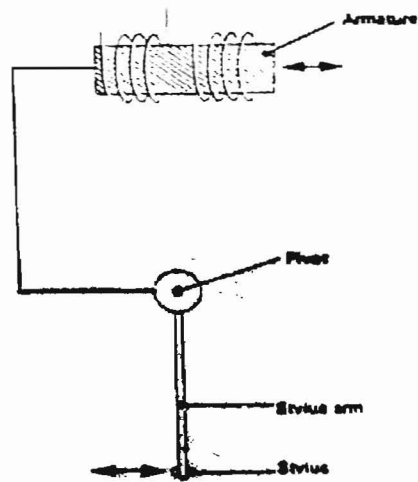
The maximum peak-to valley height (P+V) is the numerical value of the out-of-roundness. Four different circles available for this calculation. They are the least square circle (LS), the minimum zone circle (MZ), the maximum inscribed circle, and the minimum circumscribed circle (MC). Talyrond 250 is used for measuring the roundness of the balls. The least square circle is the arithmetic average of the deviations from the mean and the reference circle. The minimum zone circle consists of two concentric circles with least possible gap in-between them enclosing all the points within the two circles. Maximum inscribed circle is the largest possible circle that can be enclosed by all

the points of the reading. Minimum circumscribed circle is the smallest possible circle that encloses all the points of the measured ball.

#### 4.5.2 Talyrond 250

Talyrond 250 is a computer controlled stylus instrument manufactured by Rank Taylor Hobson Inc (UK). It has a stylus, a variable inductance pick-up (transducer) with a rotating worktable (for roundness measurement) and a vertical straightness unit (for vertical straightness measurement). Two motorized axes have been provided for measurement (the worktable and the vertical straightness unit) and one motorized axis for stylus contact. Some of the parameters that can be measured by this instrument are roundness, vertical straightness, squareness, parallelism, flatness, co-axiality, cylindricity, concentricity, eccentricity, runout. The limit of error for roundness from the worktable and the pick-up spindle is about  $0.05\mu\text{m}$ . ( $0.04\mu\text{m} + 0.0003\mu\text{m}/\text{mm}$  height over the worktable).

The deviation of the obtained spherical form the actual one is found out by rotation of the ball against the transducer with several grams gauge force. The stylus tip, a sapphire ball (diameter of 2.0mm) contacts the surface being measured, which is fixed to the rotating worktable. Minute movements are caused to the stylus due to the deviation of the measured surface. This movement of stylus is converted into variations in electric signal by using a variable inductance pick up. Figure 4.1 shows the schematic of the electronic measuring system.



*Principle of variable inductance pick-up*

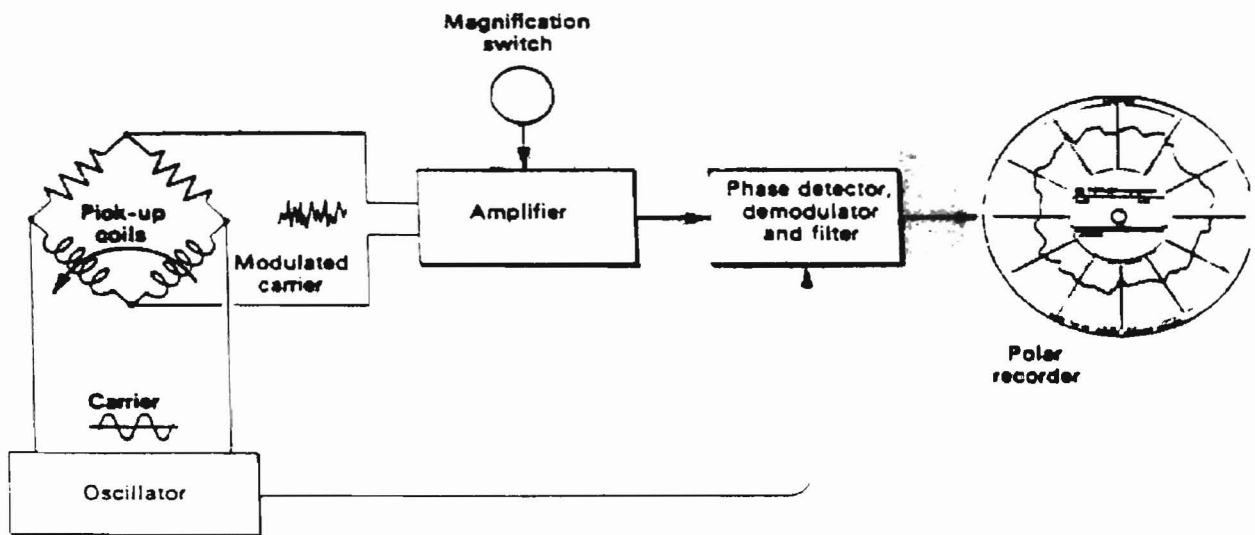


Figure 4.1 Schematic of a talysurf traverse unit laser interferometric transducer system

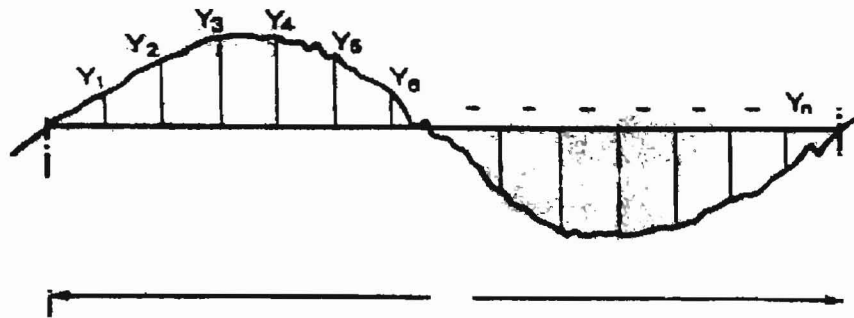
Here the variable inductance pick-up is the armature that is connected to the stylus and can move between the two coils when the stylus moves, which will alter the

inductance. The movement of the armature will unbalance the AC Bridge circuit to which the two coils are connected. This results in an output proportional to the movement and the obtained output is amplified and fed to a recorder. In order to determine the direction in which the recorder pen will move from its zero position the phase signal, which depends on the direction of movement is compared to the oscillator. A 2-stage CR networks type filter with a cut-off of 50 upr (undulations per revolutions) is used in this study. The amplitudes of irregularities with shorter wavelength remain unchanged, while the amplitudes of irregularities with longer wavelength are progressively reduced. The filter used suppresses the out-of-roundness lobes (undulations with approximately equal height and spacing) and leaves the general shape unchanged, which will result in the display of other irregularities at higher magnification.

#### 4.5.3 Evaluating the surface finish by number:

Mechanical polishing results in a surface roughness that has a more or less symmetrical profile. In the cases of fine finishing or chemo-mechanical, where the peaks are smoothed and the valleys are left intact the profile of the surface roughness might become unsymmetrical. Both Ra and Rt values are used to evaluate the surface finish. Ra represents the average roughness of the measured surface, but the information regarding the shape of the irregularities is averaged out. Rt value represents the vertical distance between the highest and lowest points in the surface profile. Figure 4.2 shows the deviation of some surface roughness parameters such as Ra and Rt. Rt can have a significant effect on the surface quality of advanced ceramic materials as they can directly represent the irregular surface defects such as scratches and pits. The cut-off

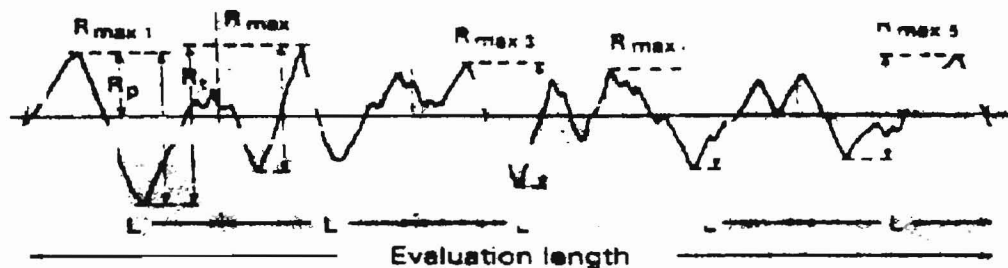
length according to the international standards (IS) is 0.25 or 0.8mm, and the evaluation length is formed by 4-6 consecutive cut-off.



*Mathematical derivation of  $R_a$  and  $R_q$*

$$R_a = \frac{|y_1| + |y_2| + \dots + |y_n|}{n}$$

$$R_q = \sqrt{\frac{y_1^2 + y_2^2 + y_3^2 + \dots + y_n^2}{n}}$$



*Derivation of some peak parameters*

- $R_{max}$  = Maximum peak-to-valley height within the sampling length  $L$
- $R_i$  = The vertical height between the highest and lowest points of the profile within the evaluation length
- $R_m$  = The mean value of the  $R_{max}$  of five consecutive sampling lengths

Figure 4.2 Deviation of  $R_a$  and  $R_t$  parameters

#### 4.5.4 Talysurf 120L

Surface finish is measured by using Rank Taylor Hobson's Talysurf 120L. This is a computer controlled stylus instrument and has a stylus laser interferometer pick-up (transducer) with a 120-mm traverse unit. A high frequency pass filter is used for measuring the surface roughness, while a low frequency pass filter is used for measuring the waviness. It has a vertical resolution of 10-nm and a horizontal resolution of 0.25- $\mu\text{m}$  for a standard conisphere diamond stylus with a tip radius of 2.0- $\mu\text{m}$ .

#### 4.6 Experimental Work

- The polishing shaft was driven using a vertical machining center (Bridgeport-Interact 412) with a stepped speed regulation in the range of 40rpm to 4,000rpm.
- The magnetic field used was measured by using a Gauss/Tesla meter.
- The polishing load was set up by adding loads on both sides of the apparatus using a pulley system, so that equal normal force can be applied on all the balls.
- The weight of the abrasives, approximately 10% of the volume of the magnetic fluid used for that particular polishing run, was found using a precision balance (Brinkmann Instruments-Resolution (0.02N)).
- The ball diameter, after each run was measured using a digital micrometer from Mitutoyo (resolution: 1 $\mu\text{m}$ ).
- The full characterization of the bearing balls is required. This includes the size variation, the specific diameter, sphericity, and surface finish. In the big batch of 55 balls the sample size was decided at 15 balls. Each ball is traced three times in approximately three orthogonal planes.

- The size variation is found out in the sample size using a comparator and comparing the polished balls against a standard ball.
- The sphericity or the roundness values are measured by using Talyrond 250 and the surface roughness is measured using 120L. The ABMA defines the sphericity of the ball as the maximum value of roundness measured on the three orthogonal planes of the ball. In the same way, the surface finish of each ball is taken as the maximum value of three traces along the three orthogonal planes of the ball.
- The sphericity was measured using Talyrond 250 (Filter: 2CR, Cutoff: 50 $\mu$ m). The out-of-roundness trace measures the maximum departure from a true circle, which in turn is denoted as its roundness.
- The surface finish of the polished balls was measured using a Talysurf 120L (Filter: 2CR, Cutoff: 0.25 mm or 0.8 mm, Evaluation length: 4-6 consecutive cut-off, Filter ISO 2CR).



## Chapter 5

### Methodology of Magnetic float polishing (MFP)

This chapter presents the methodology behind the use of magnetic float polishing involving mechanical and chemo-mechanical polishing in the finishing of advanced ceramic balls. This process basically consists of three stages, a roughing, a semi-finishing stage, and a final finishing stage. Roughing stage is one in which harder abrasives (with respect to the work materials) are used for achieving a high removal rate followed by a semi-finishing stage in which abrasives of progressively lower grain size are used. The finishing stage employs chemo-mechanical polishing (CMP) to achieve very good surface finish. CMP results in superior surface finish with minimal or no surface or sub-surface defects, such as cracks, micro-cracks, or pits on the silicon nitride balls. Material removal rates as high as  $1\mu\text{m}$  have been obtained in this process with minimal subsurface damage by using harder abrasives, such as  $\text{B}_4\text{C}$ , and  $\text{SiC}$ . The absence of surface or sub-surface damage is mainly due to the use of a flexible support system, and the use of low loads and high speeds. Final polishing of  $\text{Si}_3\text{N}_4$  balls, using  $\text{CeO}_2$  (that chemo-mechanically reacts with work  $\text{Si}_3\text{N}_4$  work material) results in high quality balls with superior surface finish ( $R_a < 5\text{nm}$ ,  $R_t < 40\text{nm}$ ). CMP is very effective for obtaining good surface finish on  $\text{Si}_3\text{N}_4$  work material and cerium oxide has been found to be the most suitable abrasive for CMP. Balls of a wide range of diameters ( $7/32''$ ,  $9/32''$ ,  $11/32''$ , and  $13/32''$ ) have been finished to a superior surface finish successfully using this process.

## 5.1 Equipment for MFP

The magnetic hydrodynamic behavior of the slurry used (abrasives suspended in magnetic fluid) is utilized for magnetic float polishing. A very low and controllable force (~1N) is applied by the abrasive on the part. The magnetic field is applied by using a bank of permanent magnets (Nd-Fe-B, Residual magnetization) with alternate N and S poles arranged below an aluminum float chamber. The abrasives are usually 5-10% of the magnetic fluid by volume. A colloidal dispersion of extremely fine (100 to 150 Å) ferromagnetic particles, usually magnetite ( $\text{Fe}_3\text{O}_4$ ), in a carrier fluid such as water or kerosene, is used as the magnetic fluid. The magnetic fluid used is water based (W-40, saturation magnetization at 25°C: 400 Gauss and viscosity at 25°C). The magnetic particles are pulled downward on applying the magnetic field, which results in the application of a buoyant force in the upward direction on all the non-magnetic particles, which in turn pushes them to the area of lower magnetic field. The ceramic balls, the float, and the abrasives all being non-magnetic float inside the chamber due to the upward buoyant force. A drive shaft is lowered to make contact with the balls in order to press the balls, so that they reach a desirable height or a level of force. Three-point contact is established when the ball is held between the float, the chamber wall, and the drive shaft. The abrasive grains under the action of the magnetic buoyancy polish the balls in this position as the spindle rotates. The flexible float helps in applying uniform low loads (~1N), which in turn results in producing a damage free surface on the ceramic balls. Larger and more uniform polishing pressure results due to the use of acrylic float (larger buoyancy force near the magnetic poles can be transmitted to the polishing area by use of this float). In order to protect the inner guide ring from wear, a urethane rubber

sheet is bonded on to it. Figure 5.1 shows the magnetic float polishing apparatus for finishing a small batch of advanced ceramic balls. Figure 5.2 is modification of this apparatus used for polishing a large batch of balls.

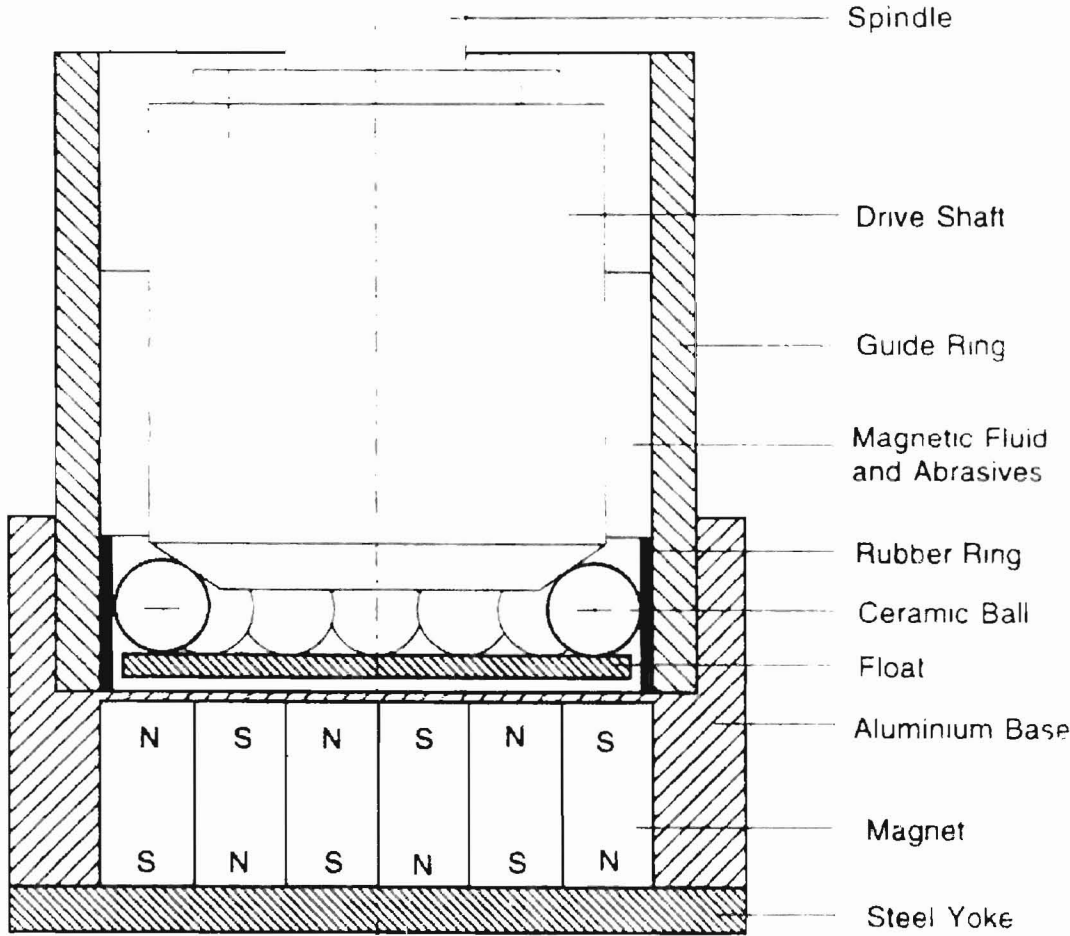


Figure 5.1 Schematic of apparatus for MFP of a small batch of advanced ceramic balls

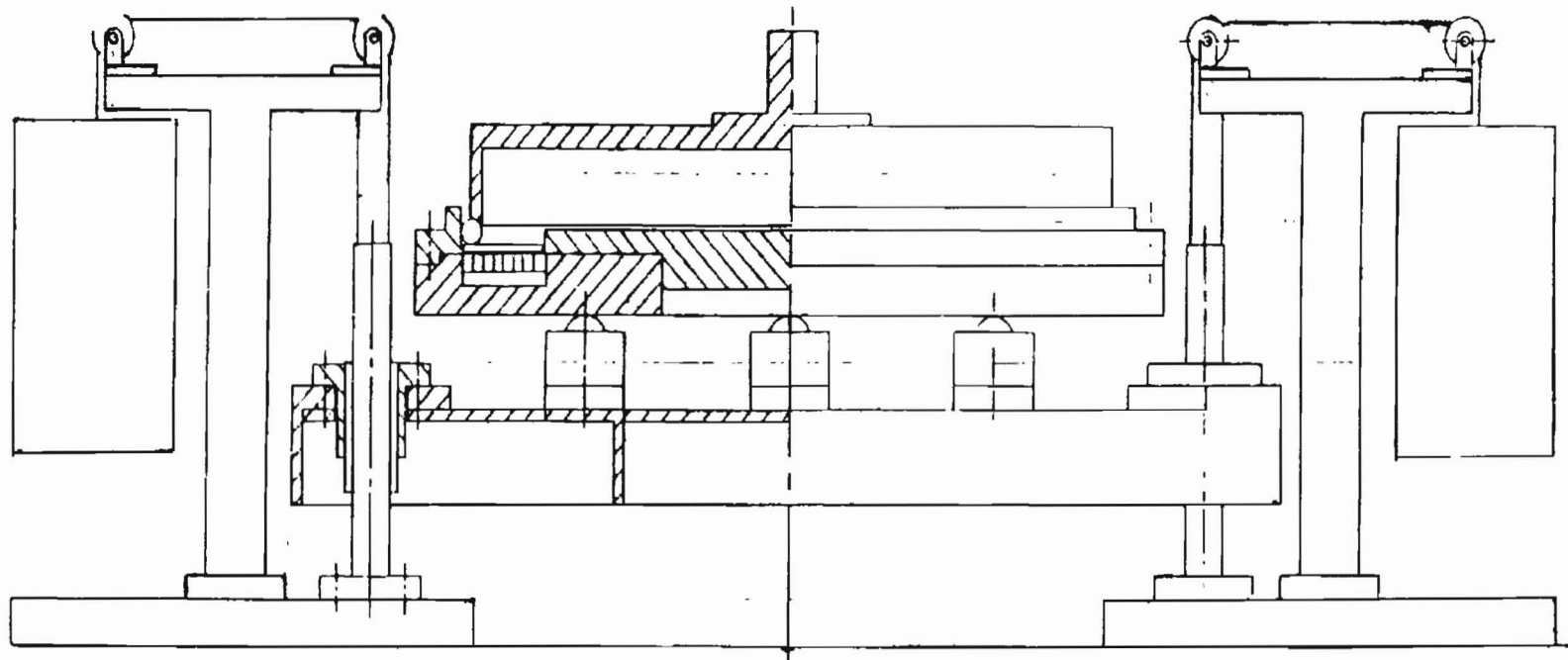


Figure 5.1 Apparatus for MFP of a large batch of advanced ceramic balls [Komanduri, Umehara, Jiang, and Cao, 1998]

## 5.2 Mechanical polishing

In magnetic float polishing abrasives of decreasing hardness and of decreasing grit size are used in order to control the material removal, the sphericity and the surface finish. The mechanism by which material removal takes place in case of  $\text{Si}_3\text{N}_4$  is by micro-fracture because of higher hardness of the abrasive and the inherent brittleness of the work material. In this case the material removal occurs by micro-fracture due to cleavage and not due to grain pullout, grains fracture, and large fracture. Also in case of magnetic float polishing, unlike conventional polishing where high loads and low speeds are used, low loads and high speeds are used. These reasons along with a very flexible system prevent any occurrence of sub-surface or surface damage.

## 5.3 Chemo-mechanical polishing (CMP)

As mentioned earlier the mechanism of material removal in the final stages of polishing is by chemical action of the softer cerium oxide ( $\text{CeO}_2$ ) with the  $\text{Si}_3\text{N}_4$  work material. Jiang (1998) suggested the possibility of CMP of  $\text{Si}_3\text{N}_4$  by  $\text{CeO}_2$  by considering the thermal analysis of flash temperature and the flash duration encountered during the polishing process. The main function of  $\text{CeO}_2$  is that it performs the CMP by participating directly in the chemical reaction (oxidation-reduction reaction) with the  $\text{Si}_3\text{N}_4$  work material leading to the formation of  $\text{SiO}_2$ . The heat from the chemical reaction is generated from the friction between the polishing shaft and the balls when rotating at higher speeds.  $\text{CeO}_2$  is harder than  $\text{SiO}_2$ , but significantly softer than  $\text{Si}_3\text{N}_4$ . So it is able to remove the brittle layer of  $\text{SiO}_2$  product on the surface of  $\text{Si}_3\text{N}_4$  effectively without damaging the  $\text{Si}_3\text{N}_4$  substrate due to abrasion. The flowing of water and  $\text{CeO}_2$

provide the kinetic action which removes the removal of reaction products from the interface. The CMP by  $\text{CeO}_2$  on  $\text{Si}_3\text{N}_4$  results in the formation of an outer layer of  $\text{SiO}_2$  and an intermediary layer of silicon oxinitride ( $\text{Si}_x\text{O}_y\text{N}_z$ ) on the top of the silicon nitride substrate. Thus, the tribo-chemical action instead of the mechanical fracture is the main reason for the extremely smooth and damage free surfaces accomplished on the  $\text{Si}_3\text{N}_4$ .

## Chapter 6

### Optimum Polishing Conditions in MFP of A Large Batch of Silicon Nitride Balls Using the Taguchi Approach

#### 6.1 Introduction

Various parameters that affect the quality of ceramic balls finished by the MFP process, include the magnetic field strength, the workmaterial, the abrasive used (material and grain size), the rotational speed of the shaft, the type of the magnetic field used (water based or hydrocarbon based), the % volume of the abrasive in the magnetic field, and the stiffness of the system. Three parameters are considered to be of major influence on the surface quality for a given abrasive-workmaterial combination [Jiang, 1998]. These parameters are namely, (1) the polishing force, (2) the abrasive concentration, (3) and the polishing speed. One of the important factors that influence the sphericity of balls is the uniformity of the groove formed on the float. Table 6.1 [Jiang, 1998] shows the conditions for finishing a small batch (13 balls) of 0.5" silicon nitride ( $\text{Si}_3\text{N}_4$ ) balls. Table 6.2 shows the properties of the abrasives used for this purpose. Since the weight of the balls in the larger batch (55 balls) polished is very much higher ( -4 times) than that of the small balls, optimal loading and speed conditions have to be found out in order to maintain the uniformity of the grooves in the roughing stage and the sphericity in the intermediate finishing stage. The polishing force applied, the polishing speed used, and the abrasive and its grit size used have been identified as the most critical variables in this case. This chapter mainly focuses on finding the optimal loading and speed conditions for polishing of a large batch of silicon nitride ( $\text{Si}_3\text{N}_4$ ) balls (0.5").

Table 6.1 Conditions for finishing a small batch (13 balls) Si<sub>3</sub>N<sub>4</sub> balls (0.5")

Stage	Abrasive		Abrasive Vol %	Speed rpm	Load N/ball	Time Hrs	Remarks
	Type	Grit Size					
1	B <sub>4</sub> C	500	10	3000	1.0	1.0	Roughing
	SiC	800	10	3000	1.0	1.0	
2	SiC	1000	10	3000	1.0	1.0	Semi-finishing
	SiC	1200	10	3000	1.0	1.0	
3	B <sub>4</sub> C	1500	10	3000	1.0	1.0	Final Finishing
	CeO <sub>2</sub>		10	3000	1.0	1.0	

Table 6.2 Abrasives used and their properties

Abrasive	Density g/cm <sup>3</sup>	Knoop Hardness Kg/mm <sup>2</sup>	Elastic modulus Gpa	Melting Point °C
B <sub>4</sub> C	2.52	2800	450	2450
SiC	3.2	2500	420	2400
CeO <sub>2</sub>	7.13	625	165	2500

The polishing machine is driven by a vertical machining center (Bridgeport NC m/c) with stepped speed regulation up to 4000 rpm. The magnetic field is measured by using a Gauss/Tesla meter. Adding loads on both sides of the pulley system already



provided set up the polishing load. In order to calculate the material removal rates, the weight reduction in the balls was measured along with the diameter of the balls after each step, which also give an indication of the material removal. The surface finish of the balls was measured using a Form Talysurf 120L (cut-off: 0.8mm, evaluation length: 6 consecutive cut-off, Filter: ISO 2CR), while the roundness was measured using Talyrond 250 (cut-off: 50 upr, filter: 2CR). Test conditions used are shown in Table 6.3.

Table 6.3 Test Conditions used

<b>Workmaterial</b>	<b>Uni-axially pressed Si<sub>3</sub>N<sub>4</sub> Balls (CERBEC)</b>  <b>Diameter : 12.7 mm (0.5")</b>  <b>Initial Sphericity : ~20 μm</b>
Abrasive	Type: B <sub>4</sub> C, SiC  Grit Size: 500, 800, 1000
Load, N/ball	2.0, 3.0, and 4.0
Speed, rpm	100, 200, and 300
Test time	1 hr./run
Magnetic Fluid	Water-based (W-40)  Saturation Magnetization at 25°C: 400 Gauss  Viscosity at 27°C: 215 Cp

## 6.2 Experiments design using Taguchi Approach

Investigation of the optimum loads and speeds for magnetic float polishing can be done using several approaches. Fisher [1971] used the single-factor approach in which only one factor was changed for a given trial run. The number of experiments needed to perform decreases as transition is made from a single-factor approach to the fractional factorial design and then to the Taguchi method [Taguchi, 1992].

Taguchi method can extract information more efficiently and more precisely compared to a single-factor by the single-factor approach. Another major advantage is that only a few number of tests are needed even in the case of large number of variables. Roy (1990), Barker (1990), Ross (1996) have shown that fractional factorial experimental design yields the same or even better results in terms of precision compared to single-factor by single-factor approach. Taguchi method overcomes most of the limitations faced by the traditional methods. A full factorial design of experiments will include all possible combination settings of the factors involved in the study resulting in a very large number of trial runs and considerable time to accomplish the task. A small fraction of the setting that produces most information from all possible combinations is selected in order to simplify the experimental effort and thus reduce the number of tests to an acceptable level. This is known as fractional-factorial design of experiments. As this method lacks proper guidelines, the experimental design and analysis of the results tend to be complex. These limitations are overcome in the Taguchi method as it simplifies and standardizes the fractional-factorial designs by developing a set of standard orthogonal arrays (OA) that can be used for many experimental situations. The method has very good consistency and reproducibility.

Taguchi developed this method in Japan after World War II, which is highly effective in the determination of optimal values for various parameters involved in a given manufacturing system. This investigation has mainly focussed on the formulation of the experiments for optimizing the load and speed conditions in the polishing of ceramic balls, rather than using it for performing a statistical analysis.

### 6.3 Approach

Each of the critical factors is considered at 3 levels to determine the optimum settings for the polishing process. The smallest, standard 3-level orthogonal array  $L_9 (3^4)$ , which has four 3-level columns, is chosen for this case. The factors for this particular case are given in the Table 6.4.

Table 6.4 Parameters used in the Taguchi method

Level	Parameters		
	A: Load	B: Speed (rpm)	C: Abrasive and Size
1	2.0N	100	B <sub>4</sub> C (500)
2	3.0N	200	B <sub>4</sub> C (800)
3	4.0N	300	B <sub>4</sub> C (1000)

#### 6.3.1 Design of the orthogonal array (OA)

The term orthogonal represents the balance present and the ability to be separated easily. Orthogonal arrays are generalized from Graeco-Latin squares. The French mathematician, Jacques Hadamard developed OA, in the 1890s.

The main functions of the mathematical arrays are

1. Any two columns of an orthogonal array form a two factorial complete design due to the pairwise balancing property of the orthogonal arrays. Averaging of the responses facilitates in offsetting the effects of one parameter on the parameter level of the one being studied. This means that all the parameters are separable from one another. This facilitates the determination of the contribution and optimum level of the each factor considered.
2. The orthogonal array (OA) technique uses the pairwise balancing property and minimizes the number of test runs to only nine in case of an experiment with a factor of 3. Table 6.5 (Ming, 1998) shows the OA with 9 rows, where each row represents a trial condition with factor levels indicated by the numbers in the row. The vertical columns correspond to the factors specified in the study and each column contains three levels 1, 2, and 3. The nine possible combinations for each column are (1,1), (1,2), (1,3), (2,1), (2,2), (2,3), (3,1), (3,2), and (3,3).

### 6.3.2 Experimental Design

Table 6.6 gives the details of the experimental design and the approach. The factors that are under consideration are load (N), the polishing shaft speed (rpm), and the abrasive used. This form the first three columns of the OA leaving the fourth and fifth column D and E open (and are designated for uncontrolled or unknown parameters in the process under study). These parameters are the roundness (sphericity) in  $\mu\text{m}$ , measured used the Talyrond 250 and the deflection in the groove of the spindle and the float, measured by a dial gauge. In Table 6.6, the vertical columns represent the levels of the polishing parameters specified in the study and each row represents a trial condition.

Table 6.5 L<sub>9</sub> (3<sup>4</sup>) Orthogonal arrays used

No.	Factors Investigated				Test Results
	A	B	C	D	
1	1	1	1	1	
2	1	2	2	2	
3	1	3	3	3	
4	2	1	2	3	
5	2	2	3	1	
6	2	3	1	2	
7	3	1	3	2	
8	3	2	1	3	
9	3	3	2	1	

Table 6.6 Design of Experiment

No.	Factors Investigated			Test Results
	Load (N)	Speed (rpm)	Abrasives and Sizes	
1	2.0	100	B <sub>4</sub> C (500)	
2	2.0	200	B <sub>4</sub> C (800)	
3	2.0	300	B <sub>4</sub> C (1000)	
4	3.0	100	B <sub>4</sub> C (1000)	
5	3.0	200	B <sub>4</sub> C (500)	
6	3.0	300	B <sub>4</sub> C (800)	
7	4.0	100	B <sub>4</sub> C (800)	
8	4.0	200	B <sub>4</sub> C (1000)	
9	4.0	300	B <sub>4</sub> C (500)	

## 6.4 Evaluation of the experimental design results

The experiments conducted are evaluated on the basis of the uniformity of the grooves formed on the spindle as well as on the float. A groove formed on the spindle can be considered to be uniform if the deflection throughout the groove is less than a unit deflection on the dial gauge, which is 1mm. The sphericity of the polished balls reflects the state of the groove. All the trials were run for duration of one hour.

### 6.4.1 Evaluation and discussion of each trial run

A qualitative evaluation of the polishing conditions has been made based on quality of the groove on the float and the deflection of the groove on the polishing spindle.

#### Trial 1:

The conditions used for this trial run were a load of 2.0 N, a speed of 100 rpm, and B<sub>4</sub>C (500) abrasive. Figure 6.1(a) shows the acrylic (Plexiglas) float after the polishing run. It can be seen that the groove on the float is highly non-uniform. There are some parts of the groove that are uniform followed by grooves in the form of bulges. In an ideal polishing run, the balls are subjected to both sliding motion and rotational motion [Childs, 1994]. As the load and the speed are less, the balls are subjected to an unwanted dragging motion. This state of the polishing is reflected by the deflection in the groove, which is in the range of 3.75 mm. This value of deflection is very high, compared to the required value of 1 mm. The sphericity of these balls is in the range of 2.50 - 3.15  $\mu\text{m}$ .

Trial 2:

The conditions used are : load of 2.0 N, speed of 200 rpm, and B<sub>4</sub>C (800) abrasive. In this case the speed is increased to 200 rpm, with a load of 2.0 N. Figure 6.1(b) shows the condition of the float after the second trial run. The condition of the groove in this case was almost similar to that of the float in the first run, even though the speed is increased to 200 rpm. The deflection of the spindle is in the range of 4.0 mm. This observation also indicated the presence of the undesirable dragging motion of the balls on the float, rather than the smooth combination of sliding and rolling motion. The sphericity of these balls is in the range of 2.65 - 3.0  $\mu\text{m}$ .

Trial 3:

The conditions used are : load of 2.0 N, speed of 300 rpm, and B<sub>4</sub>C (1000) abrasive. To investigate the effect of speed at the same load, a speed of 300 rpm is used. Figure 6.1(c) shows the condition of float after the third trial run. The deflection of the spindle is in the range of 3.5. In order to overcome the effect of dragging, the load and the speed has to overcome the effect of the weight of the balls on the polishing. The sphericity of these balls is in the range of 2.50 - 2.95  $\mu\text{m}$ .

Trial 4:

The conditions used are : load of 3.0 N, speed of 100 rpm, and B<sub>4</sub>C (1000) abrasive. In order to impart proper rolling and sliding motion to the balls, which is represented by the groove on the float, the load is increased to 3.0 N. Figure 6.1(d) shows the condition of float after the fourth trial run. In this case, the groove formed on the float is almost uniform, except for two or three bulges on the float groove. The

deflection of the spindle is in the range of 1.85 mm. The sphericity of these balls is in the range of 2.15 - 2.50  $\mu\text{m}$ .

Trial 5:

The conditions used are : load of 3.0 N, speed of 200 rpm, and  $\text{B}_4\text{C}$  (500) abrasive. Figure 6.1(e) shows the condition of float after the fifth trial run. The condition of the groove in this case is very uniform; a deflection in the range of 0.8 mm on the spindle groove also reflects this uniformity. The sphericity of these balls is in the range of 1.70 - 2.0  $\mu\text{m}$ .

Trial 6:

The conditions used are : load of 3.0 N, speed of 300 rpm, and  $\text{B}_4\text{C}$  (800) abrasive. Figure 6.1(f) shows the condition of float after the sixth trial run. The groove on the float almost resembles the groove obtained by the sixth trial run. The deflection in the range of 1.05 mm on the spindle groove also reflects this uniformity. The sphericity of these balls is in the range between 1.80 - 2.05  $\mu\text{m}$ .

Trial 7:

The conditions used are a load of 4.0 N, speed of 100 rpm, and  $\text{B}_4\text{C}$  (800) abrasive. Figure 6.1(g) shows the condition of float after the seventh trial run. The groove formed on the float is highly non-uniform and shows the formation of pits at regular interval. The deflection on the groove of the spindle is in the range of 4.5 mm. The sphericity of these balls is in the range of 3.5 - 3.95  $\mu\text{m}$ .



Trial 8:

The conditions used are : load of 4.0 N, speed of 200 rpm, and B<sub>4</sub>C (1000) abrasive. Figure 6.1(h) shows the condition of float after the eighth trial run. The groove is highly non-uniform with pits deeper than those found in the seventh one. The deflection on the groove of the spindle is in the range of 5.0 mm. The sphericity of these balls is in the range of 4.0 - 4.35  $\mu\text{m}$ .

Trial 9:

The conditions used are : load of 4.0 N, speed of 300 rpm, and B<sub>4</sub>C (1000) abrasive. Figure 6.1(i) shows the condition of float after the eighth trial run. The condition of the groove on the float is very similar to the condition after the eighth run. The deflection on the groove of the spindle is in the range of 5.0 mm. The sphericity of these balls is in the range of 4.0 - 4.4  $\mu\text{m}$ . The formation of the pits on the float is mainly due to overload, due to which the motion of the ball is restricted. Table 6.7 shows the results of the trial runs, based on the Taguchi method.

From the runs performed under various conditions it can be inferred that the conditions of Runs 5 and 6 produce balls of good roundness. The deflection of the polishing spindle groove was within the allowable level and the groove formed on the float is uniform for these two conditions. In the case of the Run 5, the material removal was 35  $\mu\text{m}$  for a polishing run time of one hour. In the case of the Run 6, the material removal was 15  $\mu\text{m}$  for the same polishing time. As the material removal rate is high for the conditions chosen in the Run 5, they are chosen for the initial roughing stage. In case of the Run 6, as the material removal rate is comparatively low, it is employed for the intermediate finishing stage. The sphericity is further improved in the intermediate

finishing stage by decreasing the grit sizes and by using SiC [Raghunandhan, 1997]. Polishing using the same conditions as in Run 6 are used for finishing the large batch (55 balls) Si<sub>3</sub>N<sub>4</sub> balls, except that chemo-mechanical polishing is employed using a much softer CeO<sub>2</sub> [Jiang, 1998].

Table 6.7 Results of the trial runs

No.	Factors Investigated			Test Results		
	Load (N)	Speed (rpm)	Abrasives	Float Groove	Deflection, mm (Polishing spindle)	Avg. Sphericity (μm)
1	2.0	100	B <sub>4</sub> C (500)	Non-uniform	4.0	2.67
2	2.0	200	B <sub>4</sub> C (800)	Non-uniform	3.75	2.72
3	2.0	300	B <sub>4</sub> C (1000)	Non-uniform	3.5	2.72
4	3.0	100	B <sub>4</sub> C (1000)	Non-uniform (bands of different sizes)	1.85	2.32
5	3.0	200	B <sub>4</sub> C (500)	Highly uniform	0.8	1.85
6	3.0	300	B <sub>4</sub> C (800)	Highly uniform	1.05	1.92
7	4.0	100	B <sub>4</sub> C (800)	Non-uniform (with pits and gouges)	4.5	3.72
8	4.0	200	B <sub>4</sub> C (1000)	Non-uniform (with pits and gouges)	5.0	4.17
9	4.0	300	B <sub>4</sub> C (500)	Non-uniform (with pits and gouges)	5.0	4.2

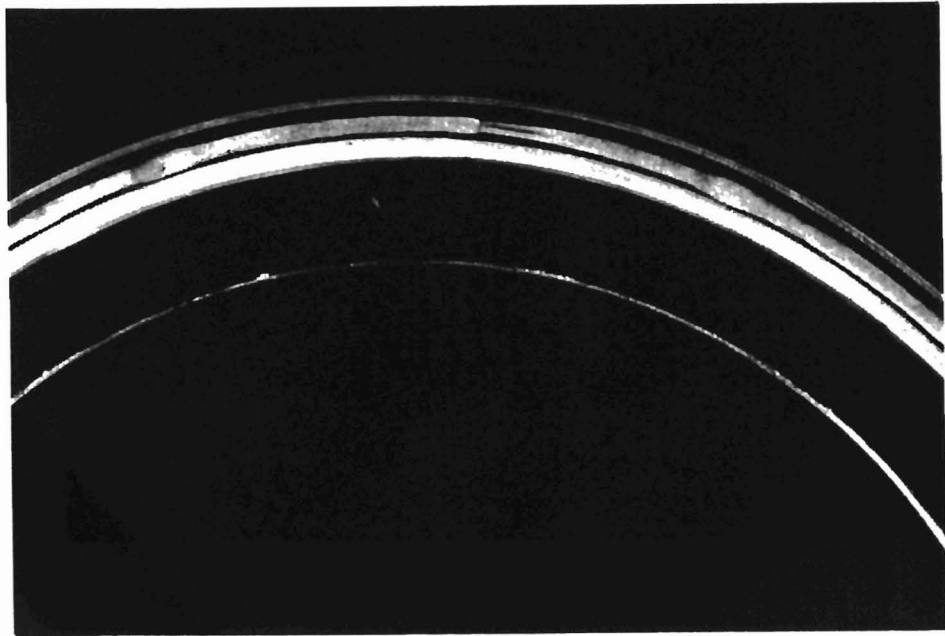


Figure 6.1(a)

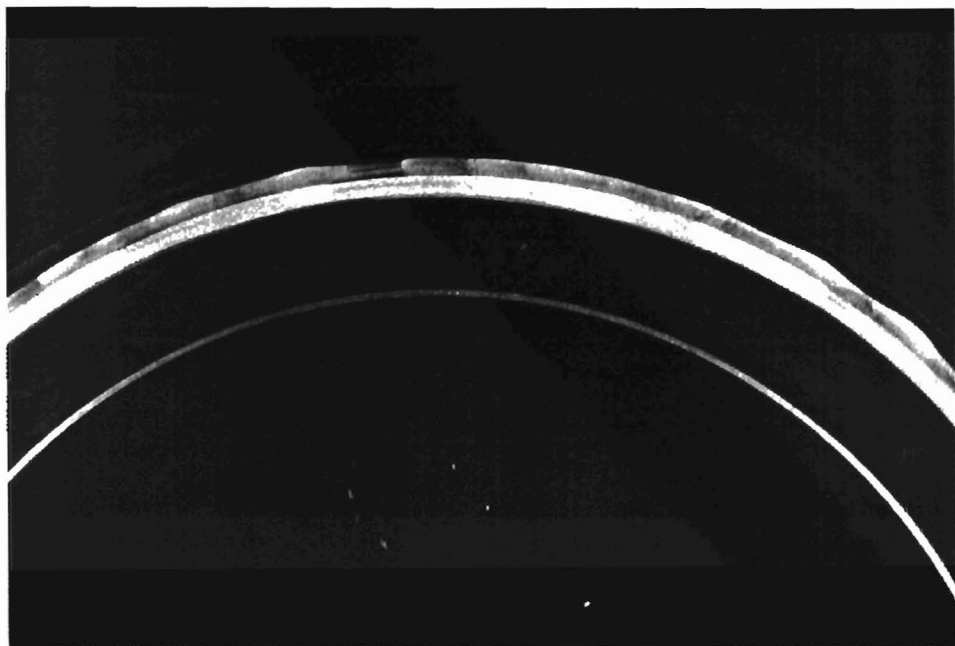


Figure 6.1(b)

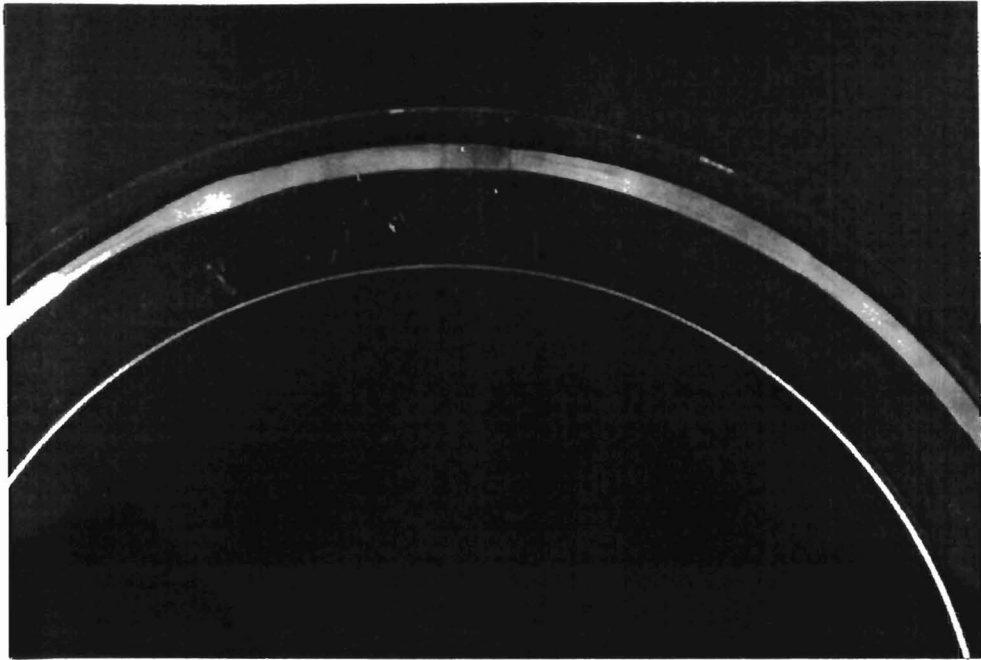


Figure 6.1(c)

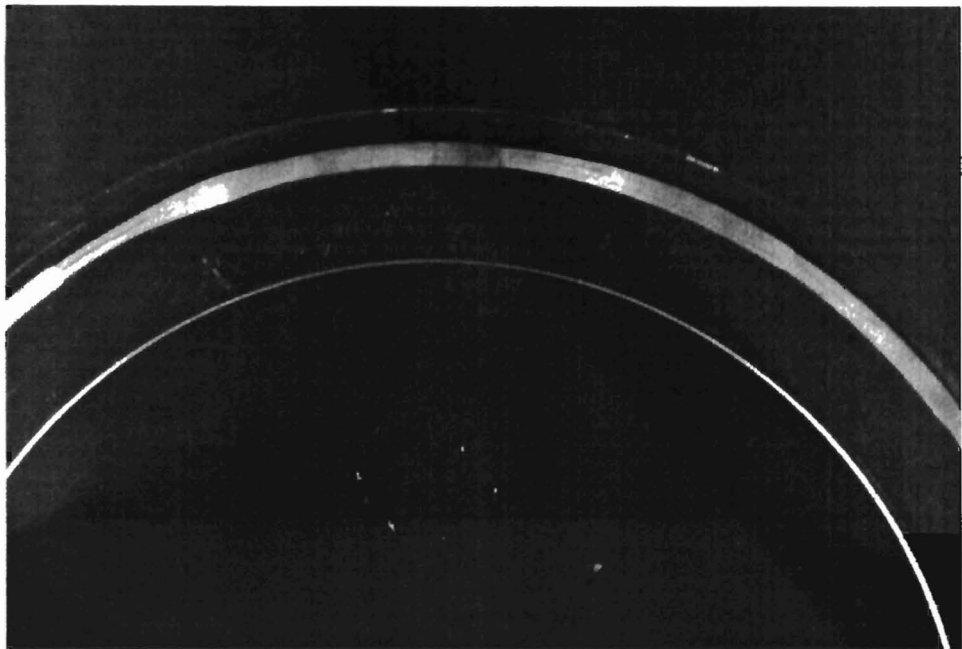


Figure 6.1(d)

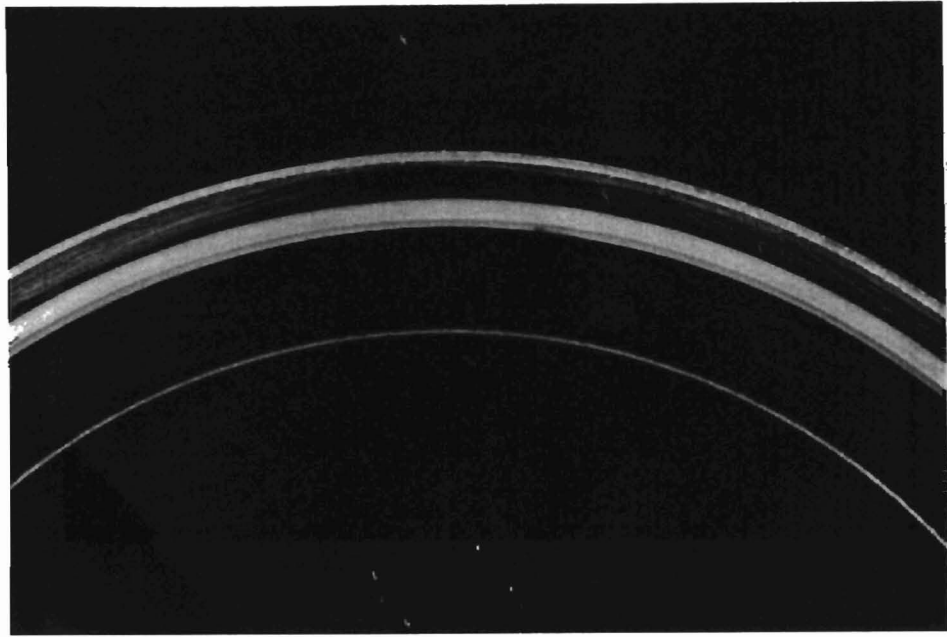


Figure 6.1(e)

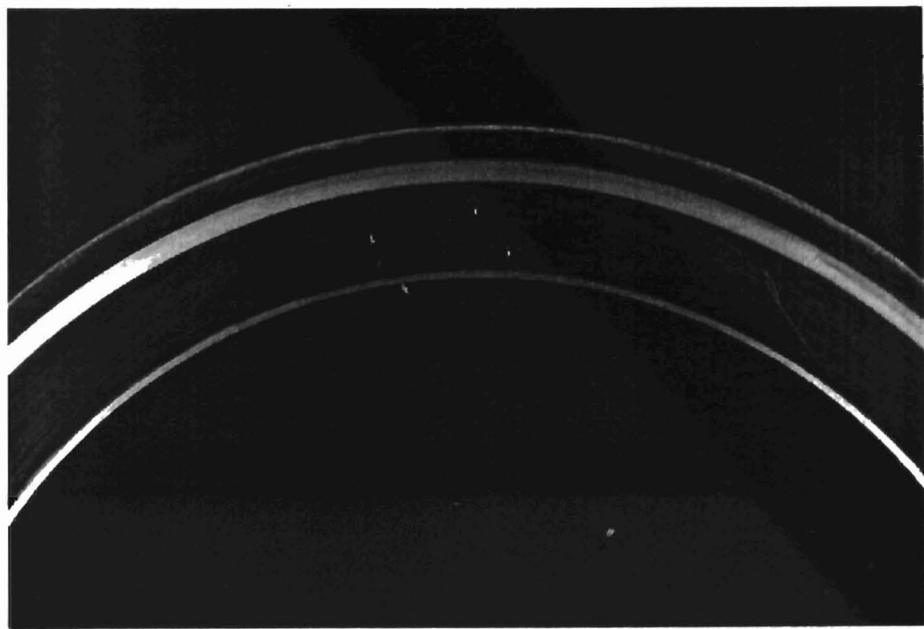


Figure 6.1(f)

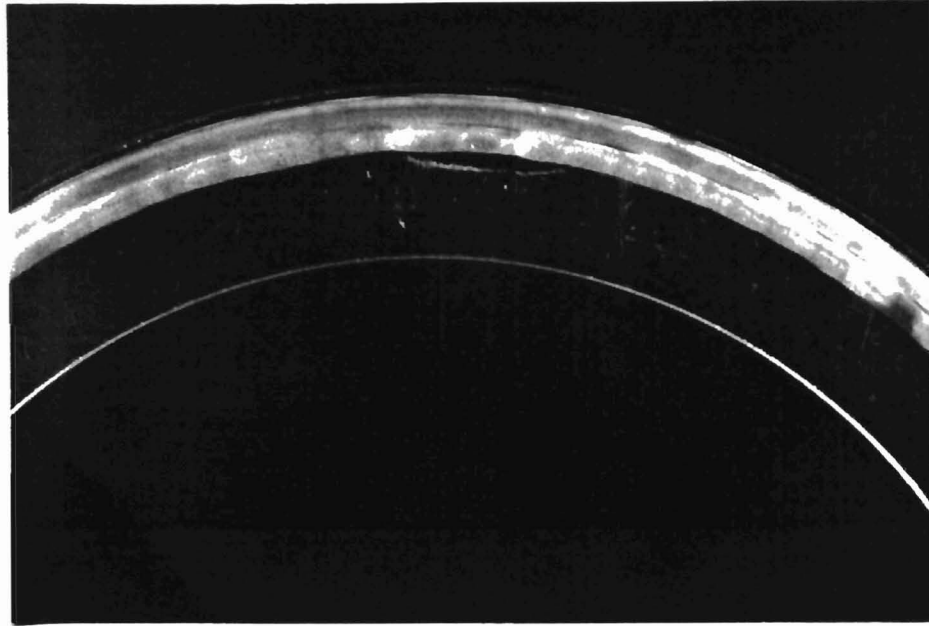


Figure 6.1(g)

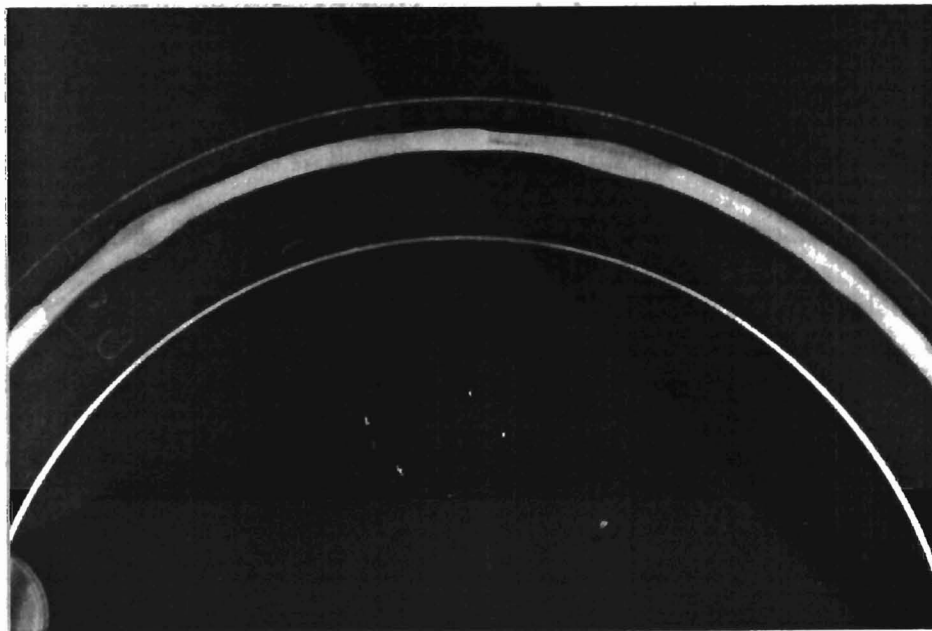


Figure 6.1(h)

## Chapter 7

### Experimental Setup of Apparatus and Process Time

Finishing of silicon nitride ( $\text{Si}_3\text{N}_4$ ) bearing balls using magnetic float polishing is a precision manufacturing process. Several factors affect the achieving of good sphericity in the polishing of ceramic balls, including coaxiality of the polishing shaft with the chamber and the drive shaft, the accuracy with which the shaft and chamber had been manufactured, and the groove on the polishing shaft. Out-of-roundness and surface finish are the most important parameters that affect the precision of the polished balls.

#### 7.1 Out-of-roundness

In the MFP process, when larger diameter portions of the ball enter the contact area, the load will increase and a larger amount of material is removed from that point. This process continues till all the peaks disappear, resulting in improved sphericity.

Geometrical accuracy as well as relative positional accuracy of the main parts of the apparatus used for polishing determines the accuracy of the apparatus. The geometric accuracy depends on the accuracy of the high speed spindle used. The relative positional accuracy depends on the adjustment and set-up of the apparatus used in the polishing process. Regarding polishing and set-up accuracy, maintaining coaxiality between the rotational axis of the polishing shaft and the polishing guide ring of the MFP apparatus is one of the most important criteria. In the following, these details are discussed briefly.

1. The geometrical accuracy of the main parts of the apparatus

- a. Out-of-roundness of the cylindrical surface of the polishing shaft.
- b. Out-of-roundness of the internal cylindrical surface of the chamber.

The geometrical accuracy depends upon the spindle rotational accuracy of the turning machine used for the fabrication of the chamber and the shaft, especially the inaccuracies in the spindle bearing, stiffness and thermal deformations.

The abrasive wear of the polishing shaft, the polishing float, and the urethane rubber ring during the polishing lead to improper polishing motion of the ball and can result in sphericity degradation. They should be re-machined or replaced periodically.

## 2. Relative positional accuracy of the apparatus

- a. The rotational axis should be perpendicular to the end surface of the shaft, which is the reference surface of the shaft to the drive spindle so that the additional inaccuracies in the rotational motion can be minimized.
- b. The rotational axis tapered should be coaxial with the polishing surface of the shaft. The machining of shaft cylindrical and conical polishing surfaces should be accomplished using one chuck mounting while taking the end surface as axial machining reference, in order to satisfy the above mentioned requirements, i.e., (a) and (b), during final precision machining stages. To re-machine the conical polishing surface after wear, the shaft axis should be set up to be coaxial to the lathe axis by taking the cylindrical surface of the shaft, as the reference.
- c. The axis of the chamber wall should be perpendicular to the chamber base. Polishing chamber is used not only for containing the polishing fluid, but also for guiding the ball track as a guide ring. To preserve relational integrity, the machining of chamber



should be done within one chuck mounting (without removing the work-piece from the lathe chuck) to machine ID and OD of the chamber for their concentricity and machine the end surface, to make perpendicularity of the end surface with respect to the chamber walls, which is the reference surface to ensure the chamber walls are perpendicular to the chamber base.

3. Coaxiality of the polishing shaft with chamber and the drive spindle
  - a. Coaxiality between drive spindle and polishing shaft: When the shaft is re-mounted to the drive spindle after the periodical re-machining, great care must be used to align the shaft axis with the drive axis. It is preferred to re-grind the shaft, without removing the shaft from the spindle by setting up a grinding unit.
  - b. Coaxiality between polishing shaft and polishing chamber: The mounting eccentricity between polishing shaft and polishing guide ring should be avoided. The improper setup or inadequate setup accuracy with even very small eccentricity is the main reason for the low sphericity. Figure-7.1 shows a typical triangle shape of a  $\text{Si}_3\text{N}_4$  ball due to eccentricity between the polishing drive shaft and the guide ring.

The purpose of the above mentioned requirements is to keep the coaxiality between the rotational axis of the polishing shaft and the polishing guide ring. This is the most frequent problem that causes poor sphericity results.

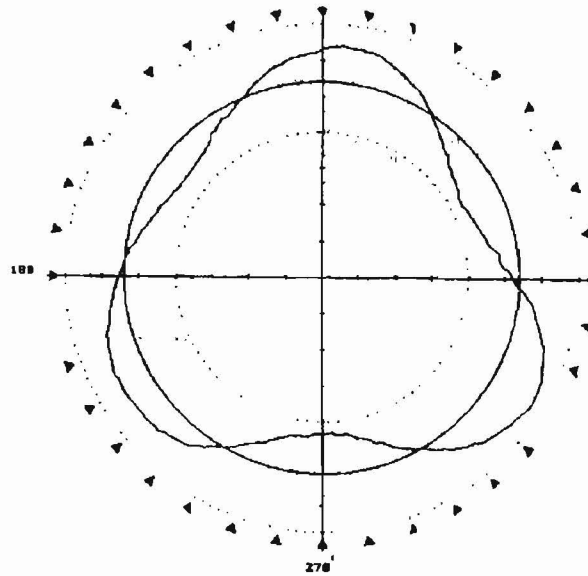


Figure 7.1 A typical eccentric  $\text{Si}_3\text{N}_4$  ball with 3 lobes

## 7.2 Surface finish

The methodology of fine mechanical polishing followed by chemo-mechanical polishing (CMP) is critical for obtaining excellent surface finish of advanced ceramic balls in the MFP process.

## 7.3 Set up of the apparatus

Magnetic float polishing is always done in a number of runs. For each polishing run the apparatus has to be set up, i.e., the polishing chamber has to be aligned with the polishing shaft or the spindle in such a way that they are coaxial. The setting up process is manual and is always subject to human error, irrespective of the accuracy and the care taken to perform it. Even a slight parallax error can cause the setting to be eccentric to the axis of the polishing shaft. This slight eccentricity in setting can cause the balls to contact

the tapered surface, higher on the one side and lower on the other side. Due to this reason, the axis of the groove gets inclined to the axis of the polishing spindle, subjecting the balls to alternate high and low loads, during rotation at high speed. This worsens the sphericity of the balls, when compared to the sphericity before polish. This results in enormous wastage of material, labor, and polishing time. Analyzing the frequency spectrum during the polish can validate the polishing setup and the occurrence of the excitation frequency in which all the elements of the polishing apparatus are in harmony indicating good set up [Srihari, 1999]. A vibrometer connected to the polishing chamber can be used for measuring these vibrating frequencies and a conclusion can be achieved of whether or not a particular polish is a good one or not.

### **7.3.1 Repeatability of the set up**

As mentioned earlier the set up process, which is manual is always subject to human error. In the case of the large batch ( $\text{Si}_3\text{N}_4$  balls) for bearing applications, (here the diameter is 0.5"), even a small error in the setting process is exaggerated. As no two settings can be the same, the setup or alignment error of one particular run gets multiplied with the setup error of the next polishing run. This leads to an increase in the deflection of the groove formed on the spindle during polishing. This results in balls of poor sphericity due to the application of non-uniform load. Assuming that a particular set up has been validated using the vibration readings for one particular run, the same set up of that particular run can be used many times, which ensures the correctness of the set up for more than one run. This method reduces the need for taking the vibration readings for all

the runs. Some of the constraints encountered in using the same setup for more than one polishing run are given below.

1. Width of the groove formed on the float
2. Stage of polishing

As discussed before, a groove is formed on the float during each polishing run. Since the same float is used for as many runs as possible for maintaining the uniformity of polishing, the width of the groove increases with each run. When the groove becomes large enough (the groove reaches the periphery of the float), the float has to be replaced. In case, the groove reaches the edge of the float, an edge crack propagates on the float, which damages the float. This condition is undesirable and will lead to the non-uniform application of load on the balls, which leads to a roundness that is less than the sphericity before that particular polish. This acts as one of the constraints for using the same setup for more than one polishing run. Using a trial and error method, it was found that after five polishing runs, the groove on the float reaches a distance of 2 mm from the edge of the float. So it was decided to have five polishing runs with the same polishing setup.

The stage of polishing also influences the possibility of using the same setup for more than one polishing run. The grit size of the abrasive greatly influences the surface finish and the sphericity of the ball. In the magnetic float polishing technique, the chamber and the polishing spindle are cleaned after each polishing run. It is ensured that abrasives of a higher grit size are not present in the polishing run, where the abrasive of a lower grit size is used. This is because; even a minutest speck of abrasive might produce a scratch, which reflects on the surface finish of that particular ball. So fresh abrasives along with fresh ferromagnetic fluid have to be used after each run. On the runs where

the transition is done, a new set up has to be done after proper cleansing of the chamber and the polishing shaft. After each polishing run, the set up is cleansed using a shop vacuum cleaner.

### **7.3.2 Process time**

One of the important features of magnetic float polishing is the short polishing process time required to finish a batch of ceramic balls. This process is much faster than the conventional lapping process, which takes ~ two weeks for finishing one batch of balls. In case of large batch balls, of sizes ranging from 7/32" to 11/32" diameter, finished using MFP, the process time was ~ 87.5 hours. The total process time can be divided into a number of elements such as the process time, the setup time, the replenishing time, and the cleansing time. Table 7.1 shows the split of the total time (process time +set up time +replenishing and cleansing time) for polishing a large batch silicon nitride balls of diameter 7/32", 9/32", and 11/32".

The total processing time for the polishing of a large batch of silicon nitride balls (0.5 or 16/32") for bearing applications can be reduced considerably if the same set up is used for more than one polishing run when compared to the time for polishing the same batch with different setups for each polishing run. The time that is required for polishing the above-mentioned batch of silicon nitride balls using MFP is some where around 100hrs. Table 7.2 shows the split of the total time (process time + set up time +replenishing and cleansing time) for polishing a large batch (55 balls) of silicon nitride balls with different setups for each polishing run.

Table 7.1 Total process time for Si<sub>3</sub>N<sub>4</sub> balls

[Large batch (55 balls), diameter 7/32", 9/32" and 11/32"]

<b>Number of polishing runs</b>	<b>35</b>
<b>Process time or polishing time</b>	<b>(35*60minutes)/60=35hrs</b>
<b>Setup Time</b>	<b>(30 minutes * 35 )/60=17.50 hrs</b>
<b>Replenishing time</b>	<b>(20 minutes * 35 )/60=11.67 hrs</b>
<b>Cleansing Time</b>	<b>(25 minutes * 35 )/60=14.58 hrs</b>
<b>Total Processing time</b>	<b>35+17.50+11.67+14.58= 78.75hrs</b>

Table 7.2 Total process time (theoretical) for Si<sub>3</sub>N<sub>4</sub> balls

[Large batch (55 balls), diameter-16/32"]

<b>Number of polishing runs</b>	<b>40</b>
<b>Process time or polishing time</b>	<b>(34*60+3*120+3*180)/60=49hrs</b>
<b>Setup Time</b>	<b>(30 minutes * 40 )/60=20 hrs</b>
<b>Replenishing time</b>	<b>(20 minutes * 40 )/60=13.33 hrs</b>
<b>Cleansing Time</b>	<b>(25 minutes * 40 )/60=16.67hrs</b>
<b>Total Processing time</b>	<b>49+20+13.33+16.67= 99hrs</b>

Table 7.3 shows the time taken for finishing the entire polishing process along with the respective material removal rate of each polishing run, in the case of a large batch (55 balls) using magnetic float polishing technique.

Table 7.3 Total processing time with MRR for finish [Large batch (55) Si<sub>3</sub>N<sub>4</sub> balls]

Sr.No	Abrasive (Grit Size)	Diameter (mm)	Material Removal (μm)	Time (min)	MRR (μm/min)
1	B <sub>4</sub> C (500)	13.488	37	60	0.616
2	B <sub>4</sub> C (500)	13.449	39	60	0.65
3	B <sub>4</sub> C (500)	13.412	37	60	0.617
4	B <sub>4</sub> C (500)	13.374	38	60	0.633
5	B <sub>4</sub> C (500)	13.334	40	60	0.667
6	B <sub>4</sub> C (500)	13.297	37	60	0.617
7	B <sub>4</sub> C (500)	13.254	43	60	0.717
8	B <sub>4</sub> C (500)	13.210	44	60	0.733
9	B <sub>4</sub> C (500)	13.164	46	60	0.767
10	B <sub>4</sub> C (500)	13.123	41	60	0.683
11	B <sub>4</sub> C (500)	13.081	42	60	0.7
12	B <sub>4</sub> C (500)	13.042	39	60	0.65
13	B <sub>4</sub> C (500)	13.004	38	60	0.633
14	B <sub>4</sub> C (500)	12.961	43	60	0.717
15	B <sub>4</sub> C (500)	12.919	42	60	0.7
16	B <sub>4</sub> C (500)	12.879	40	60	0.667
17	B <sub>4</sub> C (1000)	12.863	16	60	0.267
18	B <sub>4</sub> C (1000)	12.850	13	60	0.217

19	B <sub>4</sub> C (1000)	12.835	15	60	0.25
20	B <sub>4</sub> C (1000)	12.818	17	60	0.283
21	B <sub>4</sub> C (1000)	12.805	13	60	0.217
22	B <sub>4</sub> C (1000)	12.790	15	60	0.25
23	B <sub>4</sub> C (1000)	12.773	17	60	0.283
24	B <sub>4</sub> C (1000)	12.755	18	60	0.3
25	B <sub>4</sub> C (1000)	12.743	12	60	0.2
26	B <sub>4</sub> C (1500)	12.738	5	60	0.083
27	B <sub>4</sub> C (1500)	12.732	6	60	0.1
28	SiC (1200)	12.727	5	60	0.083
29	SiC (1200)	12.723	4	60	0.067
30	SiC (1200)	12.718	5	60	0.083
31	SiC (1200)	12.714	4	60	0.067
32	SiC (1200)	12.710	4	60	0.067
33	SiC (1200)	12.707	3	60	0.05
34	SiC (1200)	12.704	3	60	0.05
35	SiC (8000)	12.703	1	120	0.083
36	SiC (8000)	12.702	1	120	0.083
37	SiC (10000)	12.701	1	120	0.083
38	CeO <sub>2</sub>	12.701	0	180	0
39	CeO <sub>2</sub>	12.700	1	180	0.006
40	CeO <sub>2</sub>	12.700	0	180	0



Table 7.4 Split up times for the entire polishing process.

<b>Number of polishing runs</b>	<b>40</b>
<b>Process time or polishing time</b>	$(34*60+3*120+3*180)/60=49.00\text{hrs}$
<b>Setup Time</b>	$(30 * 12)/60=6.00 \text{ hrs}$
<b>Replenishing time</b>	$(20 \text{ minutes} * 40 )/60=13.33 \text{ hrs}$
<b>Cleansing Time</b>	$(10*40+25*12 )/60=11.67\text{hrs}$
<b>Total Processing time</b>	$49.00+6.00+13.33+11.67= 80.00\text{hrs}$

Using the same set up for more than one polishing run (five runs), it is found that a major portion of the total process time is reduced. In this case the setup time is only a quarter of the amount of setup time that is used if polishing is done without using different set ups for each polishing run. The cleaning time is reduced by almost 5 hours when compared to Table 7.2. Thus, this method of setting up is very useful in reducing the total process time by almost 19 hours from the method of using a different setup for each run. Based on the earlier discussion it can also be concluded that this method also increases the repeatability of the process, and decreasing the probability of human errors in alignment of the apparatus.

## Chapter 8

### Statistical Analysis

#### 8.1. Introduction

Statistical analysis of a particular process is usually done to verify whether that particular process is in the state of statistical control. A statistically controlled process is one in which, prediction is feasible and appropriate, due to controlled variation in the major parameters of the product that is being produced. The main objective of the control chart is to provide an insight into the process. Control charts basically assume that the process is stable and finds out the grand average and the average range before establishing the control limits for that particular sample size under consideration. The observed subgroup ranges and subgroup averages are compared with the predicted limits. There are two possible outcomes of this comparison:

- If the observations are consistent with the predictions, the process may be considered to be a stable process.
- If the observations are inconsistent with the predictions, the process is unstable. The inconsistency between the observations and the predictions is almost surely due to an incorrect assumption of stability rather than a violation of principles behind the calculation of the limits.

The main objective of this chapter is to investigate the variation of the critical parameters such as the roundness, the diameter of the finished balls, and the surface finish ( $R_a$  and  $R_t$ ) of the large batch  $\text{Si}_3\text{N}_4$  balls. In this case, the variation of these

parameters within a sample size selected and the variation within a subgroup size are found out. This variation can be directly related to the stability of this process.

## **8.2 Average and Range Charts**

Average charts are those which show the variation within a particular sample size for a particular batch while the range chart shows the variation within a subgroup for the entire sample size. The significance of subgroups along with their formation and use have been elaborated below.

### **8.2.1 Use of Subgroups**

The major objective of forming subgroups is to organize the data in a rational manner, which will allow the monitoring of both the location and the dispersion of the values generated by the phenomenon or the process under consideration. Several measurements are obtained from the product under observation and these values are grouped together and treated as a separate set of data.

If the subgroups display consistent behavior, then it is reasonable to assume that the process is in controlled variation or is a stable one. If the subgroups display inconsistent behavior, then the process is said to display uncontrolled variation. For example, if a subgroup size of four is selected, various measurements are made and each subgroup is summarized by the calculation of a Subgroup Average and a Subgroup Range. As long as the process remains stable and unchanging, the Subgroup Averages and Subgroup Ranges will move around within the control limits in an erratic and random manner.

### 8.2.2 Control Limits for the Subgroup Data

Control limits computed in the proper manner are robust to a lack-of control-they will usually detect a lack of control when it exists even though the out-of-control points are used in the computation

1. Compute the average and range for each of the k subgroups.
2. Compute the Grand Average,  $\bar{\bar{X}}$ , by averaging each of the k Subgroup Averages.
3. Compute the Average Range,  $\bar{R}$ , by averaging each of the k Subgroup Ranges.
4. The central line for Xbar-chart is  $\bar{\bar{X}}$ .
5. The central line for R-chart is  $\bar{R}$ .
6. Values for  $A_2$ ,  $D_3$  and  $D_4$  corresponding to the subgroup size n are chosen.
7. Multiply  $\bar{R}$  by  $A_2 = A_2 * \bar{R}$
8. Add the quantity from step-7 to the Grand Average to get the Upper Control Limit for the Xbar chart:  $UCL_{\bar{X}} = \bar{\bar{X}} + A_2 * \bar{R}$
9. Subtract the quantity from step-7 from the Grand Average to get the Lower Control Limit for the Xbar chart:  $LCL_{\bar{X}} = \bar{\bar{X}} - A_2 * \bar{R}$
10. Multiply  $\bar{R}$  by  $D_4$  to get the Upper Control Limit for the R chart:  $UCL_R = D_4 * \bar{R}$
11. Multiply  $\bar{R}$  by  $D_3$  to get the Lower Control Limit for the R chart:  $LCL_R = D_3 * \bar{R}$

The values of the constants ( $A_2$ ,  $D_3$  and  $D_4$ ) used for the particular subgroup size are given in the Table 8.1.

Table 8.1 Values of constants for different sub-group sizes

N	A <sub>2</sub>	D <sub>3</sub>	D <sub>4</sub>
2	1.880		3.268
3	1.023	-	2.574
4	0.729	-	2.282
5	0.577	-	2.114
6	0.483	-	2.004
7	0.419	0.076	1.924
8	0.373	0.136	1.864
9	0.337	0.184	1.816
10	0.308	0.223	1.777

### 8.3 Average (Xbar) and Range (R) charts for large batch and large diameter (0.5") balls

The above procedure has been applied to find out whether the process used for finishing the large diameter balls has controlled or uncontrolled variation, which directly reflects on the stability of the entire process. The batch size, sample size and subgroup size chosen for plotting the Xbar and R charts have been given below.

- Batch size = 55
- Sample size = 15
- Subgroup size, n = 8

The parameters under consideration

1. Variation in sphericity
2. Variation in Diameter
3. Variation in Surface Finish.

### **8.3.1 Variation in Sphericity**

The sphericity values (in  $\mu\text{m}$ ) have been measured for the chosen subgroups in the sample size and tabulated in Table 8.2. The UCL and LCL have been calculated for both Xbar and the R charts. Figure 8.1 shows the R chart for Sphericity. It can be found that there is controlled variation, as the control limits are not exceeded. In this case, the first point in the plot represents the maximum variation of sphericity ( $0.25 \mu\text{m}$ ). Similarly, for the thirteenth ball the maximum variation or the range is  $0.2 \mu\text{m}$ . Figure 8.2 shows the Xbar chart for sphericity. It can be seen that some points are beyond the control limits. Most of the points that are outside the control limits are below the LCL. In the case of sphericity, its not disadvantageous for points below the LCL as the main aim is to get as low a value of sphericity as possible. In this case the first point in the plot represents the average sphericity of  $0.25 \mu\text{m}$  for the tenth ball. Similarly the average sphericity for the fourteenth ball is almost  $0.30 \mu\text{m}$ . Some points that lie outside the control limits can be attributed to the eccentricity of the polishing shaft due to re-machining. As the subgroup size selected is considerably large and most of the points are within the control limits, the variation can be considered as a controlled one.

### **8.3.2 Variation in Diameter**

The diameter values in mm have been measured for the chosen subgroups in the sample size and have been tabulated in Table 8.3. The UCL and LCL have been calculated for both Xbar and the R charts. Figure 8.3 shows the R chart for the average



range of variation in the diameter within a particular ball. It can be seen that there is controlled variation, as the control limits are not exceeded. Figure 8.4 shows the Xbar chart for the variation of diameter among the sample size selected. It can be seen that all the points are within the control limits.

### **8.3.3 Variation in Surface Finish**

The surface finish values (in nm) have been measured for the chosen subgroups in the sample size and have been tabulated in Table 8.4 and 8.5. The UCL and LCL have been calculated for both Xbar and the R charts. Figures-8.5 and 8.7 show the R chart for surface finish (Ra and Rt). It can be seen that there is controlled variation, as the control limits are not exceeded. Figures 8.6 and 8.8 show the Xbar chart for surface finish (Ra and Rt). It can be seen that there are no points that lie outside the control limits so the process can be considered as stable, i.e., they exhibit a controlled variation.

Analyzing all the control charts drawn using the critical parameters measured, it can be seen that although all the points in the R-charts are within the control limits, one or two points lie outside the control limits in case of the X-bar chart. These points can be due to some eccentricity on the polishing shaft, which might have occurred during the re-machining of the shaft. Re-machining is usually done on the shaft's inclined surface in order to remove the worn surface. But the overall trends of the control charts indicate that the process is in controlled variation. Figure 8.9 and 8.10 show the roundness profile (measured with Talyrond) of a  $\text{Si}_3\text{N}_4$  ball after it is finished using magnetic float polishing. Figure 8.11 and 8.12 show the surface roughness profile, measured with Talysurf of a  $\text{Si}_3\text{N}_4$  ball after it is finished using magnetic float polishing.

Table 8.2 Measured sphericity values in  $\mu\text{m}$ . Sample Size=15, Subgroup Size, n=8.

	1	2	3	4	5	6	7	8	Total	Average	Std. Dev	Range
1	0.4	0.4	0.5	0.45	0.4	0.45	0.3	0.55	3.45	0.43125	0.075297	0.25
2	0.35	0.35	0.45	0.5	0.45	0.45	0.45	0.5	3.5	0.4375	0.0582482	0.15
3	0.5	0.35	0.45	0.4	0.35	0.4	0.35	0.4	3.2	0.4	0.0534522	0.15
4	0.45	0.45	0.4	0.5	0.45	0.5	0.5	0.45	3.7	0.4625	0.0353553	0.1
5	0.2	0.25	0.2	0.3	0.35	0.25	0.35	0.4	2.3	0.2875	0.0744024	0.2
6	0.3	0.35	0.3	0.4	0.35	0.45	0.45	0.5	3.1	0.3875	0.0744024	0.2
7	0.4	0.45	0.3	0.35	0.5	0.45	0.5	0.35	3.3	0.4125	0.0744024	0.2
8	0.45	0.35	0.3	0.35	0.3	0.45	0.45	0.45	3.1	0.3875	0.0694365	0.15
9	0.5	0.4	0.4	0.5	0.45	0.5	0.45	0.5	3.7	0.4625	0.0443203	0.1
10	0.25	0.25	0.3	0.2	0.25	0.2	0.3	0.25	2	0.25	0.0377964	0.1
11	0.5	0.4	0.45	0.5	0.45	0.4	0.45	0.35	3.5	0.4375	0.0517549	0.15
12	0.55	0.5	0.45	0.5	0.35	0.35	0.4	0.35	3.45	0.43125	0.0798995	0.2
13	0.4	0.35	0.3	0.25	0.4	0.45	0.4	0.25	2.8	0.35	0.0755929	0.2
14	0.3	0.2	0.25	0.35	0.3	0.25	0.35	0.35	2.35	0.29375	0.0562996	0.15
15	0.45	0.35	0.45	0.4	0.45	0.45	0.3	0.4	3.25	0.40625	0.0562996	0.15
										0.3891667		0.1633
Upper Control Limit, Ucl-R=0.304391				Upper Control Limit, Ucl-Xbar=0.450111								
Lower Control Limit, LCL-R=0.030047				Lower Control Limit, LCL-Xbar=0.328289								
Central Limit, CL-R=0.1633				Central Limit, CL-Xbar=0.3892								



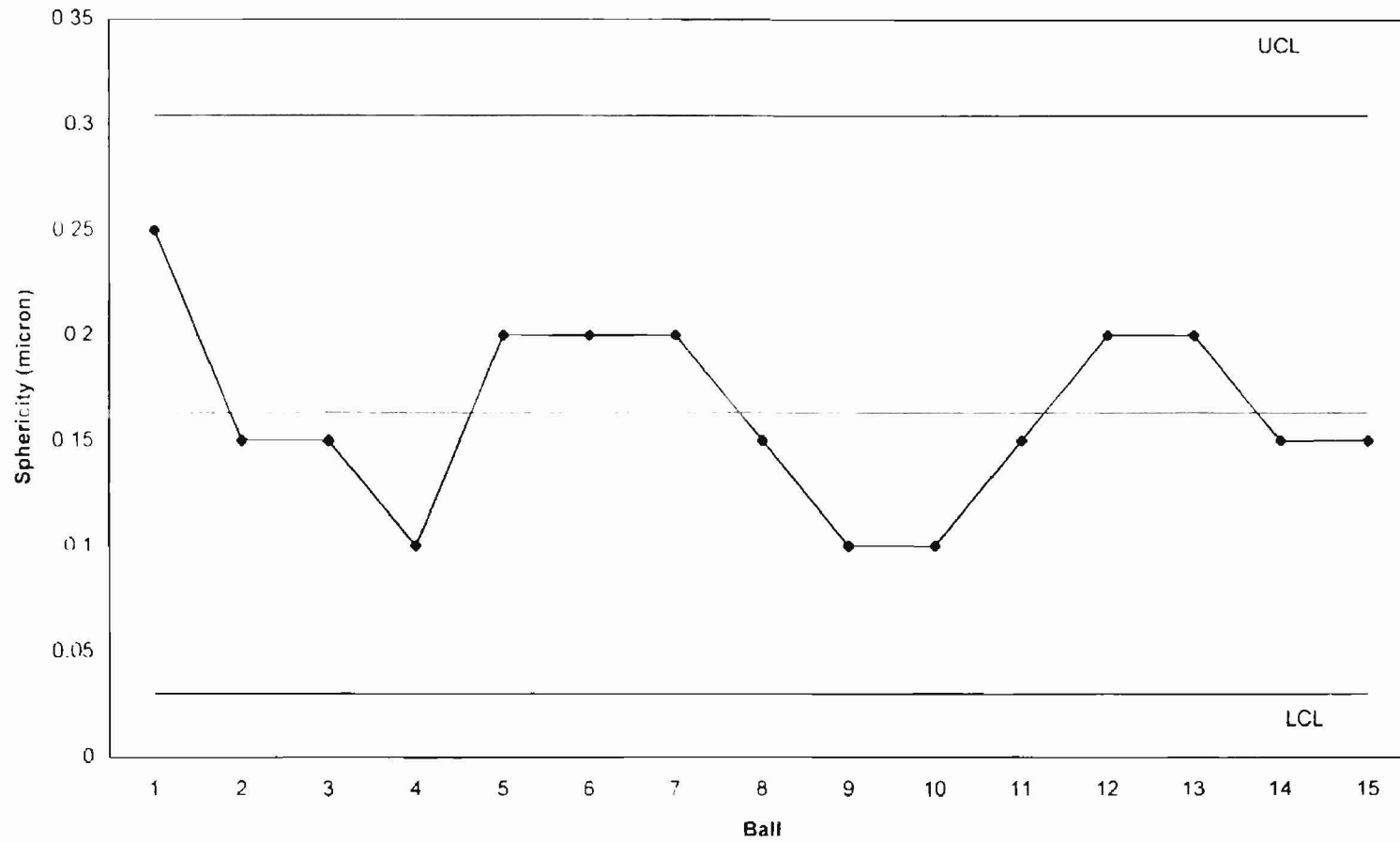


Figure 8.1 R-Chart (Variation of Sphericity within a ball)

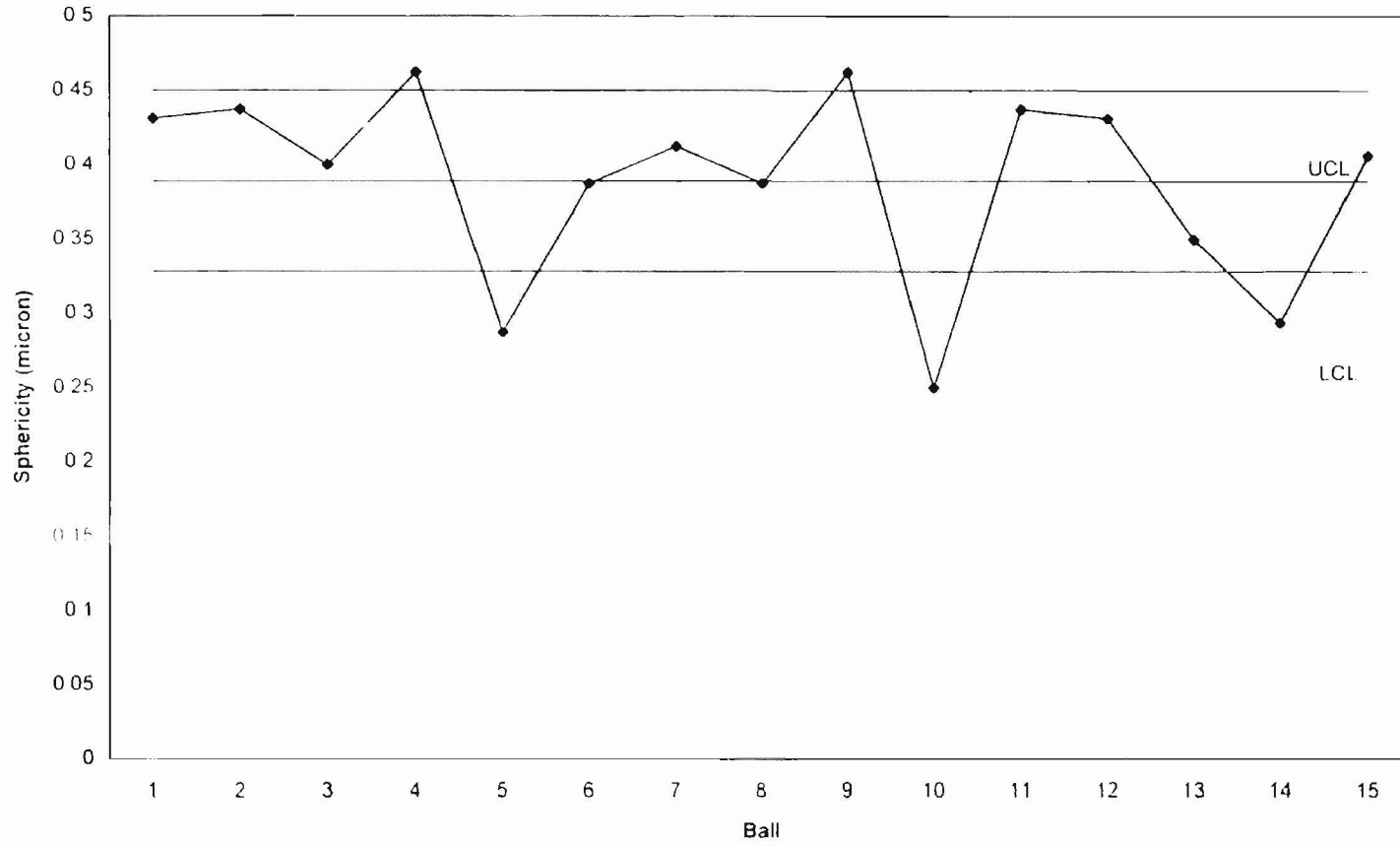


Figure 8.2 Xbar Chart (Variation of Sphericity within the Sample Size)

Table 8.3 Measured diameter values in mm. Sample size=15, Subgroup size, n=8

	1	2	3	4	5	6	7	8	Total	Mean	Range
1	12.7005	12.700375	12.700425	12.700475	12.7008	12.700675	12.70105	12.700225	101.6045	12.70056	0.000825
2	12.7004	12.700475	12.70025	12.700325	12.70105	12.7011	12.70025	12.700425	101.6043	12.70054	0.00085
3	12.700375	12.69985	12.700725	12.70065	12.700825	12.6998	12.70015	12.700275	101.6027	12.70034	0.001025
4	12.700275	12.700425	12.701125	12.700525	12.700425	12.699725	12.700225	12.700525	101.6033	12.70041	0.0014
5	12.7005	12.700475	12.700725	12.700475	12.699825	12.700425	12.700625	12.7005	101.6036	12.70045	0.0009
6	12.700375	12.70025	12.700275	12.700225	12.700375	12.700525	12.699725	12.7004	101.6022	12.70028	0.0008
7	12.700425	12.700825	12.700875	12.700175	12.700525	12.700675	12.7005	12.701025	101.6049	12.70061	0.001
8	12.699875	12.700675	12.700525	12.700325	12.700425	12.700325	12.700125	12.6998	101.6021	12.70026	0.000875
9	12.700325	12.700225	12.700625	12.700525	12.700325	12.700875	12.700625	12.701125	101.6047	12.70059	0.0009
10	12.700275	12.700275	12.700325	12.7008	12.700475	12.700525	12.700825	12.700675	101.6042	12.70053	0.00055
11	12.7005	12.700375	12.7004	12.700275	12.700125	12.700675	12.700275	12.700525	101.6032	12.7004	0.00055
12	12.700725	12.700625	12.7008	12.70105	12.700875	12.700675	12.700525	12.700675	101.606	12.70075	0.000525
13	12.700125	12.700225	12.700275	12.699875	12.699825	12.700325	12.700475	12.7004	101.6015	12.70019	0.00065
14	12.700475	12.70125	12.700525	12.700675	12.7006	12.700425	12.700875	12.700525	101.6054	12.70068	0.000825
15	12.700625	12.7005	12.700125	12.700225	12.7002	12.700325	12.700425	12.700475	101.6029	12.70036	0.0005
	Upper Control Limit, Ucl-R=0.001514				Upper Control Limit, Ucl-R=12.70076					12.70046	0.000812
	Lower Control Limit, LCL-R=0.00011				Lower Control Limit, LCL-Xbar=12.70016						
	Central Limit, CL-R=0.000812				Central Limit, CL-Xbar=12.70046						

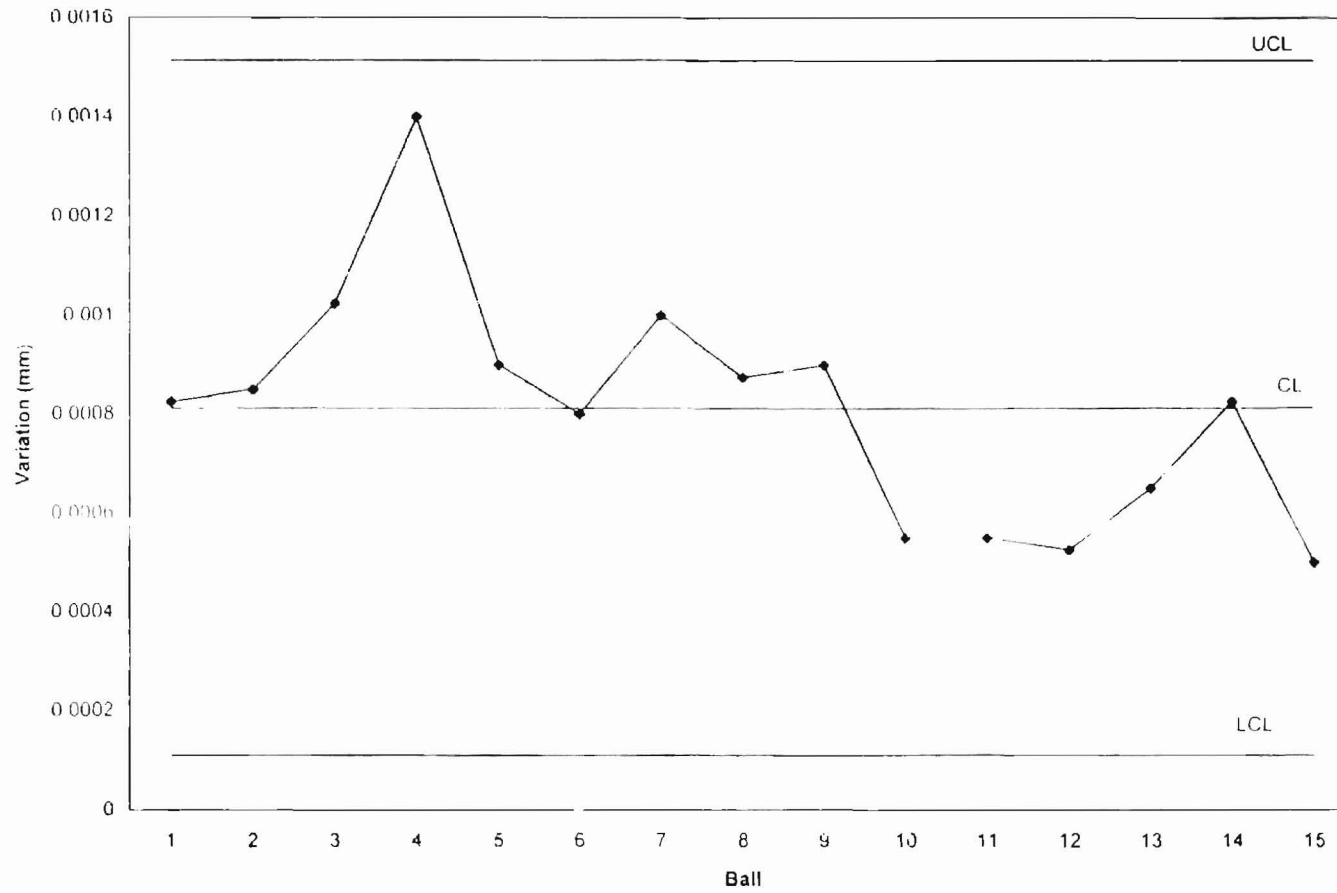


Figure 8.3 R Chart (Variation of Diameter within the ball)

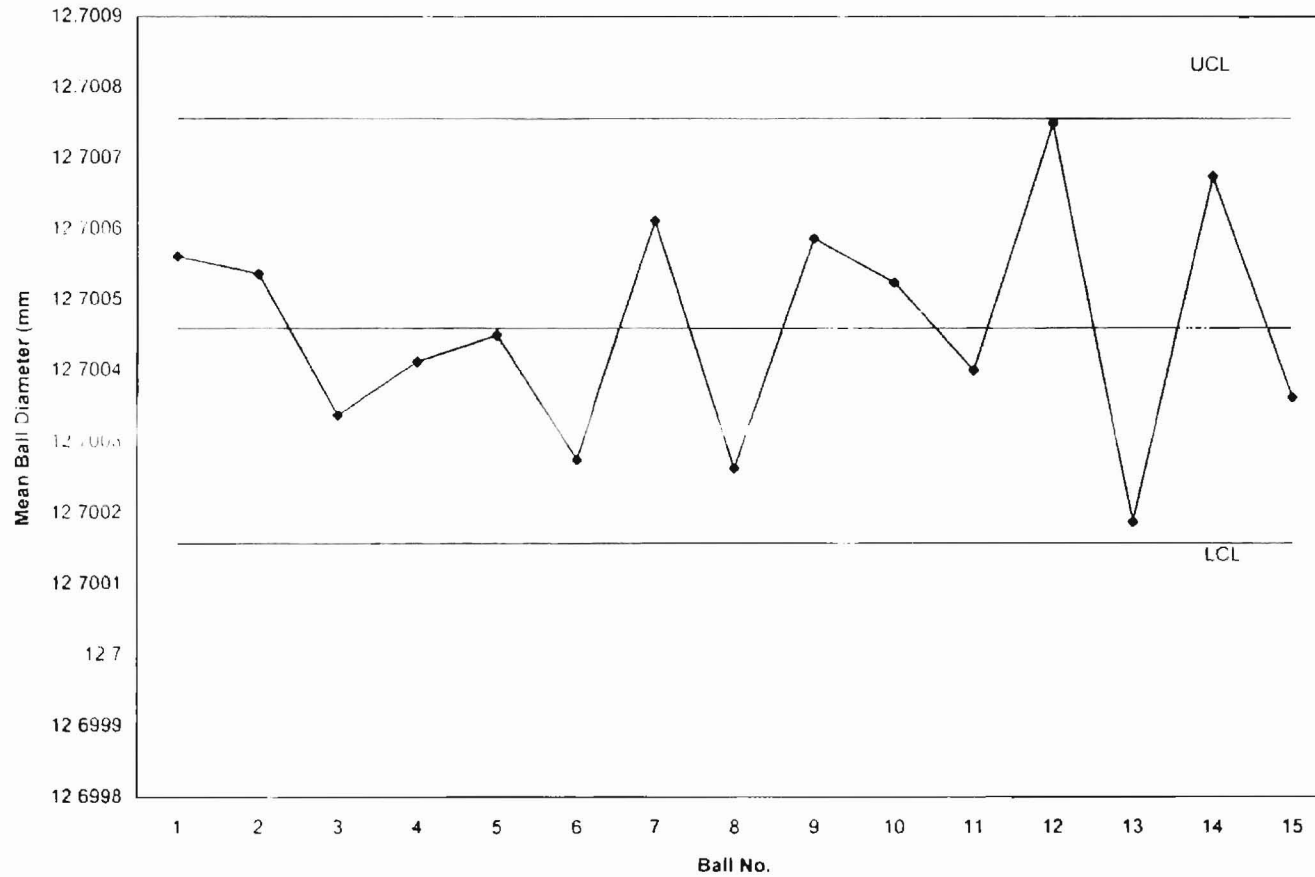


Figure 8.4 X-bar Chart (Variation of Diameter within the sample size)

Table 8.4 Measured values of Ra (nm), Sample Size=15, Subgroup size, n=8

	1	2	3	4	5	6	7	8	Total	Average	Std. Dev	Range
1	8.5	8.6	9.7	8.9	9.6	9.7	9.1	9.9	74	9.25	0.545108	1.4
2	9.4	9.7	10.1	8.1	8.7	10.2	9.1	10.2	75.5	9.4375	0.767068	2.1
3	8.7	9.1	8.6	7.9	9.2	9.5	9.3	10.3	72.6	9.075	0.706602	2.4
4	9.6	9.4	9.7	10.2	10.1	10	8.7	8.7	76.4	9.55	0.587975	1.5
5	7.9	8	8.2	8.6	7.5	8.9	9.2	9.5	67.8	8.475	0.692305	2
6	8.6	8.8	10.2	10.1	9.5	9.1	8.5	8.7	73.5	9.1875	0.672814	1.7
7	9.2	9.1	8.6	9	7.9	7.8	8.5	9.2	69.3	8.6625	0.565528	1.4
8	9.8	10.2	10.3	9.2	9.8	10.3	10.4	10	80	10	0.396412	1.2
9	9	7.4	8.1	8.5	8.9	7.5	9.2	8.6	67.2	8.4	0.676123	1.8
10	10.2	9.3	9.8	9.3	9.6	9.4	9.8	9.1	76.5	9.5625	0.358319	1.1
11	9.5	7.5	8.4	8.5	9.1	8.1	8.2	9.4	68.7	8.5875	0.693722	2
12	8.3	8.8	7.8	7.2	8.5	9	8.1	8.7	66.4	8.3	0.590399	1.8
13	9.1	9.7	8.7	8	8.3	8.6	8.2	9	69.6	8.7	0.555492	1.7
14	8.9	10	9.6	9	8.1	9.3	8.8	8.2	71.9	8.9875	0.649038	1.9
15	9.1	9.2	8.7	8.2	9.3	8.3	7.8	8.4	69	8.625	0.539179	1.5
										8.986667		1.7
	Upper Control Limit, Ucl-R=3.1699				Upper Control Limit, Ucl-Xbar=9.6208							
	Lower Control Limit, LCL-R=0.2312				Lower Control Limit, LCL-Xbar=8.3526							
	Central Limit, CL-R=1.7				Central Limit, CL-Xbar=8.9867							

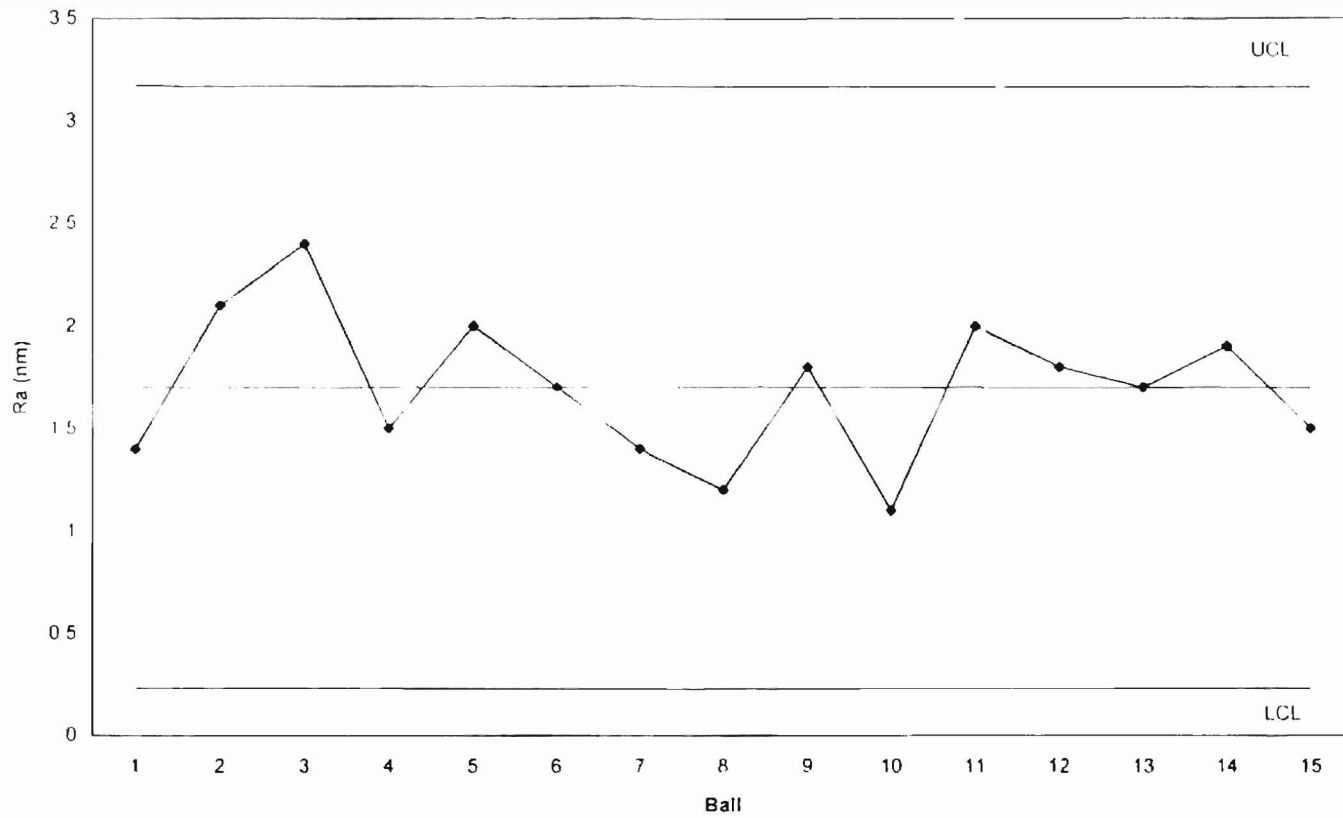


Figure 8.5 R Chart (Variation of Ra within the ball)

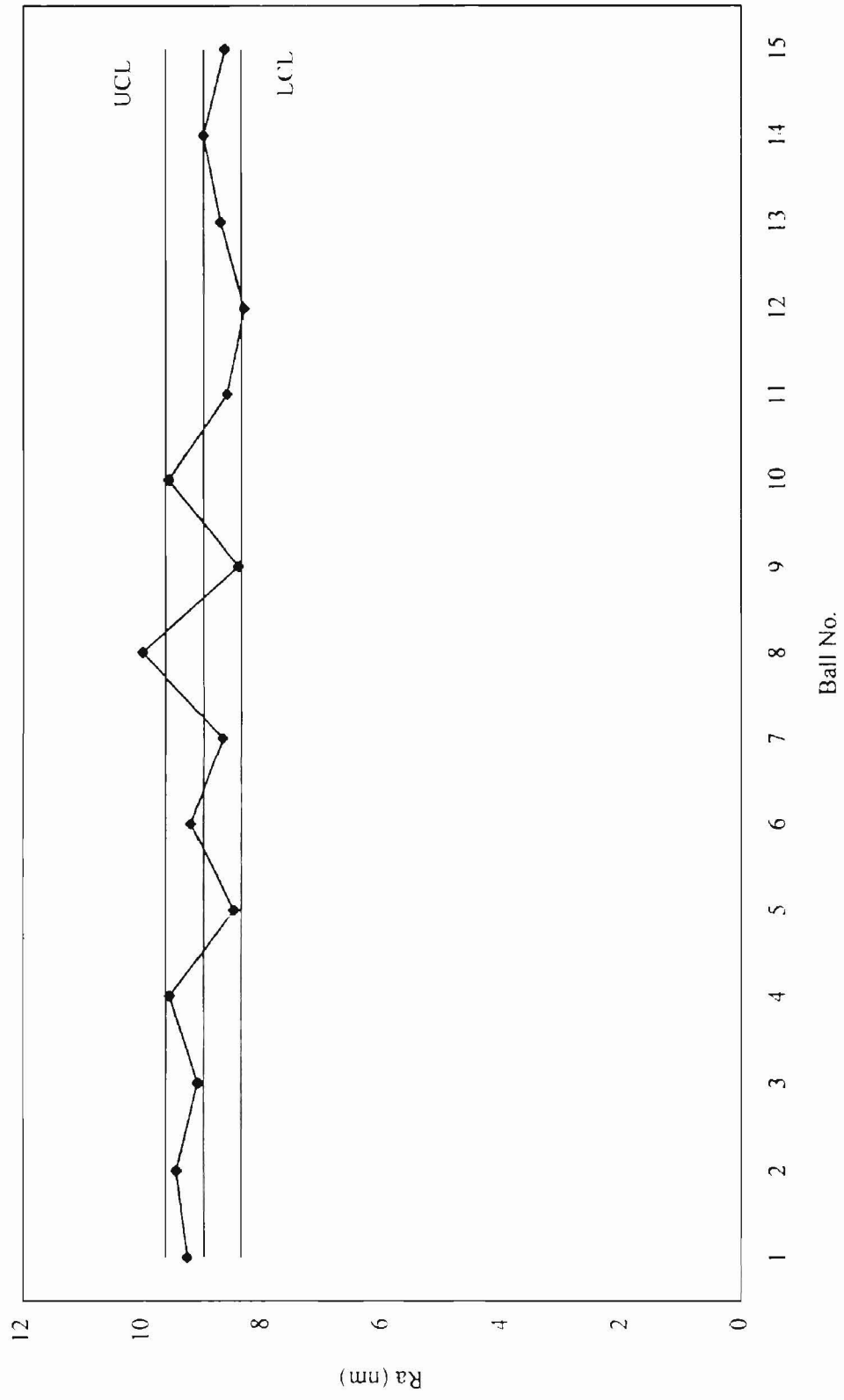


Figure 8.6 X-bar Chart (Variation of Ra within the sample size)



Table 8.5 Measured values of Rt (nm), Sample Size=15, Subgroup size, n=8

	1	2	3	4	5	6	7	8	Total	Average	Std.Dev	Range
1	98.5	125.8	108.7	169.9	181.8	141.3	103.8	142.4	1072.2	134.025	30.653	83.3
2	183.6	158.1	181.1	132.1	90.3	92.4	141.3	102.4	1081.3	135.1625	37.691	93.3
3	103.7	108.1	100.1	91.4	171.9	185	115.6	116.3	992.1	124.0125	34.732	93.6
4	114.9	129.9	141.6	138.5	175.5	170.9	122.4	97.3	1091	136.375	26.672	78.2
5	169.3	122	134.7	143.8	156.1	165.3	99.3	91.2	1081.7	135.2125	29.225	78.1
6	133.9	102.8	125.2	116.4	167.4	134.2	119.6	150.3	1049.8	131.225	20.311	64.6
7	184.3	172.9	114.7	115.4	161.7	152.5	123.8	124.4	1149.7	143.7125	27.55	69.6
8	77.8	154.1	102.6	114	155.8	152	99.3	151.9	1007.5	125.9375	31.058	78
9	107.7	88.7	83.4	82.8	162.4	109.6	159.1	67.6	861.3	107.6625	35.491	94.8
10	125.7	85.9	148.9	78	109	86.8	119.3	110	863.6	107.95	23.775	70.9
11	128.8	102.5	152.9	161.4	127.8	78.2	128.9	117.9	998.4	124.8	26.424	83.2
12	72.6	126.4	124.6	116.3	86.9	66.3	112	110.6	815.7	101.9625	23.456	60.1
13	107.2	122.7	145.9	84.5	135.1	156.9	107.7	122.1	982.1	122.7625	23.258	72.4
14	97	92.7	103.5	98.8	104.2	92.7	79.1	84.7	752.7	94.0875	8.768	25.1
15	87.4	109.5	82	97.8	113.3	92.2	112.1	103.4	797.7	99.7125	11.789	31.3
Upper Control Limit, UCL-R=133.7737					Upper Control Limit, UCL-Xbar=148.4091					121.64		71.7667
Lower Control Limit, LCL-R=9.760312					Lower Control Limit, LCL- Xbar=94.87091							
Central Limit, CL-R=71.767						Central Limit, CL-Xbar=121.64						

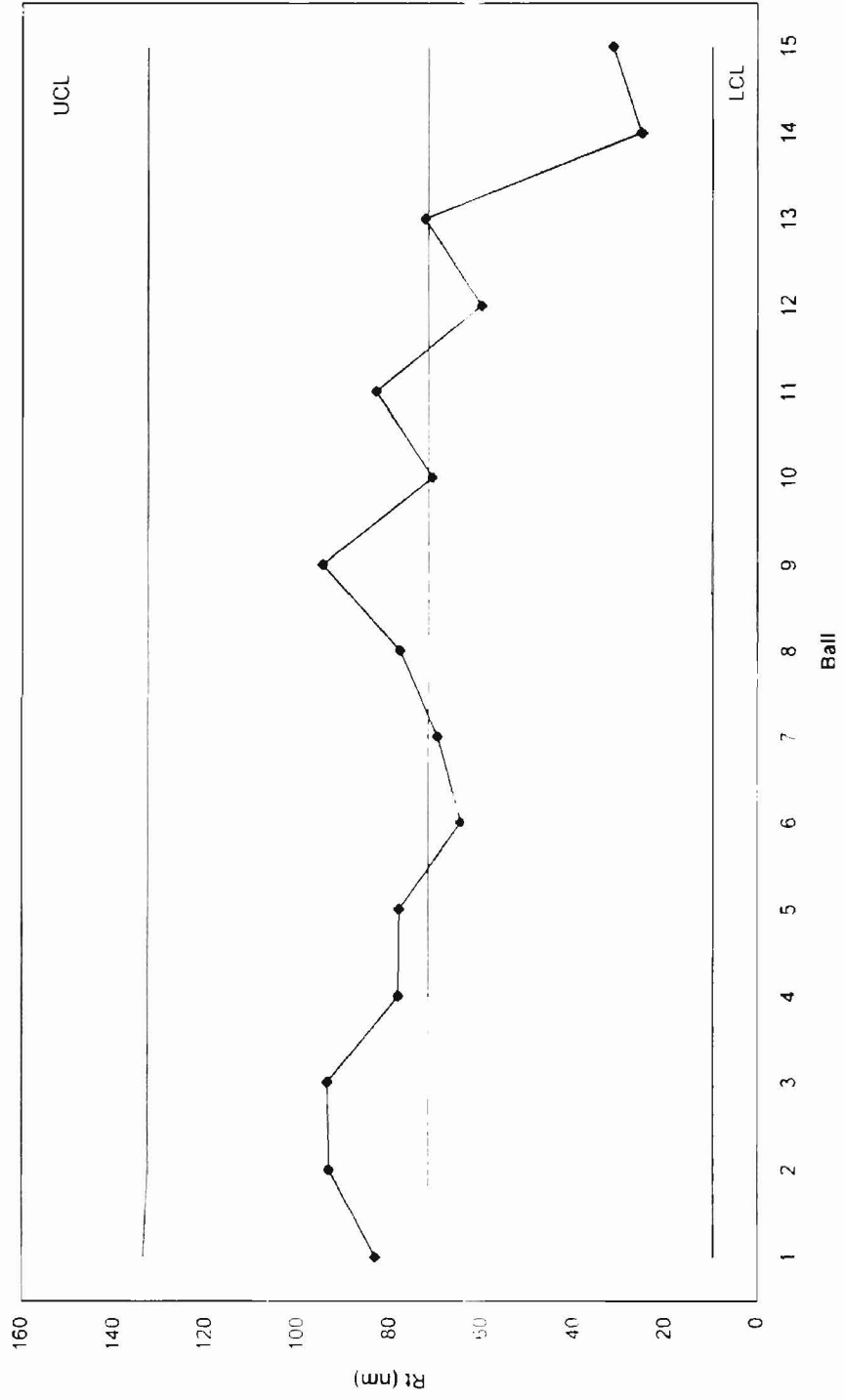


Figure 8.7 R Chart (Variation of Rt within the ball)

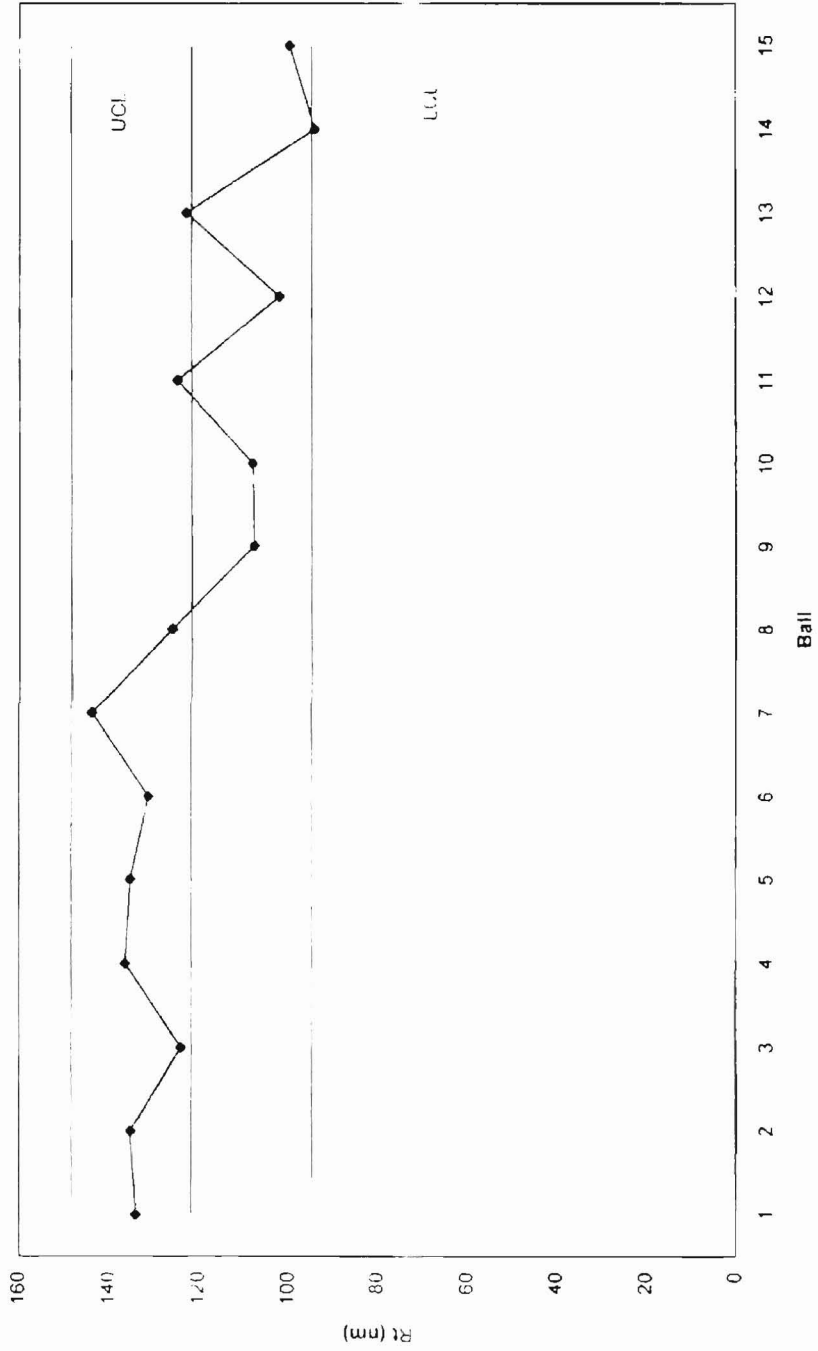
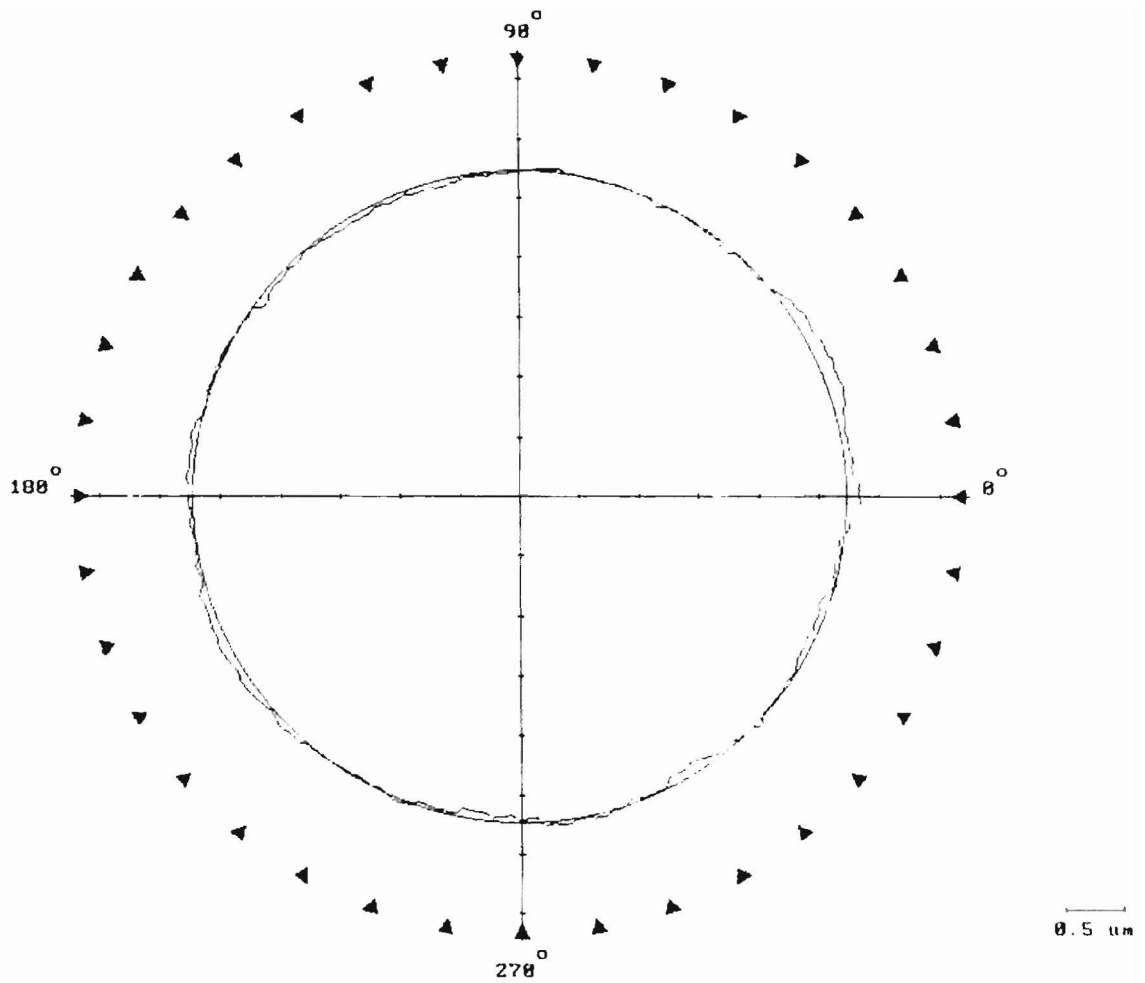


Figure 8.8 X-bar Chart (Variation of Rt within the sample size)

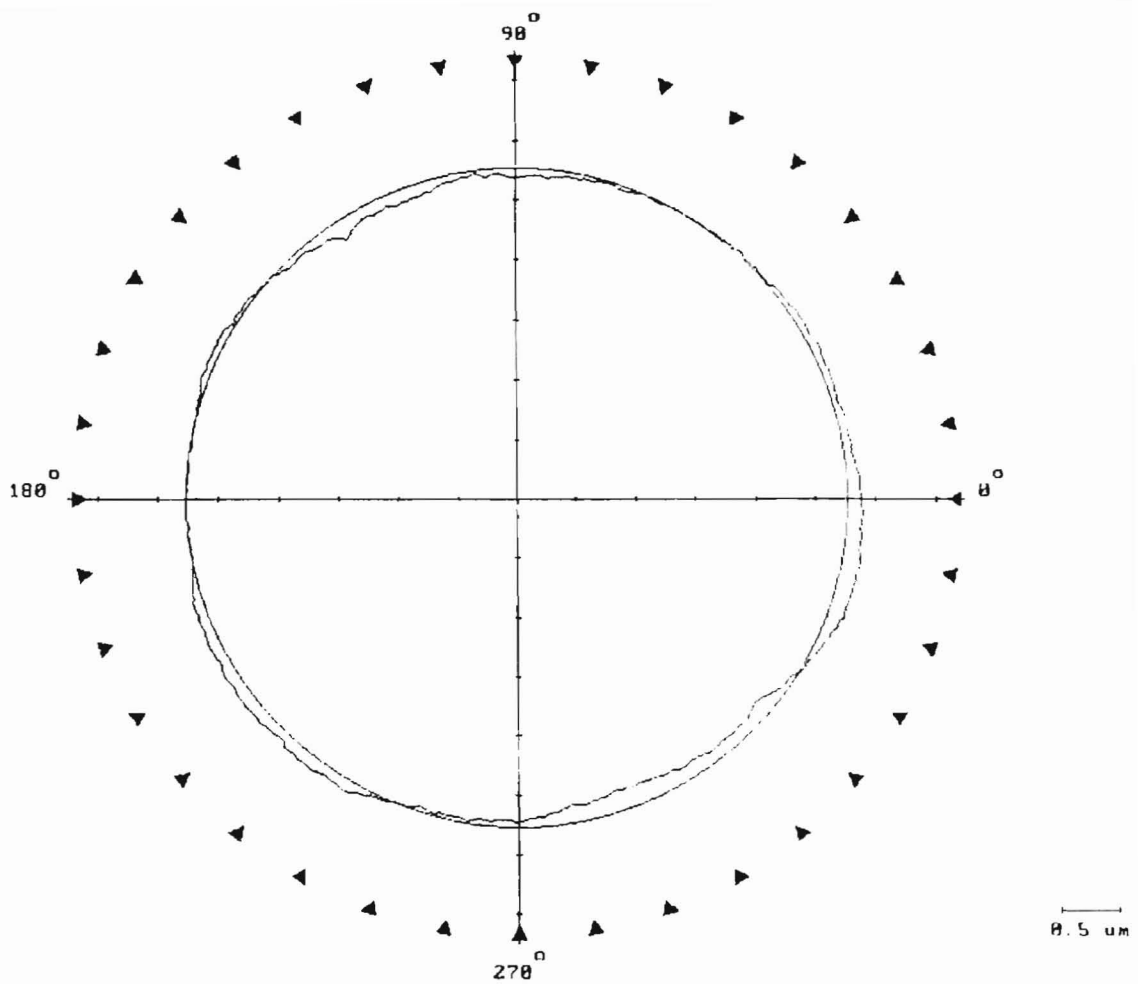


LS ROUNDNESS RESULTS

○	0.28 μm	Meas. mode	External
E	1.08 μm	Z Height	144.4 mm
∠	248.3 deg	Filter	50 upr 2CR
↗	2.05 μm	Profile	100.0 %

Datum : SPINDLE

Figure 8.9 Roundness profile of a finished Si<sub>3</sub>N<sub>4</sub> ball (Talyrond 250)



**LS ROUNDNESS RESULTS**

○	0.35 μm	Meas. mode	External
E	4.80 μm	Z Height	144.5 mm
∠	307.2 deg	Filter	50 upr 2CR
↗	9.65 μm	Profile	100.0 %

Datum : SPINDLE

Figure 8.10 Roundness profile of a finished  $\text{Si}_3\text{N}_4$  ball (Talyrond 250)

**RANK TAYLOR HOBSON**  
Form Talysurf Series

OKLAHOMA STATE UNIVERSITY

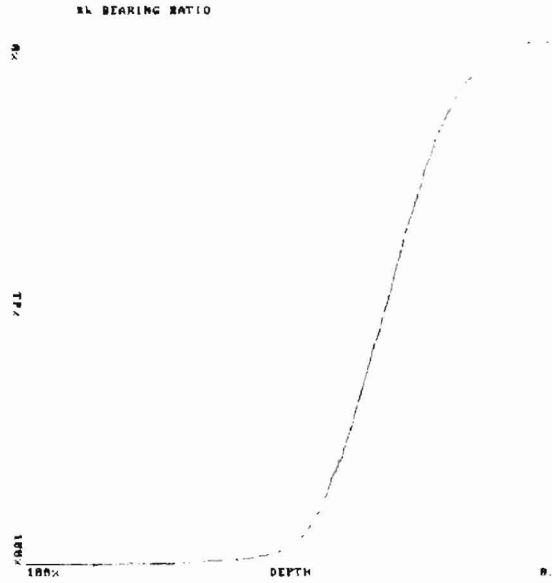
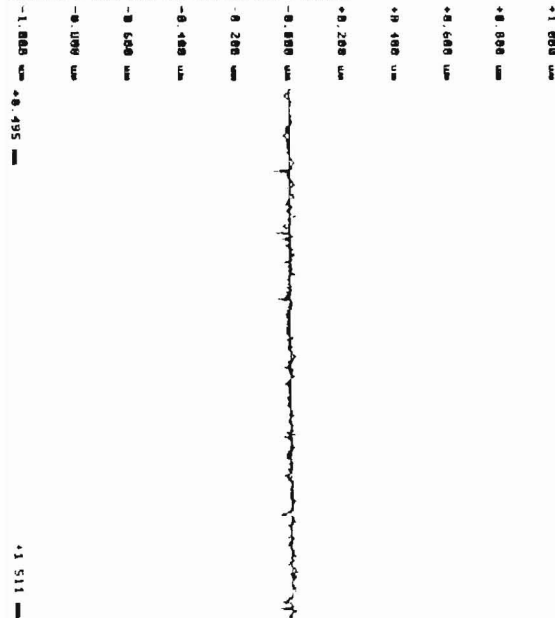
13/02/88 14:35:02  
Rough/120/4-0.25mm,100:1/Comux  
Calibrated: 05:07. 19/03/96, 112/2033, 112/1036, mra

Batch 68 Glass ball polishing w/ pad

COMPLETE MODIFIED PROFILE

Horizontal Scale : 100.000 um per division  
Horizontal Magnification : x 94.0  
Vertical Scale : 0.200 um per division  
Vertical Magnification : x 47400.0

WARNING : VERTICAL SCALE HAS BEEN ADJUSTED  
WARNING : ALL PROFILE POINTS NOT PRINTED



LS Ra4 6.76370um

Ra	0.0078 um	Rq	0.0102 um	Rp	0.0245 um
Rv	0.0653 um	Rt	0.0090 um	R11	0.0057 um
RA2	0.0745 um	R13	0.0534 um	R14	0.0740 um
Rsk	0.0904	Rku	5.9004	Delq	0.5446 deg
Lamq	0.7401 um	S	4.0930 um	Ry	0.0057 um
Rz150	0.0731 um	RzDIN	0.0720 um	Tpm	0.0221 um
Rzu	0.0683 um	R3x	0.0497 um	Rk	0.0371 um
Rpk	0.0136 um	Rvk	0.0190 um	Mr1	10.0000 %
Mr2	91.0000 %	Sm	7.4240 um	Lo	1.0154 um

Figure 8.11 Surface Roughness profile of a finished Si<sub>3</sub>N<sub>4</sub> ball (Talysurf 120L)

**RANK TAYLOR HOBSON**  
Form Talysurf Series

OKLAHOMA STATE UNIVERSITY

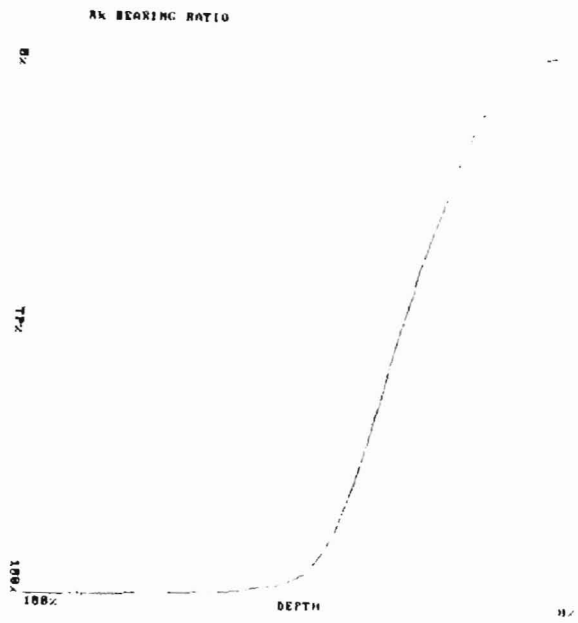
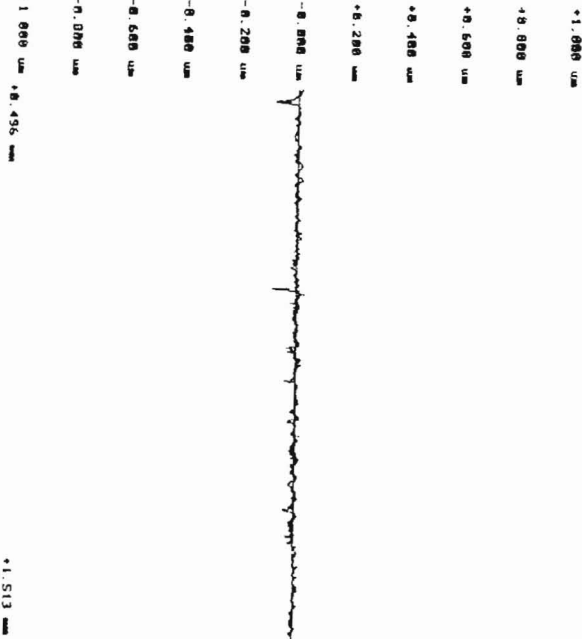
13/02/00 14:30:23  
Rough/ISO/4-0 25mm, 100:1/Convex  
Calibrated: 05:07, 19/03/96, 112/2033, 112/1836, wpp

Batch 68: Glass ball polishing w/ pad

COMPLETE MODIFIED PROFILE

Horizontal Scale : 100.000 um per division  
Horizontal Magnification : x 94.0  
Vertical Scale : 0.200 um per division  
Vertical Magnification : x 47400.0

WARNING : VERTICAL SCALE HAS BEEN ADJUSTED  
WARNING : ALL PROFILE POINTS NOT PRINTED



LS Rad 6 76.148mm

Ra	0.8808 um	Rq	0.8114 um	Rp	0.8382 um
Rv	0.8916 um	Rt	0.1218 um	Rt1	0.1062 um
Rt2	0.1218 um	Rt3	0.0682 um	Rt4	0.0682 um
Rsk	-2.0467 um	Rku	14.6864 um	Dr1q	0.5412 deg
Lamy	7.6097 um	S	3.0424 um	Ry	0.1218 um
Rx1S0	0.8835 um	RxDIM	0.0691 um	Rzm	0.0244 um
R3y	0.8555 um	R3z	0.0483 um	Rk	0.0437 um
Rpk	0.8139 um	Rvk	0.0263 um	Mt1	9.0008 %
Mt2	93.0000 %	Gz	7.2116 um	Lo	1.0172 mm

Figure 8.12 Surface Roughness profile of a finished Si<sub>3</sub>N<sub>4</sub> ball (Talysurf 120L)

## Chapter 9

### Conclusions

1. Based on the result of the trial runs (Table 6.7), which are designed using the Taguchi approach, a load and speed combination of 3 N and speed of 200 rpm for the initial roughing stage and a load of 3N and speed of 300 rpm for the intermediate semi-finishing stage are found to be the best in terms of good sphericity and uniform material removal for a large batch (55) of large diameter (17/32") silicon nitride ( $\text{Si}_3\text{N}_4$ ) balls.
2. Based on Table 7.3, an average material removal rate of  $0.672\mu\text{m/hr}$  is achieved during the initial roughing stage, while an average material removal rate of  $0.144\mu\text{m/hr}$  is achieved during the intermediate semi-finishing stage for a large batch of diameter (17/32") silicon nitride ( $\text{Si}_3\text{N}_4$ ) balls.
3. The out-of-roundness of the finished ceramic balls varied from  $0.20\ \mu\text{m}$  to  $0.55\ \mu\text{m}$  (Table 8.2), which is comparable to the Grade 10-steel ball, based on the AFBMA (Anti-friction Bearing Manufacturers Association) standards. A diametric tolerance of  $\pm 0.001\text{-mm}$  (Table 8.3) is obtained, which is also comparable to Grade 10-steel ball of AFBMA. The surface finish,  $R_a$  varied from 7.2 to 10.4 nm (Table 8.4) and  $R_t$  varied from 66.3 nm to 184.3 nm (Table 8.5), which is comparable to a Grade 3-steel ball. Based on the above conclusion, the out-of-roundness and diametric tolerance should be improved to the Grade 3-steel ball
4. By using the same set up during magnetic float polishing (for five runs), it is found that a major portion of the total process time is reduced. The set up time is reduced by



a quarter (comparing Table 7.2 and 7.4) if polishing is done without using different setups for each polishing run as compared to the process in which each run have different setups. The cleansing time is reduced by almost 5 hours, when the split-up times of the process using different setups for each run are compared to the one using the same setup for more than one run (5 runs). This method of using the same setup for five polishing runs is very useful in reducing the total process time by almost 19 hours from the method of using a different setup for each run. This method also increases the repeatability of the process decreasing the probability of human errors in the alignment of the apparatus.

5. Based on the average and the range charts (Figure 8.1-8.8) it's found that a subgroup size of 8 and a sample size of 15 are enough to find whether this particular process varies in a controlled fashion or not. Finally, based on the control charts (Figure 8.1-8.8) it is concluded that the process is in controlled variation.

## Chapter 10

### Future Work

Magnetic float polishing can be used for finishing of advanced ceramics in a highly cost-effective manner. As this method does not use the costly diamond abrasive and has faster polishing times the cost of the overall manufacturing process is low compared to the conventional lapping process.

#### 10.1 Using a single setup.

The variation in the critical parameters, such as the sphericity, the surface roughness, and the diametric tolerance has to be as low as possible. The variation in these parameters can be held within a very minimal value depending on the validity of the setup. Future research must concentrate on modifying the apparatus in such a way that the entire process should be done in one setup. Analyzing the frequency spectrum can check the initial validity of the setup. This method of using a single setup will decrease the total process time by almost 50%. This method decreases the possibility of the occurrence of the human error and removes the possibility of the polishing process being affected by repeatability. The main result of this step will be very good sphericity and diametric tolerance values.

#### 10.2 Extending MFP to finish single crystal silicon balls.

One of latest innovations in the electronic industry is the fabrication of an integrated chip circuit on the surface of a single crystal silicon ball (diameter of 1 mm).

Figure 10.1 shows a conceptual view of such a chip. This requires a spherical surface with a high degree of surface finish, a very good sphericity and a very good diametric tolerance. Magnetic float polishing (MFP), which has been successfully implemented for advanced ceramic balls can also be extended to finish these single crystal silicon balls.

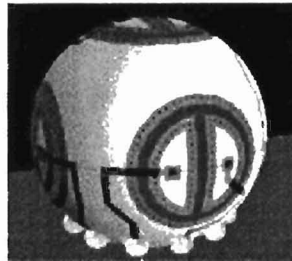


Figure-10.1 Integrated chip on a single crystal silicon ball

MFP also known as a “gentle” finishing process due its low load and high speed conditions can be ideal for finishing balls of small diameters without any surface or sub-surface damage. Modification of the polishing shaft and the chamber used is suggested for this purpose.

## References

- Aramaki, H., Shoda, Y., Morishita, Y., Sawamoto, T., "The Performance of Ball Bearings With Silicon Nitride Ceramic Balls in High Speed Spindles for Machine Tools," *Journal of Tribology*, October 1988, Vol.110, pp.693.
- Khuperkar, A. M., "Finishing of Glass Balls by Chemical-Mechanical Polishing (CMP) Using Cerium Oxide-Expanding The Process Capabilities of Magnetic Float Polishing (MFP) Technology," Masters Thesis, December 1999.
- Bhagavathula, S. R., and Komanduri, R., "On Chemo-mechanical Polishing of Silicon Nitride with Chromium Oxide Abrasive," *Philosophical Magazine A*, 74/4, 1996, 1003-1017.
- Buchner, K., " A Comparison of Spindle Ball Bearings with Steel or Ceramic Balls for Very High Speed Applications," *Creative Use of Bearing Steels*, ASTM STP 1195, J. J. Hoo, ED., American Society of Testing Materials, Philadelphia, 1993, 121-133.
- Burrier, H. I. And Burk, C., "Fatigue and Wear Behavior of NBD-200 Silicon Nitride Balls," *Ceramic Bearing Development*, WL-TR-96-4015.
- Cento, P., Dareing, D. W.. " Ceramic Materials in Hybrid Ball Bearings." *Tribology Transactions*. Vol. 42(1999), 4, 707-714.
- Childs, T. H. C., Jones, D.A., Mahmood, S., Kato, K., Zhang, B., and Umehara, N., " Magnetic Fluid Grinding Mechanics," *Wear*, 175, (1994a), 189-198.
- Childs T. H. C.. Mahmood, S., and Yoon, H. J., " The Material Removal Mechanism in Magnetic Fluid Grinding of Ceramic Ball Bearings," *Proc. Of I. Mech. E. London*, 208, No.B1, 1994b, 47-59.

Childs T. H. C., Mahmood, S., and Yoon, H. J., " The Magnetic Fluid Grinding of Ceramic Ball Bearings," *Tribology International*, 28, No.6, 1995, 341-348.

Coats, H. P., "Method and Apparatus for Polishing Containers," US Patent 2, 196, 058; 1940.

Dezzani, M. M., Pearson, P. K., " Hybrid Ceramic Bearings for Difficult Applications." *Journal of Engineering for Gas Turbines and Power*, April 1996, Vol. 118, pp-449.

Hou, Zhen-Bing and Komanduri, R., "Magnetic Field Assisted Finishing of Ceramics- Part I: Thermal Model," *Trans ASME, J. of Tribology*, 120, (Oct.1998), 645-651.

Hou, Zhen-Bing and Komanduri, R., "Magnetic Field Assisted Finishing of Ceramics- Part II: On Thermal Aspects of Magnetic Float Polishing (MFP) of Ceramic Balls," *Trans ASME, J. of Tribology*, 120, (Oct.1998), 652-659.

Hou, Zhen-Bing and Komanduri, R., "Magnetic Field Assisted Finishing of Ceramics- Part III: On Thermal Aspects of Magnetic Abrasive Finishing (MAF) of Ceramic Rollers," accepted for publication in *Trans ASME, J. of Tribology*, 120, (Oct.1998), 660-667.

Inasaki, I., " Grinding of Hard and Brittle Materials," *Annals of the CIRP*, 36/2, 1987.

Indge, J. H., " Lapping More Science less an Art Form," *Ceramic Industry*, July 1990, 26-28.

Jiang, M., and Komanduri, R., " Application of Taguchi Method to Determine Polishing Conditions in Magnetic Float Polishing," *Wear*, 213, 1997, 59-71.

Jiang, M., and Komanduri, R., "Finishing of Si<sub>3</sub>N<sub>4</sub> balls for Bearing Applications," *Wear*, 215, 1998, 267-278.

Jiang, M., and Komanduri, R., "On the Chemo-mechanical Polishing (CMP) of Silicon Nitride Bearing Balls with Water Based CeO<sub>2</sub> Slurry," Transactions of ASME, Journal of Engineering Material and Technology, 120, Oct.1998, 304-312.

Jiang, M., and Komanduri, R., "On the Chemo-mechanical Polishing (CMP) of Silicon Nitride Bearing Balls with Various Abrasives," Wear, 220, Oct.1998, 59-71.

Jiang, M., and Komanduri, R., "Magnetic Float Polishing of Magnetic Materials," US Patent No. 05.957,753, Sep. 28,1999.

Jiang, M., and Komanduri, R., "Magnetic Float Polishing Processes and Materials Therefor," US Patent No. 05,931,718, Aug. 3,1999.

Jiang, M., "Finishing of Advanced Ceramic Balls for Bearing Applications by Magnetic Float Polishing (MFP) Involving Fine Polishing Followed by Chemo-Mechanical Polishing (CMP)," Masters Thesis, July 1998.

Kato, K., Umehara N., Adachi S., and S. Sato, " Method for Grinding using a magnetic fluid and an apparatus thereof," U.S. Patent 4831466, Apr. 18, 1989

Komanduri, R., "On the Mechanisms of Material Removal in Fine Grinding and Polishing of Advanced Ceramics," Annals of CIRP, 44/1, 1996

Komanduri, R., Umehara, N., and M. Raghunandan, " On the Possibility of Chemo-Mechanical Action in Magnetic Float polishing of Silicon Nitride," Trans ASME J of Tribology, 118, 1996, 721-727

Komanduri, R., Lucca, D. A., and Y. Tani. " Technological Advances in Fine Abrasive Process," Annals of CIRP, 46/2, 1997

Kurobe, T. and Imanaka, O., " Magnetic Field-assisted Fine Finishing," Precision Engineering, 6/3, 1984, 119-124

Lynch, T. P., "Hybrid Ceramic Bearings Increase Turbine Life: silicon nitride balls in steel races survive conditions that destroy steel bearings," Design News, March 25 1991

Raghunandan, M., "Magnetic Float Polishing of Silicon Nitride Balls," Ph. D. thesis, Oklahoma State University, 1996

Raghunandan, M., Noori-Khajavi, A., Umehara, N., and R. Komanduri, "Magnetic Float Polishing of Advanced Ceramics," Trans ASME, J of Manf. Sci. and Engg 119, (1997) 520-528

Raghunandan, M., R. Komanduri, "Finishing of Silicon Nitride Balls for High-speed Bearing Applications," Trans ASME, J of Manf. Sci. and Engg 120, (1998) 1-13

Rao, S. H., "Finishing of Ceramic Balls by Magnetic Float Polishing With Online Vibration Monitoring And Control," MS Thesis, December 1999

Ross, P. J., "Taguchi Techniques for Quality Engineering," McGraw-Hill, NY, 1996

Roy, R. K., "A Primer on the Taguchi Method," Competitive Manufacturing Series, Van Nostrand Reinhold, NY, 1990

Shinmura, T., Takazawa, K., and E. Hatano, "Study of Magnetic Abrasive Finishing," Annals of CIRP, 39/1, 1990, 325-328

Subramanian, K., Indge, J. H., et al, "Final Shaping and Surface Finishing," Ceramics and Glasses, Engineered Materials Handbook, 4, 1987

Subramanian, K., and Robert, N. K., "Grinding Advanced Ceramics: A Forecast for the 1990s," Ceramic Bulletin, 67/12, 1988

Subramanian, K., Ramanath. S., and Tricard. M., "Mechanisms of Material Removal in the Precision Production Grinding of Ceramics," J of Manf. Sci. and Engg 119, Nov. 1997, 509-519

- Tani, Y. and Kawata, K., "Development of High-efficient Fine Finishing Process Using Magnetic Fluid," *Annals CIRP*, 33/1, 1984, 217-220
- Umehara, N., "Research on Magnetic Fluid Polishing," Ph. D. thesis (in Japanese), Tohoku University, Japan, 1990
- Umehara, N., and Kato, K., "Principles of Magnetic Fluid Grinding of Ceramic Balls," *Applied Electromagnetics in Materials*, 1, 1990, 37-43
- Umehara, N., Kato, K., and Nakano, H., "Magnetic Fluid Grinding of Ceramic Rollers," *Electromagnetic forces and Applications*, Elsevier Science Publishers, 1992, 139-142
- Umehara, N., Kato, K., and Kanagawa, I., "Magnetic Fluid Grinding of Ceramic Flat Surfaces," *Electromagnetic forces and Applications*, Elsevier Science Publishers, 1992, 143-146
- Umehara, N., and Komanduri, R., "Magnetic Fluid Grinding of HIP-  $\text{Si}_3\text{N}_4$  Rollers," *Wear*, 192, 1996, 85-93
- Weinberg, G. H., and Schumaker, J. A., "Statistics An Intuitive Approach," Brooks/Cole Publishing Company, Second Edition, July 1969



## **VITA**

**Ashok Lakshmanan**

**Candidate for the Degree of**

**Master of Science**

Thesis: FINISHING OF LARGE DIAMETER AND LARGE BATCH ADVANCED CERAMIC BALLS ( $\text{Si}_3\text{N}_4$ ) FOR BEARING APPLICATIONS USING MAGNETIC FLOAT POLISHING

Major Field: Mechanical Engineering

Biographical:

Personal Data: Born in Myladuthurai, Tamilnadu, India, on August 27, 1976, the son of Lakshmanan and Baghirathi

Education: Received Bachelor of Engineering degree in Mechanical Engineering from the University of Madras, Tamilnadu, India, in May 1997. Completed the requirements for the Master of Science degree with a Major in Mechanical and Aerospace Engineering at Oklahoma State University, Stillwater, Oklahoma in July, 2000

Experience: Graduate Research Assistant in Mechanical and Aerospace Engineering Department, Oklahoma State University, Stillwater, Oklahoma, August 1998 - August 2000.